Università degli Studi di Milano
Facoltà di Scienze Matematiche, Fisiche e Naturali
Corso di Laurea in Fisica

Geometric scaling in perturbative QCD

Tesi di laurea di
Fabrizio Caola

Alla Sarah,
secondo una consolidata tradizione,
e ai miei genitori.

Felix qui potuit rerum cognoscere causas
atque metus omnis et inexorabile fatum
subiecit pedibus

Verg., Georg. II, 490-492

Geometric scaling in perturbative QCD

Fabrizio Caola

Contents

List of Figures

Introduction

HERA data on deep inelastic scattering (DIS) at small x show a very striking property: the total cross section $\sigma_{tot}^{\gamma^* p}$, which is *a priori* function of two independent variables — the photon virtuality Q^2 and the Bjorken variable x — seems to depend only on the variable $\tau = Q^2 R^2(x)$, see Fig. 1. This scaling behaviour, first noticed by Staśto, Golec-Biernat and Kwieciński [1], is usually referred as "geometric scaling".

In [1] the authors build up a simple model which captures the main features of the scaling behaviour. In their model $R^2(x) = Q_0^2 \, (x/x_0)^\lambda$, with $Q_0 = 1$ GeV, $\lambda = 0.3 - 0.4$, $x_0 = 3 \times 10^{-4}$ in order to fit the data. Though this model is in good agreement with all the HERA data (in the small x region, $x < 0.01$), its assumptions are quite arbitrary and it can't be derived from first principles, so from a theoretical point of view it is unsatisfactory.

We may then wonder whether it is possible to explain geometric scaling within the framework of perturbative QCD. To answer this question, first of all we have to improve the standard perturbative QCD in order to obtain a fully reliable theory in the kinematic region of geometric scaling. In this region indeed a "naive" perturbative treatment fails, because of many effects.

First, this region is characterised by large values of Q^2. Now, a $n-$loop contribution to an amplitude involving momenta of order Q is found to contain up to n factors $\log(Q^2/\mu^2)$ (where μ is the renormalization scale) as well as factors α_s^n, so standard perturbation theory breaks down if $\alpha_s \log(Q^2/\mu^2)$ is large, even though α_s is small. In other words, if Q^2 is large enough that $\alpha_s \log(Q^2/\mu^2) \sim 1$, all terms of order $\left(\alpha_s \log(Q^2/\Lambda^2)\right)^k$ and $\alpha_s \left(\alpha_s \log(Q^2/\mu^2)\right)^k$ must be resummed in order to achieve an accuracy up to $O\left(\alpha_s^2\right)$. This resummation is accomplished by the Dokshitzer-Gribov-Lipatov-Altarelli-Parisi (DGLAP) equation (see e.g. [2]), one of the standard tools of traditional perturbative QCD.

However, in the geometric scaling kinematic region we can't limit ourselves to the DGLAP resummation. This region indeed is characterised not only by large values of Q^2, but also by small values of x (or equivalently by large values of the center of mass energy squared for the sub-process $\gamma^* + P \to X$). Hence there are many small x phenomena that we cannot neglect. First, when x is small enough that $\alpha_s \log(1/x) \sim 1$, all terms of the form $(\alpha_s \log(1/x))^k$, which are present in the splitting functions [2], must be resummed. This time the resummation is performed by the Balitsky-Fadin-Kuraev-Lipatov (BFKL) equation [3]. Thus BFKL effects

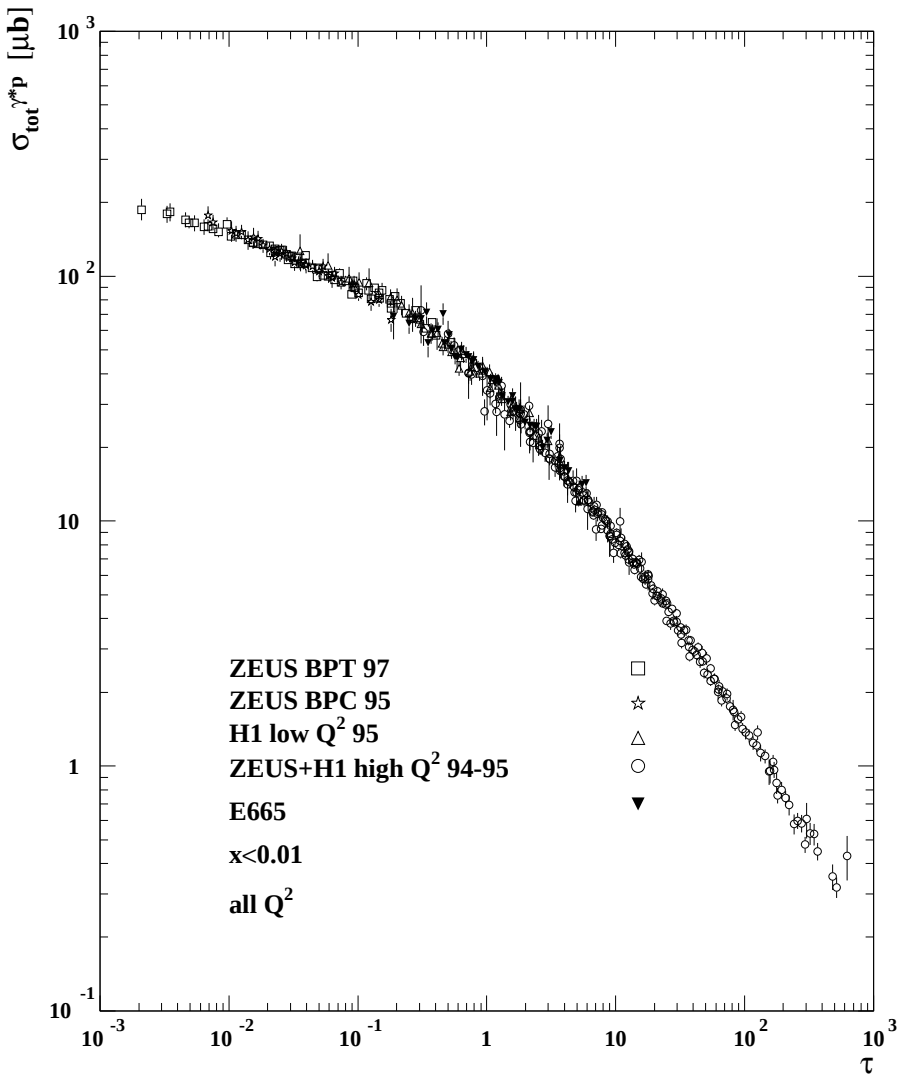

Figure 1: The original geometric scaling observation

must be considered in order to obtain a realistic splitting function for the DGLAP evolution.

Another important small-x effect could be the saturation of the parton distributions. At very high energy (i.e. at very small x) partons must recombine in order to ensure the unitarity of the theory. Both DGLAP and BFKL theories break down in this limit. The DGLAP approach fails because parton recombination is a higher twist effect, while the DGLAP equation is a leading twist result. The BFKL approach fails because it doesn't take in account multiple interactions.

Even if our knowledge of high energy QCD is far from complete, there are some interesting results, namely new evolution equations: the Balitsky/JIMWLK hierarchy [5, 6] and the Balitsky-Kovchegov [5, 7] equation. For large values of Q^2 (say $Q^2 > Q_s^2(x)$, where $Q_s(x)$ is an opportune $x-$dependent saturation scale) these equations reduce to the standard BFKL equation, while in the saturated regime $Q^2 < Q_s^2(x)$ their solutions noticeably differ from the BFKL solution. For what concerns geometric scaling, the key point with these new equations is that in the saturated regime they admit solutions with scaling behaviour.

One may then be tempted to interpret geometric scaling as a manifestation of parton saturation. However at HERA the saturation scale should be at most several GeV^2, while data exhibit scaling behaviour also for Q^2 much larger. Iancu and others [8], using BFKL methods, have shown that geometric scaling is approximatively valid also in the region $1 \lesssim \log(Q^2/Q_s^2) \ll \log(Q_s^2/\Lambda_{QCD}^2)$. This region is usually referred as the "extended geometric scaling region". At HERA a realistic estimate for the saturation scale is $Q_s \sim 2$ GeV, which would imply approximate geometric scaling for $Q^2 < 400$ Gev^2, i.e. for almost all of HERA data considered in [1].

All this seems to suggest that the geometric scaling observation at HERA is in fact a signal of parton saturation. In other words, the small-x HERA dynamics should be determined by saturation effects. But this is at least strange. First of all the derivation in [8] is a fixed coupling one and it doesn't take in account DGLAP evolution (i.e. it doesn't resum large-Q^2 logarithms). It would be astonishing if it would work in such a wide kinematic window (0.05 GeV$^2 < Q^2 < 450$ GeV^2). Furthermore, we do know that the DGLAP theory works very well in most of the geometric scaling window. For instance, the Bjorken scaling violations predicted by the DGLAP theory are clearly visible at HERA. Moreover, the parton distribution functions (PDFs) extracted from HERA data using the DGLAP evolution have been used as input for the calculation of other processes, for example for the Drell-Yan production, and they always led to results in good agreement with phenomenology.
A complete failure of the traditional DGLAP-based perturbative QCD in all the geometric scaling kinematic range seems then if not impossible at least unlikely. Hence the traditional explanation of geometric scaling in terms of saturation only is not fully convincing. In other words, a satisfactory understanding of geometric scaling in still missing.

In order to understand geometric scaling, we have first to study the true evolution in the small x HERA range. From a theoretical point of view, this study is interesting because in this regime we have to deal with a non abelian gauge theory in presence of two large scales (Q^2 and $1/x$) and with a quantum field theory near the unitarity bound. The outcomes of this study are important also from a phenomenological point of view. Consider indeed for instance the parton distribution functions extracted from HERA data. Until now indeed they are extracted using the DGLAP evolution. Hence if in the small x region the real evolution is dominated by saturation effects our HERA small x PDFs are wrong and must be

adjusted. This is not a minor problem, since the HERA PDFs will be used as input at LHC.

Summarizing, it is very important to understand the real small x behaviour of HERA data. The aim of this thesis is exactly to investigate, both from a theoretical and from a phenomenological point of view, the small x HERA region in order to understand the true nature of geometric scaling and hence of the small x evolution.

This thesis will be organised as follows. In the first chapter we will deal with standard QCD evolution equations. We will give a brief derivation of the DGLAP and BFKL equations in the context of DIS and we will revise their standard solutions. We will then show how to improve the DGLAP kernel using the BFKL one and vice versa. Chapter two will be devoted to high energy QCD. We will show that most of the known results in this area can be obtained within the framework of perturbative QCD. Following an approach pioneered by Mueller [21], we will derive the BK equation as a non linear generalization of the BFKL equation. We will then see that the BK equation can predict geometric scaling. In chapter three we will study in detail geometric scaling. First of all we will show that the traditional derivation of geometric scaling has little to do with saturation. Then we will give a derivation of geometric scaling using only the traditional QCD evolution. Finally, we will test our theory on the existing HERA data.

Chapter 1

QCD evolution equations

This first chapter will be devoted to the study of the traditional evolution equations of perturbative QCD, that is to the study of the DGLAP and BFKL equations.
In Sec. 1.1 we will introduce the deep inelastic lepton-hadron scattering (DIS) and the structure functions, just to fix the conventions.
Then in Sec. 1.2 we will review the derivation of the DGLAP equation in the context of DIS. Using the collinear factorization we will show that this equation is nothing but a renormalization group equation. Then we will calculate the leading order kernel of the DGLAP equation and by generalizing this calculation we will give an interpretation of the DGLAP theory in terms of Feynman graphs. We will close the section by quoting one of the standard solution of the DGLAP equation, the double scaling solution.
In Sec. 1.3 we will introduce the k_T factorization and we will use its symmetries to derive the BFKL equation. Then we will sketch out the calculation of the BFKL kernel and show its principal features. We won't go any further in this direction because we will calculate the full BFKL kernel in the next chapter, in the context of the colour dipole approach to DIS. After showing the traditional solutions of the BFKL equation, we will quote the main problems of the BFKL theory. In the next chapters we will show how this problems can be solved (or at least how the theory can be improved).
Sec. 1.4 will be devoted to perturbative resummations. This way we can improve the DGLAP and BFKL theory in order that they are reliable both in the high Q^2 and in the small x region. We will see that these resummations solve most of the problems of the BFKL evolution.

Our exposition will be far from complete, we will limit ourselves to a rapid overview. For a detailed discussion we refer to the literature, for example to [10] and references therein. A good and complete introduction to the BFKL theory in the context of jet physics can be found in [12].

1.1 Deep Inelastic Scattering

Consider the deep inelastic lepton-proton scattering:

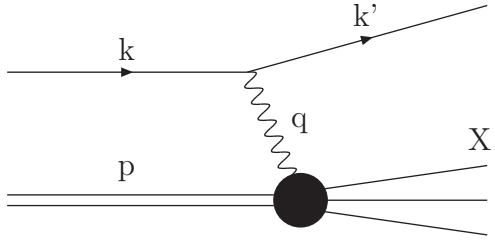

Figure 1.1: Deep Inelastic Scattering

It is customary to parametrize this process in terms of the variables[1]

$$Q^2 \equiv -q^2, \qquad x \equiv \frac{Q^2}{2p \cdot q} = \frac{Q^2}{Q^2 + s}, \tag{1.1}$$

where s is the Mandelstam variable referred to the sub-process $\gamma^* + P \to X$. It is clear from (1.1) that the small x limit corresponds to $s >> Q^2$, while the large x limit corresponds to the soft region, $s \sim 0$.

As long as only photons are exchanged (that is, no parity-breaking electroweak effects are present), the DIS cross section can be written as

$$\frac{d\sigma}{dxdQ^2} = \frac{4\pi\alpha_{em}^2}{Q^4}\left[\left[1 + \left(1 - \frac{q \cdot p}{k \cdot p}\right)^2\right] F_1 + \frac{1}{x}\left(1 - \frac{q \cdot p}{k \cdot p}\right)\left[F_2 - 2xF_1\right]\right]. \tag{1.2}$$

The structure functions $F_i = F_i\left(x, Q^2\right)$ encode all the non trivial information about the proton structure. At the lowest order in the perturbative expansion they obey the Callan-Gross relation $2xF_1 = F_2$. Even if this relation is spoiled by radiative corrections, it is often convenient to introduce the factor $R \equiv F_2/2xF_1 - 1$ and to write the cross section as

$$\frac{d\sigma}{dxdQ^2} = \frac{2\pi\alpha_{em}^2}{Q^4 x}\left[2 - 2\frac{q \cdot p}{k \cdot p} + \left(\frac{q \cdot p}{k \cdot p}\right)^2 \frac{1}{1+R}\right] F_2(x, Q^2). \tag{1.3}$$

[1] We will neglect systematically proton mass

1.2 DGLAP equation

1.2.1 Operator Product Expansion and factorization

One of the most powerful tools of perturbative QCD is the factorization theorem, which states that for a general hard process with incoming hadrons all the non-perturbative effects can be factored out into universal (i.e. process-independent) parton distribution functions.

To see how this work in DIS, we first have to write down the cross section (1.2) as $\sigma \propto L_{\mu\nu}W^{\mu\nu}$, that is to split the cross section into a leptonic part $L_{\mu\nu} = 4e^2\left(k_\mu k'_\nu + k'_\mu k_\nu - g_{\mu\nu}k\cdot k'\right)$, fully determined from QED, and a hadronic part $W^{\mu\nu} = 1/(4\pi)\int d^4x e^{iq\cdot x}\langle P|J^\mu(0)J^\nu(x)|P\rangle$, where P is the proton state and J^μ the electromagnetic current.
Following (1.2) we can parametrize the hadronic tensor as

$$W^{\mu\nu} = \left(-g^{\mu\nu} + \frac{q^\mu q^\nu}{q^2}\right)F_1 + \left(p^\mu - q^\mu\frac{p\cdot q}{q^2}\right)\left(p^\nu - q^\nu\frac{p\cdot q}{q^2}\right)\frac{F_2}{p\cdot q}. \tag{1.4}$$

Recalling the Callan-Gross relation $F_2 = 2xF_1$, we may introduce a longitudinal structure function $F_L = F_2 - 2xF_1$ and rewrite Eq. (1.4) as:

$$W^{\mu\nu} = \frac{F_L}{2x}\, e_L^{\mu\nu} + \frac{F_2}{2x}\, e_2^{\mu\nu}, \tag{1.5}$$

with

$$\begin{aligned} e_L^{\mu\nu} &= g^{\mu\nu} - \frac{q^\mu q^\nu}{q^2} \\ e_2^{\mu\nu} &= -g^{\mu\nu} - \frac{2x}{q^2}\left(p^\mu q^\nu + p^\nu q^\mu\right) - \frac{4x^2}{q^2}p^\mu p^\nu. \end{aligned} \tag{1.6}$$

$F_2/2x$ and $F_L/2x$ can be extracted from W by the mean of the projectors:

$$\Omega_2^{\mu\nu} = -\frac{1}{2}g^{\mu\nu} + \frac{3x}{p\cdot q}\, p^\mu p^\nu, \qquad \Omega_L^{\mu\nu} = \frac{Q^2}{(p\cdot q)^2}p^\mu p^\nu. \tag{1.7}$$

Using the optical theorem, we can relate the hadronic tensor to the imaginary part of the forward Compton scattering, that is

$$W^{\mu\nu} = \frac{1}{2\pi}\,\mathbf{Im}\int d^4x e^{iq\cdot x}\,\langle P|T\left(J^\mu(0)J^\nu(x)\right)|P\rangle \equiv \frac{1}{2\pi}\,\mathbf{Im}\,\langle P\,|T^{\mu\nu}|\,P\rangle\,. \tag{1.8}$$

The time ordered product of the two electromagnetic currents can be Wilson expanded. We may categorize the operators that contribute to this operator product expansion (OPE) according to the irriducible representation of the Lorentz group to which they belong, that is according to their spin. We can then write the Wilson expansion as

$$T^{\mu\nu} = \int d^4x e^{iq\cdot x}T\left(J^\mu(x)J^\nu(0)\right) \sim \sum_s C^{\mu\nu}_{\mu_1\mu_2\ldots\mu_s}(q)\;\mathcal{O}^{\mu_1\mu_2\ldots\mu_s}, \tag{1.9}$$

where $\mathcal{O}^{\mu_1\cdots\mu_s}$ is symmetric and traceless (that is it is an operator with spin s). In Eq. (1.9) "$\sim$" means that this expansion is valid for all matrix elements, provided q is much larger than the characteristic momentum in any of the external states. Having in mind (1.5), we parametrize the expansion (1.9) as

$$\sum_s C^{\mu\nu}_{\mu_1\mu_2\ldots\mu_s}(q)\ \mathcal{O}^{\mu_1\mu_2\ldots\mu_s} = \sum_s \left[\left(g^{\mu\nu} - \frac{q^\mu q^\nu}{q^2}\right) q_{\mu_1} q_{\mu_2} C_s^L + (-g^{\mu\nu} q_{\mu_1} q_{\mu_2} + \right.$$
$$\left. - g^\mu_{\ \mu_1} g^\nu_{\ \mu_2} q^2 + q^\mu g^\nu_{\ \mu_1} q_{\mu_2} + q^\nu g^\mu_{\ \mu_1} q_{\mu_2}\right) C_s^{(2)}\Big] q_{\mu_3}\ldots q_{\mu_s} \left(\frac{2}{Q^2}\right)^s \mathcal{O}^{\mu_1\mu_2\ldots\mu_s}. \quad (1.10)$$

In order to obtain a result for W, we have to evaluate the matrix element of $\mathcal{O}$ on the proton state. This matrix element can depend only on the proton momentum p, that is

$$\langle P\,|\mathcal{O}^{\mu_1\mu_2\ldots\mu_s}|\,P\rangle = 2A_s\left(p^2\right) p^{\mu_1} p^{\mu_2}\ldots p^{\mu_s}, \quad (1.11)$$

where the factor 2 is for future convenience.
Using Eq. (1.10) and (1.11) we then obtain

$$\langle P\,|T^{\mu\nu}|\,P\rangle = \sum_s \left(\frac{1}{x}\right)^s \left(2A_s\left(p^2\right) C_s^L\left(Q^2\right) e_L^{\mu\nu} + 2A_s\left(p^2\right) C_s^{(2)}\left(Q^2\right) e_2^{\mu\nu}\right). \quad (1.12)$$

Let us now discuss the contribution of an operator of dimension d and spin s to this expansion. From Eq. (1.11) it follows that the coefficient A_s has dimension $[A] = d_\mathcal{O} - s - 2$. Since $\langle P\,|T^{\mu\nu}|\,P\rangle$ is dimensionless, this implies that C_s has dimension $[C] = -d_\mathcal{O} + s + 2$. In other words, the contribution of the operator $\mathcal{O}^{\mu_1\cdots\mu_s}$ is of order

$$\left\langle P\left|C^{\mu\nu}_{\mu_1\mu_2\ldots\mu_s}(Q)\ \mathcal{O}^{\mu_1\mu_2\ldots\mu_s}\right|P\right\rangle \sim \left(\frac{1}{x}\right)^s \left(\frac{m_P}{Q}\right)^{d_\mathcal{O}-s-2} \equiv \left(\frac{1}{x}\right)^s \left(\frac{m_P}{Q}\right)^{t-2}, \quad (1.13)$$

where we have introduced the *twist* $t = d - s$.
In the deep inelastic region, $Q^2 \to \infty$, we can consider only small-twist operators, the others being suppressed by powers of $1/Q$. This approximation is usually referred as the leading twist approximation. In our case the operators with lowest possible twist are:

$$\mathcal{O}_f^{\mu_1\mu_2\mu_3\ldots\mu_s} = \overline{\psi}_f \gamma^{\mu_1}\ iD^{\mu_2}\ iD^{\mu_3}\ \ldots\ iD^{\mu_s}\psi_f - \text{traces} \quad (1.14)$$
$$O_g^{\mu_1\mu_2\mu_3\ldots\mu_s} = F_a^{\mu_1\nu}\ iD^{\mu_2} iD^{\mu_3}\ \ldots\ iD^{mu_{s-1}}\ F_{a\ \nu}^{\mu_s} - \text{traces}, \quad (1.15)$$

where the symmetrization is implicit. Here f is a flavour index, a is a colour index and D is the covariant derivative.

Let us now see how all of this can be related W, that is to the structure functions F. For definiteness we will focus on F_2, that is we will consider $T_2 \equiv \Omega_2^{\mu\nu}\langle T_{\mu\nu}\rangle$. From Eq. (1.12) we obtain

$$T_2 = \sum_s \left(\frac{1}{x}\right)^s 2C_s A_s, \quad (1.16)$$

where we have dropped the index 2 in C in order to shorten the notation. Using the Cauchy's theorem we can extract $C_k A_k$:

$$C_k A_k = \frac{1}{2\pi} \mathbf{Im} \int_0^1 dx T_2(x) x^{k-2}. \tag{1.17}$$

But recalling Eq. (1.8) this implies

$$C_k A_k = \int_0^1 dx F_2(x) x^{k-2} = \int_0^1 dx \frac{F_2(x)}{x} x^{k-1} \equiv \mathcal{M}\left[F_2/x\right](k), \tag{1.18}$$

that is $C_j A_j$ are related to F_2 by Mellin transform[2] .

Introducing

$$\begin{aligned} C_f(x,Q^2) &\equiv \int_{c-i\infty}^{c+i\infty} \frac{dN}{2\pi i} x^{-N} C_N^f(Q^2) \\ q_f(x,Q^2) &\equiv \int_{c-i\infty}^{c+i\infty} \frac{dN}{2\pi i} x^{-N} A_N^f(Q^2) \end{aligned} \tag{1.19}$$

and using the Laplace convolution theorem we obtain

$$F_2(x,Q^2) = x \sum_{i=1}^{n_f} C_i \otimes (q_i + \bar{q}_i) + C_g \otimes g, \tag{1.20}$$

$$[f \otimes g](x) \equiv \int_x^1 \frac{dy}{y} f\left(\frac{x}{y}\right) g(y),$$

where n_f is the number of active flavours.

Equation (1.20) express the factorization theorem. The *parton distribution functions* q_i, g are target dependent and are not perturbative quantities. As their name suggests, they represent (at least at the lowest order in the perturbative expansion) the probability density of finding a parton with momentum xp in a proton with momentum p.
The *coefficient functions* C_i are target independent and can be calculated in ordinary perturbative QCD, for example with DIS on parton. At leading order we have

$$C_i(x,Q^2) = e_i^2 \delta(1-x), \quad C_g(x,Q^2) = 0, \tag{1.21}$$

where e_i is the carge of the flavour i. It is always possible to choose a scheme such that (1.21) are true at all order in perturbation theory. In such schemes we can then write

$$F_2(x,Q^2) = x \sum e_i^2 \left(q_i(x,Q^2) + \bar{q}_i(x,Q^2)\right). \tag{1.22}$$

[2]The Mellin transform is nothing but a Laplace transform with respect to the variable $\xi = \log(1/x)$.

1.2.2 Renormalization group and DGLAP equation

Although the partonic distribution functions are essentially non perturbative quantities, it is possible to calculate their dependence on the energy scale using the renormalization group.

To simplify the notation, we suppose there is only one flavour. Suppose there is a typical energy scale, say a renormalization scale μ. Then $C_j = C_j\left(Q^2/\mu^2, \alpha_s(\mu^2)\right)$ and $A_j = A_j\left(\alpha_s(\mu^2)\right)$. Since F_2 is an observable, it can't depend on the renormalization scale, that is $\mu^2 \frac{d}{d\mu^2} F_2(Q^2/\mu^2, \mu^2) \equiv 0$. This in turn implies

$$0 \equiv \mu^2 \frac{d}{d\mu^2}\left(C_j\left(Q^2/\mu^2, \alpha_s(\mu^2)\right) A_j\left(\alpha_s(\mu^2)\right)\right);$$

$$\frac{1}{C_j}\mu^2 \frac{d}{d\mu^2} C_j = -\frac{1}{A_j}\mu^2 \frac{d}{d\mu^2} A_j \equiv -\gamma_j\left(\alpha_s(\mu^2)\right). \tag{1.23}$$

Since C_j is a perturbative quantity, the *anomalous dimension* γ must be perturbative too. Thus the logarithmic derivative with respect to μ^2 of A_j is a perturbative quantity, even if A_j are target-dependent and essentially non perturbative. We have the main result

$$\mu^2 \frac{d}{d\mu^2} A_j(\mu^2) = \gamma_j\left(\alpha_s(\mu^2)\right) A_j(\mu^2). \tag{1.24}$$

Introducing $t = \log\left(Q^2/\Lambda^2_{QCD}\right)$ Eq. (1.24) is rewritten as

$$\frac{d}{dt} A_j(Q^2) = \gamma_j\left(\alpha_s(t)\right) A_j(Q^2). \tag{1.25}$$

The general solution of (1.25) is

$$A_j(Q^2) = A_j(\mu^2) \exp\left(\int_{\alpha_s(\mu^2)}^{\alpha_s(Q^2)} dz \frac{\gamma_j(z)}{\beta(z)}\right) \equiv \Gamma_j(Q^2, \mu^2) A_j(\mu^2), \tag{1.26}$$

where β is the usual QCD β-function, that is $\frac{d}{dt}\alpha_s(t) = \beta\left(\alpha_s(t)\right)$. Similarly one can obtain

$$C_j\left(Q^2/\mu^2, \alpha_s(\mu^2)\right) = C_j\left(1, \alpha_s(Q^2)\right) \Gamma_j(Q^2, \mu^2) \tag{1.27}$$

In general then we can rewrite (1.18) as

$$\int_0^1 dx x^{n-2} F_2(x, Q^2) = \left[C_n\left(1, \alpha_s(Q^2)\right) \Gamma_n(Q^2, \mu^2)\right] A_n(\mu^2), \tag{1.28}$$

where we have separated the perturbative part (in square bracket) from the non perturbative one.

When more than one flavour is active (1.25) becomes a matrix equation, which can be written as

$$\frac{d}{dt}\begin{pmatrix} g(N,t) \\ q_i(N,t) \end{pmatrix} = \alpha_s(t)\begin{pmatrix} \gamma\left(N,\alpha_s(t)\right)_{gg} & \gamma\left(N,\alpha_s(t)\right)_{gq_j} \\ \gamma\left(N,\alpha_s(t)\right)_{q_ig} & \gamma\left(N,\alpha_s(t)\right)_{q_iq_j} \end{pmatrix}\cdot\begin{pmatrix} g(N,t) \\ q_j(N,t) \end{pmatrix}, \tag{1.29}$$

where we put $q_i(N,t) \equiv A_N^i(t)$.
Eq. (1.29) is the celebrated Dokshitzer-Gribov-Lipatov-Altarelli-Parisi (DGLAP) equation in Mellin space.

Defining the *splitting function* $P(x,\alpha_s(t))$ as the inverse Mellin transform of the anomalous dimension,

$$P\left(x,\alpha_s(t)\right) \equiv \frac{1}{2\pi i}\int_{c-i\infty}^{c+i\infty} x^{-n}\gamma\left(N,\alpha_s(t)\right)dN, \tag{1.30}$$

we obtain the DGLAP equation in coordinate space:

$$\frac{d}{dt}\begin{pmatrix} g(x,t) \\ q_i(x,t) \end{pmatrix} = \alpha_s(t)\begin{pmatrix} P\left(\alpha_s(t)\right)_{gg} & P\left(\alpha_s(t)\right)_{gq_j} \\ P\left(\alpha_s(t)\right)_{q_ig} & P\left(\alpha_s(t)\right)_{q_iq_j} \end{pmatrix}\otimes\begin{pmatrix} g(t) \\ q_j(t) \end{pmatrix}. \tag{1.31}$$

1.2.3 The LO solution of the DGLAP equation

In this section we will derive the leading order expression of the evolution factor Γ in Eq. (1.26). From this solution we will see that the DGLAP equation at this order resums all the logarithmic terms of the form $\alpha_s \log\left(Q^2/\mu^2\right)$.

Our starting point is just Eq. (1.28). Since $\gamma(j)$ is target-independent, we can evaluate it with DIS on parton. Our normalizations were chosen such that $A_j(p^2) = 1$ on parton state, hence for a partonic process Eq. (1.28) becomes:

$$\int_0^1 dx x^{n-2}\hat{F}_2(x,Q^2) = C_n\left(1,\alpha_s(Q^2)\right)\Gamma_n\left(Q^2,\mu^2\right), \tag{1.32}$$

where the hat is a reminder that we are dealing with partons.
The functions $\gamma_N(\alpha_s)$, $\beta(\alpha_s)$ and $C_N(1,\alpha_s)$ admit a perturbative expansion. At leading order we can write

$$\begin{aligned} &\gamma_N(\alpha_s) = \gamma_0(N) + O(\alpha_s^2), \qquad \beta(\alpha_s) = -\beta_0\alpha_s^2 + O(\alpha_s^3) \\ &C_N\left(1,\alpha_s\right) = C_0(N) + C_1(N)\alpha_s + O(\alpha_s^2). \end{aligned} \tag{1.33}$$

This in turn implies that at this level of accuracy we can write

$$\begin{aligned} &\Gamma_N\left(Q^2,\mu^2\right) = \exp\left(\int_{\alpha_s(\mu^2)}^{\alpha_s(Q^2)}\frac{\gamma_N(z)}{\beta(z)}dz\right) = \\ &= \left(\frac{\alpha_s(Q^2)}{\alpha_s(\mu^2)}\right)^{-\gamma_0(N)/\beta_0} = \left(1+\beta_0\alpha_s(Q^2)\log\left(\frac{Q^2}{\mu^2}\right)\right)^{\gamma_0(N)/\beta_0}. \end{aligned} \tag{1.34}$$

From this equation it is clear that at this order the DGLAP equation resums all the logarithms of the form $\left(\alpha_s(Q^2)\log\left(\frac{Q^2}{\mu^2}\right)\right)^k$, that is it resums all the leading logarithms (LL) of Q^2. It is easy to see that at NL the DGLAP equation resums the NLL terms $\alpha_s\left(\alpha_s(Q^2)\log\left(\frac{Q^2}{\mu^2}\right)\right)^k$ and so on.

Consider again Eq. (1.34). If we consider only the LO (and not the LL) approximation, that is if we don't consider the $\log Q^2$ resummation, we can write:

$$\Gamma_N\left(Q^2,\mu^2\right) = 1 + \gamma_0(N)\alpha_s\log\left(\frac{Q^2}{\mu^2}\right) + O(\alpha_s^2). \tag{1.35}$$

But this and Eq. (1.27) imply

$$C_N\left(Q^2/\mu^2,\alpha_s(\mu^2)\right) = \left(C_0(N) + \alpha_s(Q^2)C_1(N)\right)\left(1 + \gamma_0(N)\alpha_s(Q^2)\log\frac{Q^2}{\mu^2}\right) =$$

$$= C_0(N)\left(1 + \alpha_s\gamma_0(N)\log\frac{Q^2}{\mu^2}\right) + O(\alpha_s^2). \tag{1.36}$$

If we Mellin-antitransform this last equation we obtain

$$C\left(x,Q^2/\mu^2,\alpha_s\right) = C_0(x) + \alpha_s C_0 \otimes P_0\log\left(\frac{Q^2}{\mu^2}\right). \tag{1.37}$$

If we replace C_0 with its actual expression $C_0 = e^2\delta(1-x)$ we obtain:

$$C\left(x,Q^2/\mu^2,\alpha_s\right) = e^2\left(\delta(1-x) + \alpha_s P_0(x)\log\left(\frac{Q^2}{\mu^2}\right)\right). \tag{1.38}$$

But $C\left(x,Q^2/\mu^2,\alpha_s\right)$ is just $\hat{F}_2/x$, that is the partonic structure function. Then if we consider DIS on parton and we calculate $\hat{F}_2$, the coefficient of the logarithmic term $\log\left(Q^2/\mu^2\right)$ gives us the leading order splitting function. In the following section we will do exactly this calculation.

1.2.4 The LO splitting functions

As we have said in the previous section, to calculate the LO splitting functions all we have to do is to consider DIS on parton at $O(\alpha_s)$ (which is a perturbative process) and to pick up the coefficient of the logarithm $\log\left(Q^2/\mu^2\right)$. Logarithmic terms of this form can be produced within the framework of Feynman graphs in two ways: either by loop integrals or by phase space integrals. Tree level diagrams and loop corrections have the same kinematic structure, so their contribution to the splitting functions will be a trivial one (nonetheless they are important, since they are necessary to regularize the infrared divergences at $x \to 1$). The truly interesting part will come from phase space integrals, that is from real emission.

To see how this machinery works let us consider partonic DIS with one gluon emission. In order to obtain (1.38) we have to evaluate the two Feynman graphs

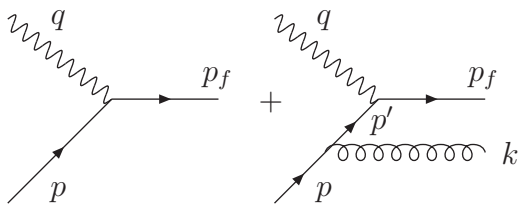

Figure 1.2: Real gluon emission in partonic DIS

in Fig. (1.2).
Consider first the diagram on the left. A straightforward calculation leads to

$$W_0^{\mu\nu} = \frac{1}{4\pi} 4e^2 \left(p^\mu p_f^\nu + p^\nu p_f^\mu - g^{\mu\nu} p \cdot p_f \right) \frac{(2\pi)^4 \delta(p + q - p_f)}{(2\pi)^3 \; 2E_f}. \tag{1.39}$$

In this case $x = 1$. Indeed

$$x = -\frac{q^2}{2p \cdot q} = -\frac{q^2}{(p+q)^2 - q^2} = \frac{q^2}{q^2 - p_f^2} = \frac{q^2}{q^2} = 1. \tag{1.40}$$

This condition must be enforced by $\delta(E_f - E_i)$. Using the relation

$$\frac{dx}{dE_f} = \frac{E_f}{p \cdot q} \tag{1.41}$$

we may write

$$\frac{\delta(E_f - E_i)}{E_f} = \frac{\delta(x-1)}{E_f \; dE_f/dx} = \frac{\delta(x-1)}{p \cdot q}. \tag{1.42}$$

Then Eq. (1.39) can be rewritten as:

$$W_0^{\mu\nu} = e^2 \left(p^\mu p_f^\nu + p^\nu p_f^\mu - g^{\mu\nu} p \cdot p_f \right) \frac{\delta(1-x)}{p \cdot q}. \tag{1.43}$$

From this it immediately follows (see (1.7)):

$$\Omega_L^{\mu\nu} W_{\mu\nu} = 0 \longrightarrow F_L = 0 \qquad \text{(Callan-Gross relation)} \tag{1.44}$$

$$\Omega_2^{\mu\nu} W_{\mu\nu} = \frac{1}{2} e^2 \delta(1-x) \longrightarrow \frac{\hat{F}_2}{x} = C_2 = e^2 \delta(1-x), \tag{1.45}$$

in agreement with (1.21).

Consider now the real gluon emission. It is convenient to introduce the Sudakov parametrization, that is

$$p = (P, 0, 0, P), \quad \eta = \frac{1}{4P}(1, 0, 0, -1), \quad k = (1-z)p + \mathbf{k}_T + y\eta, \tag{1.46}$$

where $\mathbf{k}_T = (0, k_x, k_y, 0)$ and y is fixed by the mass-shell condition $0 = k^2 = -\mathbf{k}_T^2 + (1-z)y$. In this parametrization $p' = p - k = zp - \mathbf{k}_t - y\eta$ and $p'^2 = -\mathbf{k}_T^2/(1-z)$, while the invariant phase space is

$$\frac{d^3k}{(2\pi)^3 2k^0} = \frac{1}{(2\pi)^3}\frac{d^2\mathbf{k}_T\ p\ dz}{2(1-z)p + y/(2p)}. \tag{1.47}$$

Logarithmic singularities can arise only from the quark propagator going on-shell (we are neglecting quark masses). So we are interested in the collinear region, that is in the limit $\mathbf{k}_t \to 0$, $y \to 0$. In this limit we can rewrite the phase space as

$$\frac{d^3k}{2(2\pi)^3 k^0} \approx \frac{d^2\mathbf{k}_T}{2(2\pi)^3}\frac{dz}{1-z}. \tag{1.48}$$

Since in the propagator we have an "almost-real" quark, we may use the Weizsäcker-Williams approximation:

$$i\frac{\not{p}'}{p'^2} = i\sum_{pol}\frac{u(p')\bar{u}(p')}{p'^2} + O(\mathbf{k}_T^2). \tag{1.49}$$

Consider now the matrix element for the process $p + \gamma^* \to k + p_f$. Using (1.49) we can split the squared amplitude:

$$|\mathcal{M}_{p+\gamma^*\to p_f+k}|^2 \approx |\mathcal{M}_{p'+\gamma*\to p_f}|^2\frac{1}{p'^4}|\mathcal{M}_{p\to k+p'}|^2, \tag{1.50}$$

where we have neglected terms which don't give birth to logarithms. In this approximation we can write

$$\begin{aligned} W_1 = &\left(\frac{d^3p_f}{(2\pi)^3\ 2E_f}\left|\mathcal{M}_{p'+\gamma^*\to p_f}\right|^2(2\pi)^4\delta(P_i - P_f\right)\cdot \\ &\cdot\left(\frac{d^2\mathbf{k}_T}{2(2\pi)^3}\frac{dz}{1-z}\left|\mathcal{M}_{p\to k+p'}\right|^2\frac{1}{p'^4}\right). \end{aligned} \tag{1.51}$$

Consider for the moment the first line only. With the replacement $p' \to p$ this is exactly like W_0. Let us then discuss the effects of p'. First of all, it changes the kinematics. In this case indeed we have

$$x = -\frac{q^2}{2p\cdot q} = -\frac{q^2}{2/z\ p'\cdot q} = -z\frac{q^2}{2p'\cdot q} = z, \tag{1.52}$$

hence we will have $\delta(x-z)$. Then $W^{\mu\nu}$ becomes:

$$\begin{aligned} W^{\mu\nu}_{p'+\gamma^*\to p_f} &= e^2\left(p'^\mu p_f^\nu + p'^\nu p_f^\mu - g^{\mu\nu}p'\cdot p_f\right)\frac{\delta(z-x)}{p\cdot q} = \\ &= z\ e^2\left(p^\mu p_f^\nu + p^\nu p_f^\mu - g^{\mu\nu}p\cdot p_f\right)\frac{\delta(z-x)}{p\cdot q}. \end{aligned} \tag{1.53}$$

This implies that the LO coefficient C_2 can be written as

$$C_2(x) = e^2 \left(\delta(1-x) + \int dz \left(\frac{d^2\mathbf{k}_T}{2(2\pi)^3} \frac{1}{1-z} \left| \mathcal{M}_{p\to k+p'} \right|^2 \frac{1}{p'^4} \right) (z\ \delta(x-z)) \right) = \\ = e^2 \left(\delta(1-x) + \left[\frac{d^2\mathbf{k}_T}{2(2\pi)^3} \frac{x}{1-x} \left| \mathcal{M}_{p\to k+p'} \right|^2 \frac{1}{p'^4} \right] \right). \quad (1.54)$$

Consider now the term between the square brackets. Extracting the g_s^2 term from the amplitude and recalling that in our parametrization $p'^2 = -k_T^2/(1-x)$ we obtain

$$\left[\frac{d^2\mathbf{k}_T}{2(2\pi)^3} \frac{x}{1-x} \left| \mathcal{M}_{p\to k+p'} \right|^2 \frac{1}{p'^4} \right] = \frac{g_s^2}{16\pi^2} \int \frac{dk_T^2}{k_T^2} \frac{x(1-x)}{k_T^2} \left| \mathcal{M}_{p\to k+p'} \right|^2. \quad (1.55)$$

Assume now that $|\mathcal{M}|^2/k_T^2$ is independent on k_T. Then Eq. (1.55) becomes

$$\left[\frac{d^2\mathbf{k}_T}{2(2\pi)^3} \frac{x}{1-x} \left| \mathcal{M}_{p\to k+p'} \right|^2 \frac{1}{p'^4} \right] = \alpha_s \left(\frac{x(1-x)}{4\pi k_T^2} \left| \mathcal{M}_{p\to k+p'} \right|^2 \right) \log \left(\frac{Q^2}{\mu^2} \right), \quad (1.56)$$

where μ^2 is an infrared regulator. But now from Eq. (1.56), (1.54) and (1.38) it follows that[3]

$$P_0(x) = \frac{x(1-x)}{4\pi k_T^2} \left| \mathcal{M}_{p\to k+p'} \right|^2. \quad (1.57)$$

This argument can be easily generalized to the case of more than one flavour. In this case we have four splitting functions, one for each sub-process shown in Fig. 1.3. The origin of the name *splitting functions* is then clear: $P_{j\leftarrow i} \equiv P_{ji}$ express somehow the probability for a parton i to splitting into a parton j.

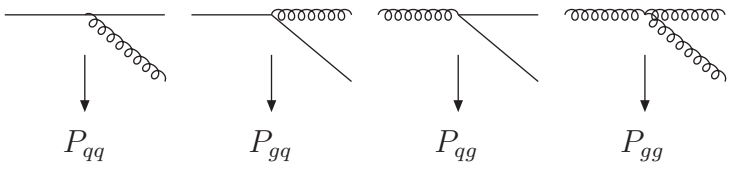

Figure 1.3: Leading order contribution to the splitting functions

[3]In fact, this splitting function is correct only if $x < 1$, i.e. it is not infrared safe. In order to obtain the true infrared regularised splitting function we have to evaluate also the virtual diagrams.

At LO one obtain [2]:

$$P_{qq}^0(x) = C_F \left[\frac{1+x^2}{(1-x)_+} + \frac{3}{2}\delta(1-x) \right], \quad C_F = \frac{4}{3} \tag{1.58}$$

$$P_{qg}^0(x) = T_R \left[x^2 + (1-x)^2 \right], \quad T_R = \frac{1}{2} \tag{1.59}$$

$$P_{gq}^0(x) = C_F \left[\frac{1+(1-x)^2}{x} \right] \tag{1.60}$$

$$P_{gg}^0(x) = 2N_c \left[\frac{x}{(1-x)_+} + \frac{1-x}{x} + x(1-x) \right] + \delta(1-x)\frac{11N_c - 4n_f T_R}{6}. \tag{1.61}$$

Note that only gluon entries are singular as $x \to 0$.

1.2.5 Feynman graphs interpretation of the LL series

We can think at the LL DGLAP evolution as a geometrical series in terms of Feynman graphs. For simplicity, we will deal only with real gluon emission.

We saw that a term $\alpha_s \log\left(\frac{Q^2}{\mu^2}\right)$ is produced by the process in Fig. (1.3a). At the same way we can produce all the logarithms $\left(\alpha_s \log\left(\frac{Q^2}{\mu^2}\right)\right)$ by iterating this mechanism, that is we can obtain the leading log series by the *gluon ladder* shown in Fig. 1.4.

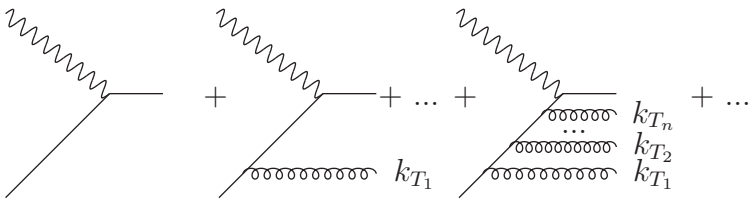

Figure 1.4: Gluon ladder

The LL series is then produced by the phase-space integrals

$$\int_{\mu^2}^{Q^2} \frac{dk_{T_n}^2}{k_{T_n}^2} \int_{\mu^2}^{k_{T_n}^2} \frac{dk_{T_{n-1}}^2}{k_{T_{n-1}}^2} \ldots \int_{\mu^2}^{k_{T_3}^2} \frac{dk_{T_2}^2}{k_{T_2}^2} \int_{\mu^2}^{k_{T_2}^2} \frac{dk_{T_1}^2}{k_{T_1}^2} = \frac{1}{n!} \log^n \left(\frac{Q^2}{\mu^2}\right). \tag{1.62}$$

Note that the LL series is generated only if $k_{T_1} \ll k_{T_2} \ll \ldots \ll k_{T_n}$, otherwise k_{T_1} would act as an ultraviolet cut-off and no large logarithms would be produced. In order to see this, consider just two gluon emission. The first quark propagator has an off-shellness equal to $-k_{T_1}^2/(1-x_1)$, while the second equal to $-(\mathbf{k}_{T_1} + \mathbf{k}_{T_2})^2/(1-x_2)$. Hence we have the factors

$$\int \frac{dk_{T_2}^2}{(\mathbf{k}_{T_1} + \mathbf{k}_{T_2})^2} \frac{dk_{T_1}^2}{k_{T_1}^2}. \tag{1.63}$$

From this it is clear that only if $k_{T_2} \gg k_{T_1}$ we have the logarithmic structure as in Eq. (1.62). This argument can be easily generalized to multiple emissions.

Consider now the first step of the ladder, $k_{T_1} = \mu$. It is just the factorization scale. Above this scale we have factorization and perturbative DGLAP equation. Non perturbative effects enter trivially, just as boundary condition. Under this scale instead there are all the non trivial non perturbative phenomena that determine the parton distribution functions.

Since the intermediate quarks are increasingly virtual as we go up the ladder, one can interpret them as components of the proton when this is probed at successively higher scales. In other words, an intermediate quark with $k_T^2 \approx Q^2$ can be thought of as a constituent of the proton made visible when the wave function of the proton is analysed with a resolution $\Delta x \sim 1/Q^2$. In this picture, the proton seen at one scale can be resolved at a finer scale into a more virtual quark and a number of gluons.

In this picture we can derive the DGLAP equation in an intuitive way. Assume indeed to consider the quark distribution at some scale Q^2 and then to slightly increase Q^2 to $Q^2 + \Delta Q^2$. This opens up a new region of phase space for the emission of a quark with transverse momentum $Q^2 < k_T^2 < Q^2 + \Delta Q^2$. This quark can be emitted both from a quark and a from gluon, with probabilities respectively equal to $\alpha_s P_{qq}(z)\Delta Q^2/Q^2$ and $\alpha_s P_{qg}(z)\Delta Q^2/Q^2$. But then at this scale we may write

$$\begin{aligned} & q\left(x, Q^2 + \Delta Q^2\right) - q\left(x, Q^2\right) = \\ & = \alpha_s \frac{\Delta Q^2}{Q^2} \int_0^1 dx' \int_0^1 dz \left(P_{qq}(z) q(x', Q^2) + P_{qg}(z) g(x', Q^2)\right) \delta(x - x'z) = \\ & = \alpha_s \frac{\Delta Q^2}{Q^2} \int_x^1 \frac{dz}{z} \left(P_{qq}(z) q\left(\frac{x}{z}, Q^2\right) + P_{qg}(z) g\left(\frac{x}{z}, Q^2\right)\right), \end{aligned} \tag{1.64}$$

which in the limit $\Delta Q^2 \to 0$ reduces to

$$Q^2 \frac{d\, q(x, Q^2)}{dQ^2} = \alpha_s \int_x^1 \frac{dz}{z} \left(P_{qq}(z) q\left(\frac{x}{z}, Q^2\right) + P_{qg}(z) g\left(\frac{x}{z}, Q^2\right)\right), \tag{1.65}$$

i.e. to the (fixed coupling) evolution equation for q.

1.2.6 The double scaling solution

In order to see how the DGLAP equation works in practice, in this section we will derive one of its standard solutions, the double scaling solution. This is a solution valid in the region of large Q^2 and small x, that is it may be valid in the kinematic window of geometric scaling.

We start from the expression

$$F_2(x, Q^2) = x \sum_{i=1}^{n_f} e_i^2 \left(q_i(x, Q^2) + \overline{q}_i(x, Q^2)\right). \tag{1.66}$$

It is convenient to introduce the singlet and non singlet quark distributions, defined respectively as

$$q_S \equiv \sum_{i=1}^{n_f} (q_i + \bar{q}_i), \qquad q_{NS} \equiv \sum_{i=1}^{n_f} \left(\frac{e_i^2}{\langle e^2 \rangle} - 1 \right) (q_i + \bar{q}_i), \tag{1.67}$$

where $\langle e^2 \rangle \equiv \frac{1}{n_f} \sum_{i=1}^{n_f} e_i^2$.
Then Eq. (1.66) becomes

$$F_2(x,t) = \langle e^2 \rangle \, x \, (q_S(x,t) + q_{NS}(x,t)), \tag{1.68}$$

while the DGLAP equation (1.31) becomes

$$\frac{d}{dt} \begin{pmatrix} g \\ q_S \end{pmatrix} = \alpha_s(t) \begin{pmatrix} P_{gg} & P_{gq} \\ P_{qg} & P_{qq}^S \end{pmatrix} \otimes \begin{pmatrix} g \\ q_S \end{pmatrix}, \tag{1.69}$$

$$\frac{d}{dt} q_{NS} = \alpha_s(t) P_{qq} \otimes q_{NS}. \tag{1.70}$$

In order to find the solution to these equations, it is convenient to work in the N-Mellin space. In this space indeed the leading order solution for a generic parton distribution $p(N,T)$ is just

$$p(N,t) = p(N,t_0) e^{\frac{1}{\beta_0} \gamma(N) \zeta}, \tag{1.71}$$

with $\zeta \equiv \log(t/t_0)$. If we want the solution in the x space, we must antitransform Eq. (1.71):

$$p(x,t) = \int_{c-i\infty}^{c+i\infty} \frac{dN}{2\pi i} e^{\xi N} p(N,t), \tag{1.72}$$

where $\xi = \log(1/x)$.

Assume for the moment that all the singularities of the initial condition $p(N,t_0)$ are to the left of those of $\gamma(N)$ (which are always poles on the real axis at non-positive integer values of N). Then at small x, i.e. at large ξ, the integral may be evaluated by the saddle point method, with the saddle point condition

$$\xi_s + \frac{1}{\beta_0} \frac{d\gamma}{dN} \zeta = 0. \tag{1.73}$$

We may thus obtain the leading small x behaviour of the DGLAP equation by expanding the matrix of the anomalous dimensions around its rightmost singularity, determining the corresponding splitting functions by inverse Mellin transformation, and then solving the resulting simplified DGLAP equation. It is convenient to work with new parton distribution defined as $Q \equiv xq$, $G \equiv xg$. Because of the x factor the anomalous dimensions associated to Q and G are not the same as the ones associated to q and g. However it is trivial to obtain the relation between γ_{AB} and γ_{ab}:

$$\gamma_{AB}(N) = \gamma_{ab}(N+1), \tag{1.74}$$

where $A, B = Q, G$ and $a, b = q, g$.

Expanding the LO anomalous dimensions γ_{AB} obtained from the splitting functions (1.58) we obtain:

$$\gamma_S(N) = \frac{1}{N}\begin{pmatrix} 2C_A & 2C_F \\ 0 & 0 \end{pmatrix} + \begin{pmatrix} \frac{11}{6}C_A - \frac{2}{3}T_R n_f & -\frac{3}{2}C_F \\ \frac{4}{3}T_R n_f & 0 \end{pmatrix} + O(N)$$
$$\gamma_{NS}(N) = \frac{C_F}{N+1} + \frac{C_F}{2} + O(N+1), \tag{1.75}$$

where $C_A = N_c = 3$. From what we have said it is clear that q_{NS} behaves like xq_S or xg, hence it may be neglected at small x. In the following then we will consider only the singlet distribution.

In order to solve the DGLAP equation we have to diagonalize the anomalous dimension matrix (1.75). The resulting eigenvalues are

$$\lambda_+ = 2C_A\frac{1}{N} + \left(\frac{11}{6}C_A + \frac{2}{3}T_R n_f - \frac{4}{3}\frac{C_F}{C_A}T_R n_f\right) \tag{1.76}$$
$$\lambda_- = -\frac{4}{3}\frac{C_F}{C_A}T_R n_f, \tag{1.77}$$

with associated eigenvectors

$$Q_+ = \frac{2}{3}\frac{T_R n_f}{C_A}NG_+, \qquad Q_- = -\frac{C_A}{C_F}G. \tag{1.78}$$

Note that only λ_+ is singular at $N = 0$, hence in the small x limit F_2 will be dominated by the "large" eigenvector G_+.

In x space the eigenfunctions obey the following decoupled differential equations:

$$\begin{aligned} &\left(\frac{\partial^2}{\partial\xi\partial\zeta} + \delta_+\frac{\partial}{\partial\xi} - \gamma^2\right)G_+(\xi,\zeta) = 0 \\ &\left(\frac{\partial}{\partial\zeta} - \delta_-\right)G_-(\xi,\zeta) = 0, \end{aligned} \tag{1.79}$$

with

$$\delta_+(\xi,\zeta) = \frac{11 + \frac{2n_f}{27}}{\beta_0}, \quad \delta_- = \frac{16}{27\beta_0}n_f, \quad \gamma^2 = \frac{12}{\beta_0} \tag{1.80}$$

and $\beta_0 = 11 - \frac{2}{3}n_f$.

From what we have said, the evolution is dominated by G_+, which obeys a two dimensional wave equation with 'time' $\frac{1}{2}(\xi + \zeta)$ and 'space' $\frac{1}{2}(\xi - \zeta)$. From this some properties of the solution G_+ follow. First of all, the equation is essentially symmetrical in ξ and ζ, hence G_+ evolves equally in x and t (up to the small asymmetry induced by the damping term proportional to δ_+). Any further asymmetry in ξ and ζ must thus come from the boundary condition. Moreover, the

propagation is "timelike" into the forward light-cone at the origin $(\xi, \zeta) = (0, 0)$, along the "characteristics" ξ =constant and ζ =constant. Furthermore, at a given point (ξ, ζ), G_+ depends only on the boundary conditions contained within the backward light cone formed by the two characteristics through (ξ, ζ), that is to calculate $G_+(\xi, \zeta)$ is is unnecessary to know what happens at smaller values of x or larger values of t. Note finally that the equation is linear, hence contributions to G_+ from different parts of the boundary are simply added together.

Let us now write the solutions of Eq. (1.79). The solution to the second equation is trivial, we only have to integrate. Thus the general solution is:

$$G_- (\xi, \zeta) = e^{-\delta_- \zeta} G_- (\xi, 0) \,. \tag{1.81}$$

For the first equation, if we write $z = 2\gamma\sqrt{\xi\zeta}$ it becomes a Bessel equation. Then the general solution for G_+ is

$$\begin{aligned} G_+(\xi, \zeta) &= I_0 \left(2\gamma\sqrt{\xi\zeta} \right) e^{-\delta_+ \zeta} G_+(0, 0) + \\ &+ \int_0^\xi d\xi' I_0 \left(2\gamma\sqrt{(\xi - \xi')\zeta} \right) e^{-\delta_+ \zeta} \frac{\partial}{\partial \xi'} G_+ \left(\xi', 0 \right) + \\ &+ \int_0^\zeta d\zeta' I_0 \left(2\gamma\sqrt{\xi(\zeta - \zeta')} \right) e^{-\delta_+ (\zeta - \zeta')} \left(\frac{\partial}{\partial \zeta'} + \delta_+ \right) G_+ \left(0, \zeta' \right) , \end{aligned} \tag{1.82}$$

with

$$I_0(z) \equiv \sum_{n=0} \infty \frac{\left(\frac{1}{4} z^2 \right)^n}{(n!)^2} = \frac{1}{\sqrt{2\pi z}} e^z \left(1 + O\left(\frac{1}{z} \right) \right) . \tag{1.83}$$

Obviously the behaviour of G depends on the boundary conditions. Let us consider two classes of relevant boundary conditions. First assume that $G(x, t_0) \approx$ constant for small x. In this case the leading singularity comes from the anomalous dimension, hence our argument applies. Expanding the Bessel function I_0 in Eq. (1.82) we obtain:

$$G(\sigma, \rho) \approx G_+(\sigma, \rho) \approx \frac{\mathcal{N}}{\sqrt{4\pi\sigma}} e^{2\gamma\sigma - \delta_+ \frac{\sigma}{\rho}} \left(1 + O\left(\frac{1}{\sigma} \right) \right) , \tag{1.84}$$

where we have introduced the double scaling variables

$$\sigma \equiv \sqrt{\xi\zeta}, \qquad \rho \equiv \sqrt{\xi/\zeta}. \tag{1.85}$$

Assume now that $G(x, t_0) \propto x^{-\lambda}$, with $\lambda > 0$. In this case we can't neglect the singularity of the boundary condition. Evaluating the Mellin inversion integral (1.72) in the saddle point approximation we obtain

$$G(\sigma, \rho) \approx e^{\lambda\sigma\rho + \left(\frac{\gamma^2}{\lambda} - \delta_+ \right)} . \tag{1.86}$$

For small enough x this behaviour overwhelms the behaviour of Eq. (1.84). However, if ζ is large enough, that is if $\rho \leq (\gamma/\lambda)$, the leading behaviour is again the one of Eq. ((1.84).

Hence we obtain a universal prediction for F_2: if ζ is large enough indeed we have

$$\begin{aligned} F_2(\sigma,\rho) \approx Q_+ = \frac{2}{3}\frac{T_R n_f}{C_A}\frac{\partial G_+}{} \approx \\ \approx \frac{\mathcal{N}}{\sqrt{4\pi\sigma}}\frac{\gamma}{\rho}\exp\left(2\gamma\sigma - \delta_+\frac{\sigma}{\rho}\right)\left[1 + O\left(\frac{1}{\rho}\right) + O\left(\frac{1}{\sigma}\right)\right], \end{aligned} \tag{1.87}$$

where the boundary dependence is only in the trivial overall factor $\mathcal{N}$.
This means that away from the boundaries perturbative QCD allows us to predict in a parameter-free way (i.e. independently of the precise form of the boundary conditions) the asymptotic behaviour of F_2.

Let us summarize our results. Recalling Eq. (1.84) we can say that: $\log G(\sigma,\rho)$ at fixed ρ is asymptotically a linear function of σ, with slope independent of ρ (up to terms which vanish as $1/\rho$), while at fixed σ it is asymptotically a flat function of ρ. In other words, $\frac{\log G(\sigma,\rho)}{\sigma}$ is asymptotically independent of both ρ and σ, up to corrections which vanish as $1/\rho$ and $1/\sigma$. This property is usually referred as the "double asymptotic scaling" of G, hence the solution Eq. (1.87) is called the double scaling solution of the DGLAP equation.

1.3 BFKL equation

1.3.1 The high energy region and large x-logarithms

In the previous section we have shown that the (LO) DGLAP equation resums all the contributions of the form $\left(\alpha_s \log Q^2\right)^k$, hence it is fundamental when we are in the high virtuality region. Assume now that we are in the high energy region, $s \gg Q^2$.

If s is such that $\alpha_s \log(s/Q^2) = \alpha_s \log(1/x) \sim 1$, we have to resum all the contributions of the form $\left(\alpha_s \log(1/x)\right)^k$ to obtain an accuracy up to $O(\alpha_s)^2$. Let us see if the DGLAP equation can perform this resummation. Consider again Eq. (1.34). It is clear then that the leading order DGLAP equation resums terms of the form $\left(\alpha_s \log(Q^2) \log(1/x)\right)^k$, that is it resums the double leading log series (DLL) . Unfortunately this resummation neglects those terms which contain the leading power of $\log(1/x)$ but which aren't accompanied by the leading power of $\log(Q^2)$. The resummation of these terms, which are present in the evolution of the parton densities, is accomplished by the BFKL equation [3].

This section will be devoted to the derivation of the BFKL equation. There are many approach to BFKL theory. We will follow the k_T factorization one, since it exploits explicitly the parallelism between DGLAP and BFKL equations.

1.3.2 k_T factorization and BFKL-like equation

In order to obtain the BFKL equation, we need a more general form of the factorization theorem (1.20). It is possible to prove that the two-particle reducible contribution to an inelastic $\gamma^* P \to X$ scattering satisfies, at least at leading log x (LLx), the fundamental factorization [9]:

$$\sigma(x, Q^2) = \int_x^1 \frac{dy}{y} \int_0^{W^2/4} \frac{dk^2}{k^2} C\left(\frac{y}{x}, \frac{Q^2}{k^2}, \alpha_s(\mu^2)\right) f(y, k^2, \mu^2), \tag{1.88}$$

where σ is the adimensional cross-section, k is a transverse momentum, W is the square of the center-of-mass energy for the subprocess $\gamma^* P \to X$, C is a perturbatively calculable quantity and f is the *unintegrated parton distribution*, which is related to the usual integrated one by

$$F(x, Q^2) = \int_0^{Q^2} \frac{dk^2}{k^2} f(x, k^2). \tag{1.89}$$

Eq. (1.88) expresses the k_T *factorization theorem*.

For our purposes it is useful to introduce $S^2 = \Lambda^2/x$, $l^2 = \Lambda^2/y$, so that (1.88) becomes

$$\sigma(S^2/\mu^2, Q^2/\mu^2, \mu^2) = \int_0^\infty \frac{dl^2}{l^2} \int_0^\infty \frac{dk^2}{k^2} C\left(\frac{S^2}{l^2}, \frac{Q^2}{k^2}, \alpha_s(\mu^2)\right) f\left(\frac{l^2}{\mu}, \frac{k^2}{\mu^2}, \mu^2\right), \tag{1.90}$$

where the formal extension of the integration limits is of no consequence for our application (provided that the definitions of C and f are suitably extended). The symmetry of (1.90) is now totally manifest. Just as the high virtuality limit corresponds to $Q^2 \to \infty$ at fixed S^2, so the high energy limit is now $S^2 \to \infty$ at fixed Q^2.

Eq. (1.90) assumes a simpler form in the Mellin space. If we define

$$\sigma(N, M, \mu^2) := \int_0^\infty \frac{dS^2}{S^2} \left(\frac{\Lambda^2}{S^2}\right)^N \int_0^\infty \frac{dQ^2}{Q^2} \left(\frac{\Lambda^2}{Q^2}\right)^N \sigma\left(\frac{S^2}{\mu^2}, \frac{Q^2}{\mu^2}, \mu^2\right), \qquad (1.91)$$

the double factorization (1.90) can be expressed as

$$\sigma(N, M) = C\left(N, M, \alpha_s(\mu^2)\right) f(N, M, \mu^2) \qquad (1.92)$$

To derive the BFKL equation from (1.92), we will adopt the following strategy: first we will show how the mass factorization (and hence the DGLAP equation) follows from (1.88), then we will use the manifest symmetry of (1.88) to obtain the high energy factorization (and hence the BFKL equation).

Consider then the large Q^2 limit. We can rewrite (1.92) as

$$\sigma(N, Q^2/\mu^2, \mu^2) = \int_{c-i\infty}^{c+i\infty} \frac{dM}{2\pi i} \left(\frac{Q^2}{\Lambda^2}\right)^M C(M, N, \alpha_s\left(\mu^2\right)) f(N, M, \mu^2) \qquad (1.93)$$

Since the Mellin transform of $(\Lambda^2/Q^2)^k \log^n(\Lambda^2/Q^2)$ is $n!/(M-k)^{n+1}$, it follows that the leading singularity at large Q^2 is at $M = 0$, singularities further to the left vanish as powers of $1/Q^2$ (and hence they are neglected in the leading twist approximation).

It is possible to prove that in a nonabelian gauge theory only two-particle reducible diagrams can contain logarithmic singularities [10],[11]. Hence the two-particle irreducible unintegrated distribution function has at most a pole at $M = 0$, while the two-particle reducible coefficient function may contain (and in fact it does) logarithmic singularities which correspond to multiple poles at $M = 0$. We may then perform a Laurent expansion of the coefficient function

$$C\left(N, M, \alpha_s\mu^2\right) = \sum_{i=-\infty}^{\infty} C_k\left(N, \alpha_s(\mu^2)\right) M^{-M-1}, \qquad (1.94)$$

so that at leading twist we have

$$C(N, Q^2/\Lambda^2, \mu^2) = \sum_{m=0}^{\infty} \frac{1}{m!} C_m\left(N, \alpha_s(\mu^2)\right) \left(\log(Q^2/\Lambda^2)\right)^m \qquad (1.95)$$

The logarithmic singularities are generated perturbatively, so $C_m(N, \alpha_s)$ will begin at $O(\alpha_s^m)$.

We can proceed similarly with f. Power counting arguments [11] show that f is regular at $M = 0$, so

$$f(N, M, \mu^2) = \sum_{i=0}^{\infty} f_i(N, \mu^2) M^i, \tag{1.96}$$

with

$$f_m(N, \mu^2) = \frac{1}{m!} \int_0^{\infty} \frac{dk^2}{k^2} \left(\log(\mu^2/k^2)\right)^m f(N, k^2/\mu^2, \mu^2). \tag{1.97}$$

To obtain the leading twist behaviour of F_2, we must combine Eq. (1.94) and (1.96) and keep only the $M = 0$ singularities. Moreover, at leading log accuracy, we have to keep only terms like $\left(\alpha_s \log(Q^2)\right)^k$. Since $C_m(N, \alpha_s)$ begins at $O(\alpha_s^m)$, this implies that at leading log in (1.96) only the first term survives. But $f_0(N, \mu^2)$ is the integrated distribution function $F(N, \mu^2)$, so we obtain from (1.93) the mass factorization theorem:

$$\sigma(N, Q^2/\mu^2, \mu^2) = C(N, Q^2/\mu^2, \alpha_s(\mu^2)) F(N, \mu^2) + O(1/Q^2) \tag{1.98}$$

From (1.98) the general DGLAP-like equation (1.25) and the general solution (1.28) follow immediately.

We can now exploit the symmetry between N and M to derive an energy factorization theorem. Let us consider the high-energy limit $S^2/\Lambda^2 \to \infty$. From [10],[11] it follows that only two-particle reducible graphs produce logarithmic singularities. Moreover, it can be shown by explicit calculation that only two-gluon reducible graphs grow logarithmically. We may then separate two-gluon reducible graphs from the others (two-quark reducible and two-particle irreducible), see Fig(1.5).

For the two-gluon reducible contribution Eq. (1.88) holds, so in analogy with (1.93) we can write

$$\sigma^{(2)}(M, S^2/\mu^2, \mu^2) = \int_{c-i\infty}^{c+i\infty} \frac{dN}{2\pi i} \left(\frac{S^2}{\Lambda^2}\right)^N C\left(N, M, \alpha_s(\mu^2)\right) f(N, M, \mu^2). \tag{1.99}$$

Just as the leading twist contribution were determined by $M = 0$ singularities, so the high-energy large logarithms arise from $N = 0$ singularities. We then expand C and f around $N = 0$. Recalling that (as for the M-behaviour) f has at most a pole at $N = 0$, while C has multiple poles, we can write

$$\begin{aligned} C\left(N, M, \alpha_s(\mu^2)\right) &= \sum_{-\infty}^{\infty} C_n\left(M, \alpha_s(\mu^2)\right) N^{-n}, \\ f(N, M, \mu^2) &= N^{-1} \sum_{0}^{\infty} f_n(M, \mu^2) N^n \end{aligned} \tag{1.100}$$

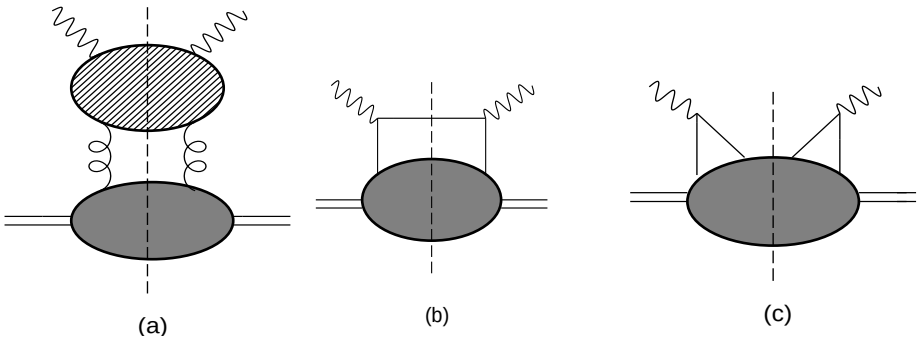

Contributions to the forward scattering. (a) is two-gluon reducible, (b) is two-gluon irreducible but two-quark reducible, (c) is two-particle irreducible. At high Q^2 (a) and (b) are leading twist and evolve, while (c) is higher twist and hence power-suppressed. At high S^2 none of them are power suppressed, but only (a) evolves, while (b) and (c) are asymptotically constant.

Figure 1.5: Contributions to the forward amplitude.

with

$$\begin{aligned} f_n(M,\mu^2) &= \frac{1}{n!}\int_0^\infty \frac{dl^2}{l^2}\left(\log(\mu^2/l^2)\right)^n l^2 \frac{\partial}{\partial l^2} f(M, l^2/\mu^2, \mu^2) = \\ &= -\frac{1}{n!}\int_0^1 dy\,(\log y)^n \frac{\partial}{\partial y} f(M, y, \mu^2). \end{aligned} \tag{1.101}$$

Defining[4] $F(M,\mu^2) \equiv f_0(M,\mu^2)$ we can write in analogy with (1.98)

$$\begin{aligned} \sigma(M, S^2/\mu^2, \mu^2) = C\left(M, S^2/\mu^2, \alpha_s(\mu^2)\right) F(M,\mu^2) + \\ +\sigma^q(M, S^2/\mu^2, \mu^2) + O(1/S^2), \end{aligned} \tag{1.102}$$

where $\sigma^q(M)$ contains the two-gluon irreducible terms (which approach a constant in the high energy limit)[5].

Using the results of the DGLAP section then from (1.102) it follows immediately:

$$S^2 \frac{\partial}{\partial S^2} F(M, S^2) = \chi\left(M, \alpha_s(S^2)\right) F(M, S^2), \tag{1.103}$$

$$\sigma(M, S^2/\mu^2) = C\left(M, 1, \alpha_s(S^2)\right) \Gamma_M(S^2, \mu^2) F(M, \mu^2), \tag{1.104}$$

with

$$\Gamma_M(S^2,\mu^2) \equiv \exp\left(\int_{\alpha_s(\mu^2)}^{\alpha_s(S^2)} \frac{d\alpha}{\beta(\alpha)} \chi(M,\alpha)\right) \tag{1.105}$$

[4]Note that this definition of $F(M,\mu^2)$ is not directly related to $F(N,\mu^2)$

[5]In (1.98) such a contribution is neglected since it is in the higher twist, see Fig(1.5).

If we hold the coupling fixed, we can write our evolution equation as

$$\frac{d}{dt}\sigma(N,t) = \gamma(N,\alpha_s)\sigma(N,t) \tag{1.106}$$

$$\frac{d}{d\xi}\sigma(\xi,M)) = \chi(M,\alpha_s)\sigma(\xi,M), \tag{1.107}$$

where $\xi = \log(1/x)$.

Eq. (1.106) and (1.107) express respectively the (fixed coupling) DGLAP and BFKL evolution. Since the BFKL kernel is calculated at fixed coupling, we may refer to (1.107) as the true BFKL equation. Let us now discuss the running coupling. We have derived these equations starting from the k_T factorization, which holds surely only at LLx. Hence we can't trust Eq. (1.106) and Eq. (1.107) at NLLx. But running coupling effects are NLLx, thus we can't trust our equations if the coupling runs. In other words, our derivation is valid only with fixed coupling. For the DGLAP equation, we have seen in the previous section that the collinear factorization is an all-order result, so we can let the coupling run without problems. Unfortunately there isn't an analogous result for the high-energy factorization, hence we must limit ourselves to the fixed coupling BFKL equation.

In the derivation of our equation, we considered for simplicity only one parton type. Consider now all the quark flavours and the gluon. In Sec. 1.2.6 we have shown that we can diagonalize the anomalous dimension matrix and consider separately the evolution of the two eigenvectors G_+ and G_-. Moreover, it is possible to prove that [23] only the gluon entries of the anomalous dimension matrix contain LLx singularities. From this it follows that only one evolution has $x-$logarithms, hence that only $G \equiv G_+$ obeys the BFKL equation, while $\frac{d}{d\xi}G_- = 0$ (for a detailed discussion, see [22]).

To sum up our results, we obtained that in the limit $Q^2 \to \infty$, x fixed the evolution is described by the DGLAP equation

$$\frac{d}{dt}G(N,t) = \gamma\left(N,\alpha_s(t)\right)G(N,t), \tag{1.108}$$

while in the limit $x \to 0$, Q^2 fixed (in particular at fixed α_s) the evolution is described by the BFKL equation

$$\frac{d}{d\xi}G(\xi,M) = \chi(M,\alpha_s)G(\xi,M), \tag{1.109}$$

where G is the eigenfunction associated to the largest eigenvalue γ of the γ_{ij} singlet matrix.

1.3.3 The BFKL kernel

It is clear from the discussion above that the BFKL kernel can be calculated evaluating the process in Fig. (1.6),

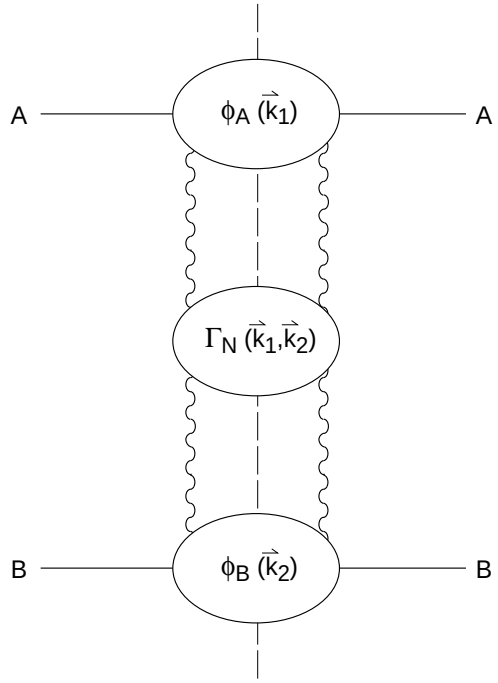

Figure 1.6: Gluon-mediated DIS

where A is the virtual photon and B the proton.

We are interested in the forward $A+B \to A+B$ scattering amplitude T, since from the optical theorem **Im** T is related to the total cross section σ.
Using the k_T factorization theorem we can write

$$\sigma \sim \int \frac{d^2\mathbf{k}_1}{k_1^2} \int \frac{d^2\mathbf{k}_2}{k_2^2} \phi_A(\mathbf{k}_1)\phi_B(\mathbf{k}_2) \int_{c-i\infty}^{c+i\infty} \frac{dN}{2\pi i} \Gamma_N(\mathbf{k}_1, \mathbf{k}_2), \tag{1.110}$$

where $\mathbf{k}_i$ are transverse momentum vectors of the gluons with virtuality $-(\mathbf{k})^2$, ϕ_i are suitable (unintegrated) structure functions, Γ_N is the $g-g$ kernel and $s = 2p_A p_B$ is the squared invariant mass of the colliding particles.

It can be proved (see e.g. [12]) that the $g-g$ kernel obeys a generalised BFKL equation:

$$N\ \Gamma_N(\mathbf{k}_1, \mathbf{k}_2) = \delta_2(\mathbf{k}_1 - \mathbf{k}_2) + \int d^2\mathbf{k} K(\mathbf{k}_1, \mathbf{k}) \Gamma_N(\mathbf{k}, \mathbf{k}_2). \tag{1.111}$$

In order to obtain the x evolution equation (1.107) we have to invert the N-Mellin transform (remember $N \leftrightarrow d/d\xi$).

At the integrated level we thus obtain

$$\frac{dG(\xi,Q^2)}{d\xi} = \int_{-\infty}^{\infty} \frac{dk^2}{k^2} K\left(\alpha_s, \frac{Q^2}{k^2}\right) G(\xi,k^2) = K \otimes G. \tag{1.112}$$

We may perform an M-Mellin transform to undo the convolution in (1.112). Eq. (1.109) is then obtained, with

$$\chi(M,\alpha_s) = \int_0^{\infty} \frac{dQ^2}{Q^2} K\left(\alpha_s, \frac{Q^2}{k^2}\right) \left(\frac{Q^2}{k^2}\right)^{-M}. \tag{1.113}$$

Note that the N-Mellin transform in Eq. (1.110) is perform with respect to the symmetric variable s/k_1k_2. Previously we defined it with respect to s/Q^2, with Q^2 the virtuality of one of the two particles (say $Q^2 = k_1^2$). This difference is irrelevant at LO, but at NLO it must be taken in account and it modifies the relation (1.113) between χ and K.

Order by order in perturbation theory the Feynman graphs leading to K are symmetric upon the exchange $\mathbf{k}_1 \leftrightarrow \mathbf{k}_2$. This in turn implies

$$\frac{1}{Q^2} K\left(\frac{Q^2}{k^2}\right) = \frac{1}{k^2} K\left(\frac{k^2}{Q^2}\right) \tag{1.114}$$

and hence a symmetry upon the exchange $M \to 1-M$ in the kernel χ. This symmetry is spoiled by running coupling effects.

The BFKL kernel χ is known up to $O(\alpha_s^2)$. An approximate form for the NLL contribution is also known, [13]. One may wonder how we can write a $O(\alpha_s^3)$ BFKL kernel if we know that the BFKL equation holds only at LLx. Now, explicit calculations have shown that this equation should hold also at NLLx. Moreover, we will see in the next chapter that within the framework of the ABF formalism one can show that G obeys a (running coupling) BFKL-like equation order by order in perturbation theory. Hence we can legitimately consider the BFKL kernel at any given order in perturbation theory. If we write

$$\chi(\alpha_s, M) = \alpha_s \chi_0(M) + \alpha_s^2 \chi_1(M) + O(\alpha_s^3) \tag{1.115}$$

then

$$\chi(\alpha_s, M) = \alpha_s \frac{N_c}{\pi} \left(2\psi(1) - \psi(M) - \psi(1-M)\right) \equiv \alpha_s \chi_0(M), \tag{1.116}$$

where $\psi(x) = \Gamma'(x)/\Gamma(x)$ and Γ is the Euler gamma function. Note the symmetry $M \leftrightarrow 1-M$. The kernel χ_0 is shown if Fig. 1.7.

The perturbative expansion (1.115) is very unstable, see Fig. 1.8. Even for α_s very small, the NL term completely overwhelms the LO term. This bad behaviour of the perturbative series can be understood and regularized in the context of the ABF formalism, as we will see in Sec. 1.4.

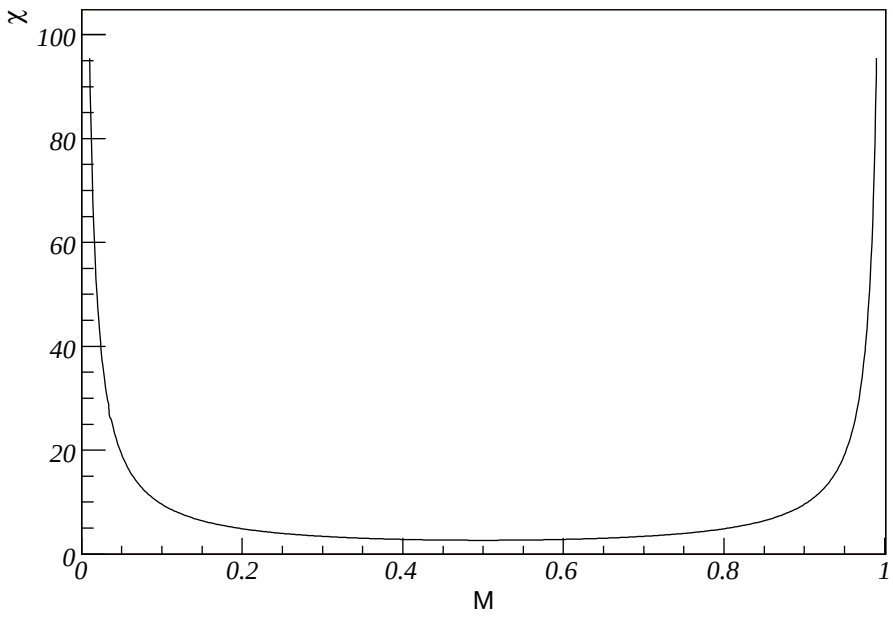

Figure 1.7: The LO BFKL kernel

1.3.4 Standard solutions of the BFKL equation

The general solution of the LO BFKL equation (1.109) in $M-$Mellin space is

$$G(\xi, M) = G(\xi_0, M) e^{\alpha_s \chi_0(M)\xi} \tag{1.117}$$

By taking the inverse Mellin transform we obtain

$$G(\xi, t) = \frac{1}{2\pi i} \int_{c-i\infty}^{c+i\infty} G(\xi_0, M) e^{\alpha_s \chi_0(M)\xi + Mt} \tag{1.118}$$

If t and ξ are both large, we can evaluate (1.118) in the saddle point approximation. The saddle condition is

$$\frac{d}{dM} \left(\alpha_s \chi_0(M)\xi + Mt\right)_{M=M_0} = 0, \ \longrightarrow \ \chi_0'(M) = -\frac{t}{\alpha_s \xi} \equiv -R. \tag{1.119}$$

We can then distinguish three interesting regions.

Consider first the limit $R \to \infty$, that is the limit $Q^2 \to \infty$, x fixed. In this case the general solution (1.118) is determined by the behaviour of χ near the origin. We can then expand

$$\chi_0(M) = \frac{N_c}{\pi} \left(\frac{1}{M} + 2\zeta(3) M^2 + 2\zeta(5) M^4 + ... \right), \tag{1.120}$$

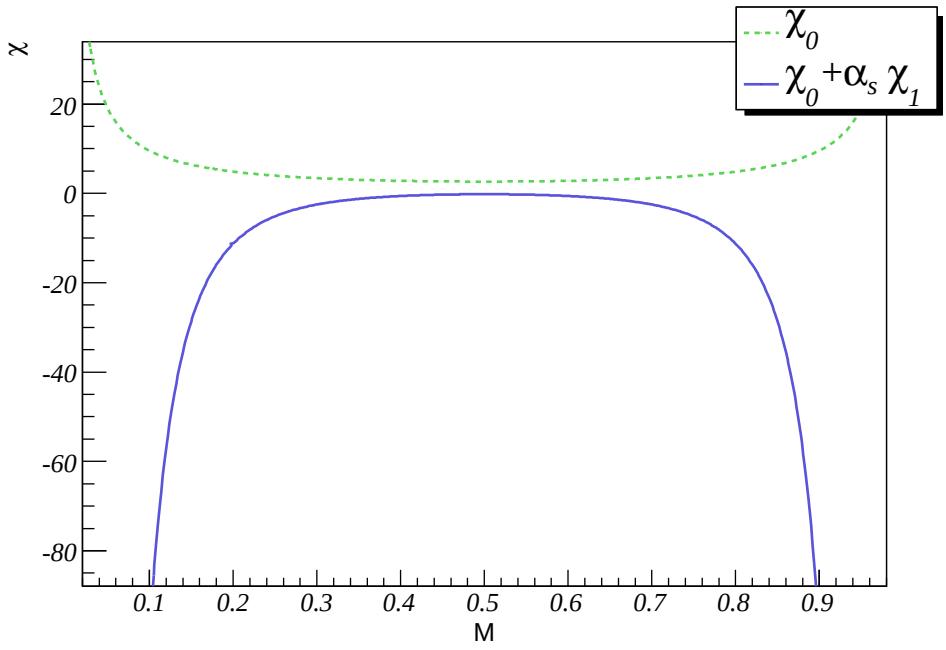

Figure 1.8: The NL BFKL kernel , $\alpha_s = 0.2$

where $\zeta(x)$ is the Riemann-zeta function. Keeping only the $M = 0$ pole we obtain $M_0 = \sqrt{\frac{\alpha_s N_c}{\pi}\frac{\xi}{t}}$ and

$$G(\xi, t) \propto \exp\left(\sqrt{\frac{4\alpha_s N_c}{\pi}\xi t}\right), \tag{1.121}$$

that is the fixed coupling version of the double scaling solution (1.84) (if we neglect the small damping term proportional to δ_+). This solution is quite obvious, since the $R \to \infty$ region is exactly the double scaling region.

Consider now the limit $R \sim 0$, that is the limit $x \to 0$ with Q^2 fixed. We expect this region being dominated by the large x-logarithms, which aren't resummed in the DLL approximation. We expect then a departure from the double scaling solution. In fact if $R \sim 0$ we may expand χ_0 near its minimum, that is near $M = 1/2$:

$$\chi_0(M) = \frac{N_c}{\pi}\left(4\log 2 - \psi''(1/2)\left(M - \frac{1}{2}\right)^2 + ...\right), \tag{1.122}$$

which leads to the asymptotic behaviour

$$G(\xi, t) \propto \exp\left(\alpha_s \chi_0(1/2)\xi\right) \approx x^{-\lambda_0}, \quad \lambda_0 = \alpha_s \frac{N_c}{\pi} 4\log 2. \tag{1.123}$$

This is the *Pomeron* prediction.

Finally, consider the limit $R \to -\infty$. This corresponds to the region $Q^2 \to 0$ with x large but fixed. This is the photoproduction limit. We then expect a linear vanishing of G in Q^2. In Mellin space this limit correspond to the $M \sim 1$ region. Expanding χ_0 near $M = 1$ we then obtain

$$M_0 = 1 - \sqrt{\frac{\alpha_s N_c}{\pi}\frac{\xi}{|t|}}, \qquad G(\xi, t) \propto Q^2 \exp\left(\sqrt{\frac{4\alpha_s N_c}{\pi}\xi|t|}\right). \tag{1.124}$$

We obtain the right qualitative behaviour, even though quantitatively we can't trust (1.124), since near $Q^2 \approx 0$ non perturbative effects must be important.

1.3.5 Problems with the BFKL evolution

The standard BFKL approach has a series of major problems. First of all, we have said that the BFKL equation can be derived only at LLx. The original BFKL equation was written as an evolution equation for the unintegrated gluon distribution $\mathcal{F}$. In this context, we can't say if the BFKL theory holds also beyond the leading order. The key point is the validity of a BFKL-like equation, that is of a universal property of the unintegrated gluon distribution. Explicit calculations have shown that at NLLx the BFKL theory should hold, that is the calculations of different processes have all given the same result for $\mathcal{F}$. Of course this is not a proof, but rather a hint of the validity of the BFKL theory. However, at NNLLx one can see that different processes lead to different results for $\mathcal{F}$. Hence we do know that at NNLLx the original BFKL theory fails. However, if we limit ourselves to the integrated distribution G, then in the next section we will show that a BFKL-like equation holds order by order in perturbation theory. Within that context we will show that all the traditional problems with the running coupling version of the BFKL equation can be solved.
Another major problem of the BFKL theory is the perturbative instability. We have seen that for reasonable values of α_s the NL correction $\alpha_s\chi_1$ completely overwhelms the leading order term. This problem too can be solved with perturbative resummations, as we will show in the next section.

Apart from these, the standard BFKL approach has other two problems, namely the violation of unitarity and the infrared diffusion. Consider the genuine BFKL prediction, i.e. the Pomeron solution. With a quadratic kernel the complete solution is

$$G(\xi, t) \propto \frac{1}{\sqrt{-2\alpha_s N_c \psi''(1/2) y}} \exp\left(\alpha_s \frac{N_c}{\pi} 4\log 2\xi + \frac{t}{2} + \frac{\pi}{\alpha_s N_c}\frac{1}{4\psi''(1/2)}\frac{t^2}{\xi}\right) =$$

$$= \frac{Q\ \pi}{\sqrt{\beta\alpha_s\frac{N_c}{\pi}\xi}}\ x^{-\alpha_s\frac{N_c}{\pi}\lambda} \exp\left(-\frac{t^2}{2\alpha_s\frac{N_c}{\pi}\beta\xi}\right), \tag{1.125}$$

with $\lambda = 4\log 2 \approx 2.77$ and $\beta = -2\psi''(1/2) \approx 33.66$.
The first problem of (1.125) is unitarity. Froissart-Martin theorem states that

a cross section can grow at most as $\log^2(s)$, that is $\log^2(1/x)$. Since $\lambda > 0$, Eq. (1.125) violates asymptotically the bound. This violation is typical of linear evolution, as we shall see in the next chapter.
Another problem is the infrared diffusion. Consider $\phi = G/Q$, where G is the hard Pomeron solution (1.125). Neglecting the dilatation factor $e^{\alpha_s N_c/\pi\lambda\xi}$ ϕ is solution of the diffusion equation

$$\frac{\partial\phi}{\partial\xi} = \frac{\beta}{2}\frac{\partial^2\phi}{\partial t^2}, \tag{1.126}$$

which express t-diffusion with time variable ξ. Eq. (1.126) implies that as the energy grows the infrared region of transverse momenta becomes more relevant, that is the perturbative treatment fails.

It is not clear whether these problems persist also after the perturbative resummations of both $\log Q^2$ and $\log 1/x$ terms. We know that these resummations ameliorate the situation, but both the violation of unitarity and the infrared diffusion seem to persist. However we will see in the next chapter that these problems can be solved within the framework of the BK theory, which should be the correct theory in the very high energy regime.

1.4 Improving DGLAP and BFKL: the ABF formalism

In the previous sections we have obtained two evolution equations that resum terms of the form $\left(\alpha_s \log Q^2\right)^k$ (DGLAP equation, t evolution) and $\left(\alpha_s \log 1/x\right)^k$ (BFKL equation, x evolution). Both the equations in the DLL approximation resum the $\left(\alpha_s \log Q^2 \log 1/x\right)^k$ contributions.

We may then ask if it is possible to resum both $\left(\alpha_s \log 1/x\right)^k$ and $\left(\alpha_s \log Q^2\right)^k$. The answer is yes, thanks to the Altarelli-Ball-Forte (ABF) formalism. This section will be devoted to the explanation of this technique.

1.4.1 Fixed coupling duality

In a region such that Q^2 and $1/x$ are large both DGLAP (1.108) and BFKL (1.109) equations are valid. Their mutual consistency implies a *duality relation* [14],[15] between the kernels γ and χ:

$$\chi\left(\alpha_s, \gamma(\alpha_s, N)\right) = N, \quad \gamma\left(\alpha_s, \chi(\alpha_s, M)\right) = M. \tag{1.127}$$

In order to obtain (1.127), consider the N-Mellin transform of Eq. (1.109):

$$\int_0^\infty d\xi e^{-N\xi} \frac{d}{d\xi} G\xi, M = \chi(M, \alpha_s) G(N, M). \tag{1.128}$$

Integration by parts leads to

$$\left[e^{-N\xi} G(\xi, M)\right]_0^\infty + N G(N, M) = \chi(M, \alpha_s) G(N, M). \tag{1.129}$$

The square bracket on the l.h.s provides an N independent boundary condition, say $H_0(M) \equiv G(0, M)$. Solving for $G(N, M)$ we find

$$G(N, M) = \frac{H_0(M)}{N - \chi(M, \alpha_s)}. \tag{1.130}$$

The leading twist behaviour of $G(N, t)$ is determined by the rightmost singularity of $G(N, M)$ in the M-plane, the contributions of additional singularities further on the left being suppressed by powers of Q^2. Perturbative singularities are given by solutions of the equation $\chi(\alpha_s, M) = N$, while singularities of the boundary condition $H_0(M)$ are non perturbative. If we suppose that the leading singularity is a perturbative one, we obtain

$$G(N, t) = \int_{c-i\infty}^{c+i\infty} \frac{dM}{2\pi i} e^{Mt} \frac{H_0(M)}{N - \chi(\alpha_s, M)} = -\frac{H_0(M_s)}{\chi'(\alpha_s, M_s)} e^{M_s t}, \tag{1.131}$$

where M_s is such that $\chi(\alpha_s, M_s) = N$.
Consider now the analogous DGLAP solution

$$G(N, t) = \tilde{H}_0(N) e^{\gamma(\alpha_s, N) t}. \tag{1.132}$$

Provided the t-independent boundary condition $\tilde{H}_0(N)$ is related to $H_0(M)$ by $\tilde{H}_0(N) = -\frac{H_0(M_s)}{\chi'(\alpha_s, M_s}$, the solutions (1.131) and (1.132) coincide (up to higher twist and nonperturbative terms) if $M_s = \gamma(N)$, that is if the duality relations (1.127) hold.

Using (1.127), knowledge of LO and NLO BFKL kernel determines the coefficients of the expansion of $\gamma(\alpha_s, N)$ in powers of α_s at fixed $\frac{\alpha_s}{N}$:

$$\gamma(\alpha_s, N) = \gamma_s\left(\frac{\alpha_s}{N}\right) + \alpha_s\gamma_{ss}\left(\frac{\alpha_s}{N}\right) + ... \tag{1.133}$$

To see how this works write down the duality relation in the form

$$\alpha_s\chi_0\left[\gamma_s\left(\frac{\alpha_s}{N}\right) + \alpha_s\gamma_{ss}\left(\frac{\alpha_s}{N}\right) + ...\right] +$$

$$+\alpha_s^2\chi_1\left[\gamma_s\left(\frac{\alpha_s}{N}\right) + \alpha_s\gamma_{ss}\left(\frac{\alpha_s}{N}\right) + ...\right] + ... = N \tag{1.134}$$

and expand in α_s at α_s/N fixed:

$$\chi_0\left(\gamma_s\left(\frac{\alpha_s}{N}\right)\right) + \alpha_s\chi_0'\left(\gamma_s\left(\frac{\alpha_s}{N}\right)\right)\gamma_{ss}\left(\frac{\alpha_s}{N}\right) + \alpha_s\chi_1\left(\gamma_s\left(\frac{\alpha_s}{N}\right)\right) + ... = \frac{N}{\alpha_s}. \tag{1.135}$$

From this we find

$$\chi_0\left(\gamma_s\left(\frac{\alpha_s}{N}\right)\right) = \frac{N}{\alpha_s}, \tag{1.136}$$

$$\gamma_{ss}\left(\frac{\alpha_s}{N}\right) = -\frac{\chi_1\left(\gamma_s\left(\frac{\alpha_s}{N}\right)\right)}{\chi_0'\left(\gamma_s\left(\frac{\alpha_s}{N}\right)\right)}. \tag{1.137}$$

This new expansion contains all the logarithmic singularities we want to resum: if for example we write

$$\gamma_s\left(\frac{\alpha_s}{N}\right) = \sum_{k=1}^{\infty} g_k^{(s)}\left(\frac{\alpha_s}{N}\right)^k \tag{1.138}$$

then the associated splitting functions reads

$$P_s(\alpha_s\xi) \equiv \int_{c-i\infty}^{c+i\infty}\frac{dN}{2\pi i\alpha_s}e^{N\xi}\gamma_s\left(\frac{\alpha_s}{N}\right) = \sum_{k=1}^{\infty}\frac{g_k^{(s)}}{(k-1)!}(\alpha_s\xi)^{k-1}. \tag{1.139}$$

Similarly P_{ss} resums the subleading singularities $\alpha_s\left(\alpha_s\log(1/x)\right)^k$ and so on. Note that the splitting function coefficients are factorially suppressed with respect to those of the anomalous dimension, hence the radius of convergence of P_s is infinite. This is very important, since it ensures that we can use our results even for very small x.

Obviously analogous results hold for χ; in this case the expansion $\chi_s + \chi_{ss} + ...$ resum all the contributions of the form $\alpha_s^n\left(\alpha_s\log(Q^2/\Lambda^2)\right)^k$.

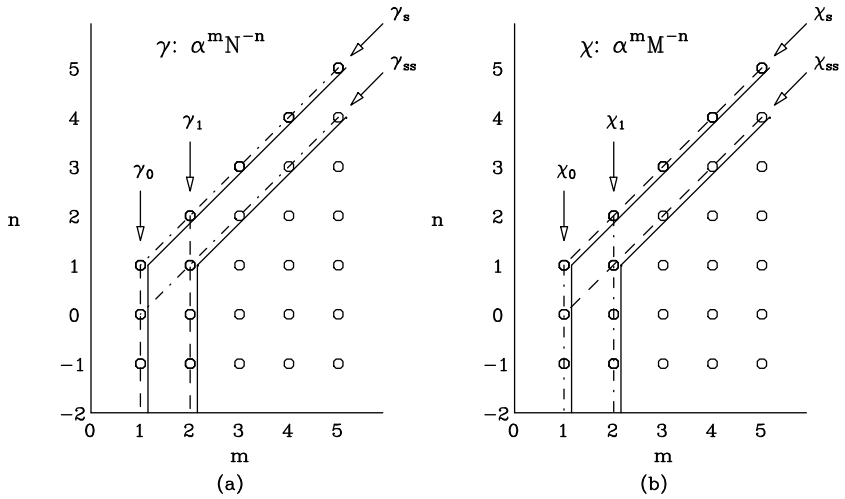

Graphical representation of different expansions of (a) γ and (b) χ in powers of α_s and (a) $1/N$ and (b) $1/M$. Vertical lines correspond to terms of the same fixed order in α_s, while diagonal lines correspond to terms of the same order in α at fixed α_s/N (a) or α_s/M (b). The solid lines denote terms of the same order in the DL expansion. Note that the traditional (vertical) and the duality-obtained (diagonal) expansions have in general one common term, which is the term retained in the DLL approximation.

Figure 1.9: Double leading expansion

We may then reorganize the expansion of our kernels into a *double leading* (DL) expansion, organized in terms of "envelopes" of the contributions summarized in Fig. 1.9. Consider for example γ. Up to NLO the DL expansion is

$$\gamma(\alpha_s, N) = \left[\alpha_s\gamma_0(N) + \gamma_s\left(\frac{\alpha_s}{N}\right) - a\frac{\alpha_s}{N}\right] +$$

$$+\alpha_s\left[\alpha_s\gamma_1(N) + \gamma_{ss}\left(\frac{\alpha_s}{N}\right) - \alpha_s\left(\frac{b_2}{N^2} + \frac{b_1}{N}\right) - b_0\right] + ... \qquad (1.140)$$

The terms a and b_i remove double counting terms, corresponding to those terms in Fig.1.9a with $(m,n) = (1,1),(1,0),(2,1),(2,2)$. In particular we obtain $a = \alpha_s N_c/\pi$ (the DLL term) and $b_2 = g_2^s = 0, b_1 = g_1^{ss} = n_f N_c\left(5 + 13/(2N_c^2)\right)/(18\pi^2)$, $b_0 = -\left(11/2N_c^3 + n_f\right)/\left(6\pi N_c^2\right)$.

1.4.2 The momentum conservation constraint

The DL expansion (1.140) can be further improved if we consider momentum conservation constraints.
Remember the OPE expansion (1.12). The spin two operator in (1.14) is just the stress-energy tensor. Since it is a conserved tensor, its anomalous dimension must vanish (see e.g. [19]).
This in turn implies $\gamma_{qq}(\alpha_s, 2) + \gamma_{gq}(\alpha_s, 2) = 0$ and $\gamma_{qg}(\alpha_s, 2) + \gamma_{gg}(\alpha_s, 2) = 0$, or (recall (1.74)) $\gamma_{QQ}(\alpha_s, 1) + \gamma_{GQ}(\alpha_s, 1) = 0$ and $\gamma_{QG}(\alpha_s, 1) + \gamma_{GG}(\alpha_s, 1) = 0$. But from this it follows

$$\gamma(\alpha_s, 1) \equiv \gamma^+(\alpha_s, 1) = 0, \qquad \gamma^-(\alpha_s, 1) = \gamma_{QQ}(\alpha_s, 1) - \gamma_{QG}(\alpha_s, 1). \tag{1.141}$$

We can then improve (1.140) by adding a term which implement the condition $\gamma(\alpha_s, 1) = 0$. From the DL point of view such a term is subleading, but it may be important for the phenomenology.

Let us now consider the BFKL kernel χ. The momentum conservation constraint also explains the bad behaviour of the traditional perturbative expansion of χ. Duality indeed implies

$$\chi\left(\alpha_s, 0\right) = \chi\left(\alpha_s, \gamma(\alpha_s, 1)\right) = 1 \tag{1.142}$$

Since $\chi_0(M) \sim 1/M$ for $M \sim 0$, because of momentum conservation the perturbative expansion *must* be badly behaved. A simple model for this behaviour is to think of replacing α_s/M with

$$\alpha_s/(M + \alpha_s) = \alpha_s/M - \alpha_s/M^2 + ... \tag{1.143}$$

in order to satisfy the momentum conservation constraint.

Consider now the DL expansion

$$\chi(\alpha_s, M) = \left[\alpha_s \chi_0(M) + \chi_s\left(\frac{\alpha_s}{N}\right) - \frac{N_c}{\pi}\frac{\alpha_s}{M}\right] +$$
$$+\alpha_s\left[\alpha_s \chi_1(M) + \chi_{ss}\left(\frac{\alpha_s}{N}\right) - \alpha_s\left(\frac{c_2}{M^2} + \frac{c_1}{M}\right) + c_0\right] + ... \tag{1.144}$$

At LO the momentum conservation constraint is satisfied exactly. Indeed $\gamma_0(1) = 0$ and $[\chi_0((M) - N_c/\pi M] \sim M^2$ near $M = 0$. At NLO the constraint is not exactly satisfied because the constant contribution to χ_1 does not vanish, even though it is numerically very small. We can then restore the constraint by adding a (subleading) correction.

The bad behaviour of the perturbative expansion is tamed in the DL reorganization, see Fig. 1.10. The new expansion is stable up to $M < 0.3 - 0.4$. Furthermore in this region χ evaluated in the DL expansion is very close to the exact DGLAP dual. This show that in this region the dominant contribution to χ (and thus to γ) comes from the resummation of large-Q^2 logarithms.
Beyond $M \sim 0.4$ the DL expansion becomes unstable because of the $M = 1$ singularities. In the next section we will see how to stabilize these singularities exploiting the full symmetry of χ.

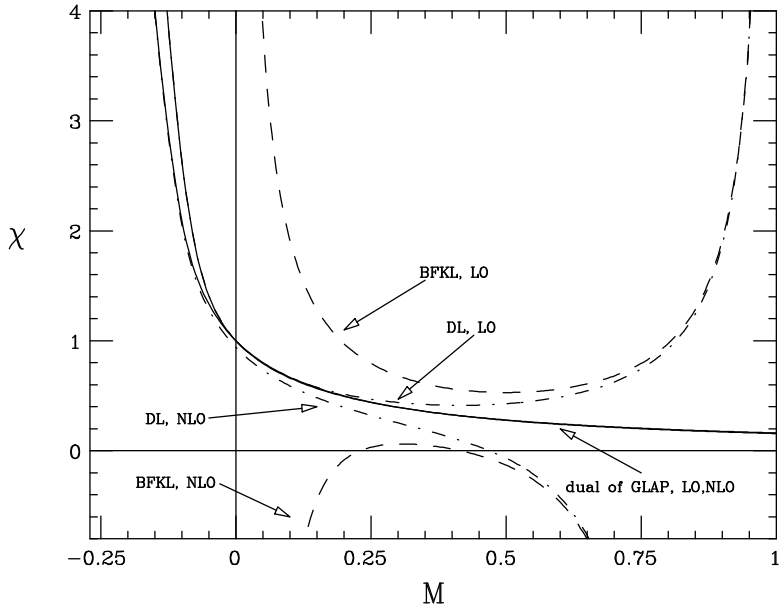

Figure 1.10: Different approximations to the the χ functions

1.4.3 Fixed coupling symmetrization

We said that order by order in perturbation theory the kernel $K(\mathbf{k}_1, \mathbf{k}_2)$ is symmetric upon the exchange $k_1 \leftrightarrow k_2$, that is χ is symmetric upon the exchange $M \leftrightarrow 1 - M$. However this symmetry can be spoiled by two effects: an asymmetric choice for the N-Mellin transform and running coupling.

With the coupling held fixed, the kernel asymmetry is due only to the choice of the definition of ξ. If we choose a symmetric definition for ξ, for example $\xi = \log(s/\sqrt{Q^2 k^2})$, the resulting (fixed coupling) kernel χ_σ must be symmetric. It can be shown [16] that the effect of changing variables from the symmetric $\xi = \log\left(s/\sqrt{Q^2 k^2}\right)$ to the DIS $\xi = \log\left(s/Q^2\right)$ choice is a change of the kernel χ from χ_σ to χ_Σ. The symmetric and the DIS kernels are related by [16]

$$\chi_\Sigma\left(M + \frac{1}{2}\chi_\sigma(M)\right) = \chi_\sigma(M) \to \chi_\sigma\left(y - \frac{1}{2}\chi_\Sigma(y)\right) = \chi_\Sigma(y), \tag{1.145}$$

where we have omitted the dependence on α_s in order to shorten the notation. The regularization of $M = 1$ poles is then done in three steps: first we perform the DL resummation of $M = 0$ poles, then we determine the associated χ_σ through (1.145) and symmetrize it, finally we going back in DIS variables by using (1.145) in reverse.

We will perform this regularization in a toy model, pretending that the all-order anomalous dimension is $\alpha_s \gamma_0(N)$, that is $\chi = \chi_s$. This corresponds to a

leading $\log Q^2$ (or collinear) approximation to the BFKL kernel. The calculation with the real DL kernels can be found in [4].

In order to perform this change of variables it is convenient to define for a generic kernel $\chi(\alpha_s, M)$ an "off-shell" generalization $\bar{\chi}(\alpha_s, M, N)$ such that

$$\chi(\alpha_s, M) = \bar{\chi}(\alpha_s, M, \chi(\alpha_s, M)). \tag{1.146}$$

Using duality relations (1.127) the on-shellness condition (1.146) can be rewritten as

$$N = \bar{\chi}(\alpha_s, \gamma(\alpha_s, N), N), \tag{1.147}$$

We then obtain $\chi(\alpha_s, M$ or $\gamma(\alpha_s, N)$ by putting either N or M "on-shell" (i.e. set $N = \chi(\alpha_s, M)$ or $M = \gamma(\alpha_s, N)$) in the off-shell relation $N = \bar{\chi}(\alpha_s, M, N)$.

With the off-shell kernels the change of variables is trivial. The (non symmetrized) off-shell version of χ_σ is obtained simply by the shift $M \to M + N/2$ in χ_s. Then we can perform the desired symmetrization. Note the this is allowed at leading $\log Q^2$, because the symmetrizing terms are by construction free of poles at $M = 0$ and thus subleading in $\log Q^2$. Finally we can return to the DIS kernel χ_Σ by performing the inverse shift $M \to M - N/2$. We thus obtain the kernels

$$\begin{aligned}
\bar{\chi}_\sigma(\alpha_s, M, N) &= \chi_s\left(\frac{\alpha_s}{M + N/2}\right) \to \chi_s\left(\frac{\alpha_s}{M + N/2}\right) + \chi_s\left(\frac{\alpha_s}{1 - M + N/2}\right), \\
\bar{\chi}_\Sigma(\alpha_s, M, N) &= \chi_s\left(\frac{\alpha_s}{M}\right) + \chi_s\left(\frac{\alpha_s}{1 - M + N}\right).
\end{aligned} \tag{1.148}$$

Consider the large-N behaviour of $\bar{\chi}_\Sigma \sim \chi_s\left(\frac{\alpha_s}{M}\right) + \chi_s\left(\frac{\alpha_s}{N}\right) = \chi_s\left(\frac{\alpha_s}{M}\right) + O\left(\frac{\alpha_s}{N}\right)$. Putting M on shell we obtain $N = \chi_s\left(\frac{1}{\gamma_0(N)}\right) + O\left(\frac{\alpha_s}{N}\right) = N + O\left(\frac{\alpha_s}{N}\right)$, thus the resummation does not spoil the identification of the resummed kernel with the DGLAP result at large N. This in turn guarantees that the resulting anomalous dimension matches smoothly to the DGLAP anomalous dimension.

Our resummed kernel (1.148) is still unsatisfactory, since it violates the momentum conservation constraint because of the symmetrizing term. However this violation in subleading. Near $M \sim 0$ the symmetrizing contribution behaves as $\chi_s(\alpha_s/(1 - M + N)) = \chi_s(\alpha_s)(1 + O(N))$. From the on-shellness relation $N = \chi(\alpha_s, M) = \chi_s(\alpha_s/M) = O(\alpha_s/M)$ it follows immediately $O(N) = O(\alpha_s/M)$, then the momentum violation is $O(\alpha_s) = O\left(\alpha_s^{n+1} M^{-n}\right)$, thus next-to-leading in a DL expansion. We can then enforce momentum conservation without spoiling the restored symmetry by simply adding the subleading term

$$\chi_m(\alpha_s, N) = c_m(\alpha_s) f_m(N), \tag{1.149}$$

with $f_m(1) = 1$, $f_m(0) = f_m(\infty) = 0$. The infinity condition ensures that the extra term does not spoil the large-N identification of the resummed kernel with the DGLAP result, while the condition $f_m(0) = 0$ ensures that χ_m is subleading, since $c_m = O(\alpha_s)$.

Let us now turn to the generic properties of the symmetrized on-shell kernels. From the momentum conservation condition in DIS variables, $\chi(\alpha_s, 0) = 1$ we obtain

$$1 = \chi_\Sigma(\alpha_s, 0) = \chi_\sigma\left(\alpha_s, 0 - \frac{1}{2}\chi_\Sigma(\alpha_s, 0)\right) = \chi_\sigma\left(\alpha_s, -\frac{1}{2}\right),$$

$$\chi_\sigma\left(\alpha_s, \frac{3}{2}\right) = \chi_\sigma\left(\alpha_s, 1 + \frac{1}{2}\right) = \chi_\sigma\left(\alpha_s, -\frac{1}{2}\right) = 1. \tag{1.150}$$

Going back in DIS variables these in turn imply

$$\chi_\Sigma(\alpha_s, 0) = \chi_\Sigma(\alpha_s, 2) = 1. \tag{1.151}$$

Since in the central region $M \sim 1/2$, $\chi = O(\alpha_s)$ and thus rather less than one, momentum conservation implies that, at least for small enough values of α_s the symmetrized kernel will have a minimum order by order in the DL expansion. Since the change of variables from symmetric to DIS variables is just a shift $M \to M - N/2$, there will be a minimum in DIS variables too.

Consider now the position and curvature around the minimum. By construction χ_σ has a minimum for $M = 1/2$, while the minimum of χ_Σ is displaced. Moreover, differentiating (1.145) with respect to M we obtain

$$\chi'_\Sigma(\alpha_s, M) = \frac{\chi'_\sigma\left(\alpha_s, M - 1/2\chi_\Sigma(M)\right)}{1 + \frac{1}{2}\chi'_\sigma\left(\alpha_s, M - \frac{1}{2}\chi_\Sigma(M)\right)}$$

$$\chi''_\Sigma(\alpha_s, M) = \frac{\chi''_\sigma\left(\alpha_s, M - 1/2\chi_\Sigma(M)\right)}{\left(1 + \frac{1}{2}\chi'_\sigma\left(\alpha_s, M - \frac{1}{2}\chi_\Sigma(M)\right)\right)^3}. \tag{1.152}$$

The minimum of χ_Σ is then at M_s, determined by $M_s = \frac{1}{2} + \frac{1}{2}\chi_\Sigma(\alpha_s, M_s)$, which implies

$$\chi_\sigma\left(\alpha_s, \frac{1}{2}\right) = \chi_\Sigma(\alpha_s, M_s), \qquad \chi''_\sigma\left(\alpha_s, \frac{1}{2}\right) = \chi''_\Sigma(\alpha_s, M_s), \tag{1.153}$$

that is the intercept and curvature of χ_Σ and χ_σ are the same.

1.4.4 Running coupling effects

So far we considered only fixed coupling duality. When one goes beyond LLx, that is beyond leading-order approximation for χ, running coupling effects can't be neglected.

In M space the usual running coupling $\alpha_s(t)$ becomes a differential operator $\hat{\alpha}_s$, since in Mellin space $t \leftrightarrow -\partial_M$. Hence the BFKL evolution equation (1.109) becomes [17]

$$\frac{d}{d\xi}G(\xi, M) = \chi(\hat{\alpha}_s, M)G(\xi, M). \tag{1.154}$$

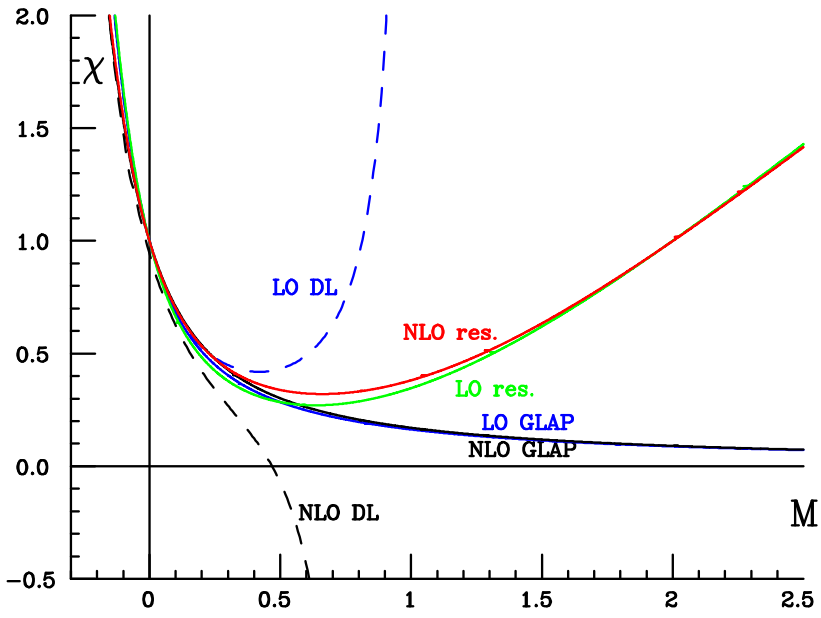

Plot of different BFKL kernels in DIS variables. Note that at NLO only the symmetrized kernel (denoted by NLO_{res}) has a minimum.

Figure 1.11: Effects of symmetrization

Since M and $\hat{\alpha}_s$ do not commute,

$$\left[\hat{\alpha}_s^{-1}, M\right] = -\beta_0 + \alpha_s\beta_0\beta_1 + ..., \tag{1.155}$$

Eq. (1.154) is meaningless if we don't fix an operator ordering. Different ordering choices correspond to different choices for the running coupling argument.

In order to see this, we consider the BFKL equation (1.112) with two different arguments of the running coupling. Let us start with the traditional argument $t = \log\left(Q^2/\mu^2\right)$. We then write Eq. (1.112) as:

$$\frac{dG(\xi,t)}{d\xi} = \int_{-\infty}^{\infty} dt' \sum_{p=i}^{\infty} \alpha_s(t)^p K_L^{(p)}(t-t') G\left(\xi, t'\right). \tag{1.156}$$

Consider now the Mellin transform of the r.h.s.:

$$\int dt \int dt' \alpha_s(t) K_L(t-t') G(\xi,t') e^{-Mt} =$$

$$= \alpha_s(-\partial_M) \int dt' e^{-Mt'} G(\xi,t') \int dt K_L(t-t') e^{-M(t-t')} = \hat{\alpha}_s \chi_L(M) G(\xi,M). \tag{1.157}$$

We see that if the coupling runs as usual with Q^2 the derivative w.r.t. M in (1.154) acts both on the kernel and on G.

Assume now that the coupling runs with k^2. Then Eq. (1.112) becomes:

$$\frac{dG(\xi,t)}{d\xi} = \int_{-\infty}^{\infty} dt' \sum_{p=i}^{\infty} \alpha_s(t')^p K_R^{(p)}(t-t') G\left(\xi, t'\right), \tag{1.158}$$

with $t' = \log(k^2/\mu^2)$. In Mellin space the r.h.s. becomes

$$\int dt \int dt' \alpha_s(t') K_R(t-t') G(\xi,t') e^{-Mt} =$$

$$= \left[\alpha_s(-\partial_M) \int dt' e^{-Mt'} G(\xi,t')\right] \int dt K_L(t-t') e^{-M(t-t')} = \chi_L(M) \hat{\alpha}_s G(\xi,M) \tag{1.159}$$

In this case the derivative w.r.t. M acts only on G and not on the kernel.

Consider now the symmetrizing procedure of the previous section. Because it is based on the interchange $Q^2 \leftrightarrow k^2$, it is now clear that the running coupling symmetrized version of $\hat{\alpha}_s^k f(M) = \frac{1}{2}\left(\hat{\alpha}_s^k f(M) + f(1-M)\hat{\alpha}_s^k\right)$.

1.4.5 LO running coupling duality

In this section we will consider the leading running coupling effects, that is we will deal with the one-loop expansion for $\hat{\alpha}_s$

$$\hat{\alpha}_s = \frac{\alpha_s}{1 - \beta_0 \alpha_s \frac{d}{dM}} \tag{1.160}$$

and with kernels linear in $\hat{\alpha}_s$:

$$\chi = \hat{\alpha}_s \phi(\alpha_s, M). \tag{1.161}$$

Note that ϕ could obviously be the leading order χ_0.

In this approximation the double Mellin transform of (1.154) becomes

$$\left(1 - \beta_0 \alpha_s \frac{d}{dM}\right) NG(N,M) + F(M) = \alpha_s \phi(M) G(N,M), \tag{1.162}$$

where $F(M)$ is a boundary condition.
The general solution of (1.162) can be written as

$$G(N,M) = H(N,M) +$$

$$+ \int_{M_0}^{M} dM' \exp\left[\frac{M-M'}{\beta_0 \alpha_s} - \frac{1}{\beta_0 N} \int_{M'}^{M} dM'' \phi(M'')\right] \frac{F(M')}{\beta_0 \alpha_s N}, \tag{1.163}$$

where $H(N,M)$ is the solution of the homogeneous equation

$$H(N,M) = H(N,M_0) \exp\left[\frac{M-M_0}{\beta \alpha_s} - \frac{1}{\beta_0 N} \int_{M_0}^{M} dM' \phi(M')\right]. \tag{1.164}$$

If we change the integration variable from M' to

$$y(M,M') = \frac{1}{\beta_0 \alpha_s N} \int_{M'}^{M} \left[N - \alpha_s \phi(M'')\right] dM'', \tag{1.165}$$

then Eq. (1.163) becomes

$$G(N,M) = H(N,M) + \int_0^{y,M,M_0} e^{-y} \frac{F\left(M'(y,M)\right)}{N - \alpha_s \phi\left(M'(y,M)\right)} dy, \tag{1.166}$$

with H proportional to e^{-y}. Since $y \to \infty$ in the limit $\alpha_s \to 0$, α_s/N fixed, the homogeneous term vanishes to all orders in the perturbative expansion. The perturbative solution then is reproduced only by the inhomogeneous term.

Consider now the N Mellin transform of the inhomogeneous term:

$$G(N,t) =$$

$$= \int_{c-i\infty}^{c+i\infty} \frac{dM}{2\pi i} \exp\left[Mt + \frac{M - M_0}{\beta_0 \alpha_s} - \frac{1}{\beta_0 N} \int_{M_0}^{M} dM'' \phi(M'')\right] \frac{I(N,M)}{N}, \tag{1.167}$$

where

$$I(N,M) = \int_{M_0}^{M'} dM' \exp\left[\frac{M_0 - M'}{\beta_0 \alpha_s} + \frac{1}{\beta_0 N} \int_{M_0}^{M'} dM'' \phi(M'')\right] \frac{F(M')}{\beta_0 \alpha_s}. \tag{1.168}$$

We can solve (1.167) in the saddle point approximation. Assuming $I(N,M)$ to be a smooth function of M the saddle condition is

$$t + \frac{1}{\beta_0 \alpha_s} - \frac{1}{\beta_0 N} \phi(M_s) = \frac{1}{\beta_0 \alpha_s(t)} - \frac{1}{\beta_0 N} \phi(M_s) = 0. \tag{1.169}$$

Identifying M_s with the anomalous dimension γ_s and ϕ with χ_0 we obtain

$$\chi_0\left(\gamma_s\left(\frac{\alpha_s(t)}{N}\right)\right) = \frac{N}{\alpha_s(t)}, \tag{1.170}$$

that is a running coupling generalization of the leading order duality relation Eq.(1.136). Substituting back the saddle condition in the exponent of Eq. (1.167) we get (differentiating the duality relation with respect to t)

$$\frac{M_s}{\alpha_s(t)\beta_0} - \frac{M_0}{\alpha_s \beta_0} - \frac{1}{\beta_0 N} \int_{M_0}^{M_s} dM' \phi(M') = \int_{t_0}^{t} dt' \gamma_s\left(\frac{\alpha_s(t')}{N}\right), \tag{1.171}$$

where $\alpha_s = \alpha_s(t_0)$.

Performing the saddle integral we obtain

$$G(N,t) = \sqrt{\frac{N\beta_0\alpha_s}{-\phi'(M_s)}} \exp\left(\int_{t_0}^{t} dt' \gamma_s\left(\frac{\alpha_s(t')}{N}\right)\right) \frac{I(N,M_s)}{N} + ... \tag{1.172}$$

Eq. (1.172) has two major problems: first it seems to violate factorization because of the t-dependent factor M_s in the boundary condition I, second it seems to violate duality because the t-dependent prefactor $1/\sqrt{-\phi'(M_s)}$ spoils the identification of the anomalous dimension γ_s. Both this problems are fictitious.

In order to check duality, consider the prefactor $1/\sqrt{-\phi'(M_s)}$. Differentiating the duality relation it can be rewritten as

$$\frac{1}{\sqrt{-\phi'\left(\gamma_s\left(\alpha_s(t')/N\right)\right)}} = \exp - \left[\frac{1}{2}\log -\phi'\left(\gamma_s\left(\alpha_s(t')/N\right)\right)\right] =$$

$$= \exp\left[\beta_0 \int_{t_0}^{t} dt' \frac{\phi''\left(\alpha_s(t')/N\right)\phi\left(\alpha_s(t')/N\right)}{2\phi'^2\left(\alpha_s(t')/N\right)}\alpha_s(t')\right] \times \frac{1}{\sqrt{-\phi'(M_s(t_0)}} =$$

$$= \exp\left[\int_{t_0}^{t} dt' \Delta\gamma_{ss}\left(\alpha_s(t')/N\right)\right] \frac{1}{\sqrt{-\phi'\left(\left(\alpha_s(t_0)/N\right)\right)}}. \tag{1.173}$$

The t_0 dependent factor can be absorbed in a redefinition of the boundary condition. Duality is then preserved provided we add to γ the extra factor $\Delta\gamma_{ss}$. We can treat the same way all the contributions generated by the saddle expansion. The result is a new anomalous dimension of the form [18]

$$\gamma_{rc}\left(\alpha_s(t')/N\right) = \gamma_s\left(\alpha_s(t')/N\right) + \beta_0\alpha_s(t)\Delta\gamma_{ss}\left(\alpha_s(t')/N\right) +$$

$$+ \left[\beta_0\alpha_s(t)\right]^2 \Delta\gamma sss\left(\alpha_s(t')/N\right) + ... \tag{1.174}$$

Consider now factorization. $I(N, M_s)$ can be written in terms of the variable y, Eq. (1.165), as

$$I(N, M_s) = \int_0^{y(M_s)} dy e^{-y} \frac{F(M'(y, M_0))}{N - \phi(M'(y, M_0))} \tag{1.175}$$

If we take $1-\alpha_s/N\phi < 0$ and $M' < M_0$, then in the perturbative limit $y(M_s) \to \infty$. Factorization is thus preserved, since the t dependence disappears to all orders in the perturbative expansion (even though the boundary condition still depends on t_0 because $M' = M'(y, M_0)$).

Exploiting this property we can rewrite the general solution (1.167) as

$$G(N,t) = \int_{c-i\infty}^{c+i\infty} \frac{dM}{2\pi i M} e^{Mt} \exp\left[\frac{M - M_0}{\beta_0\alpha_s} - \frac{1}{\beta_0 N}\int_{M_0}^{M} dM''\phi(M'')\right] \frac{I(N, t_0)}{N}. \tag{1.176}$$

In the next subsection we will try to solve explicitly Eq. (1.176) with approximate kernels ϕ.

Note that in this section we have shown that the running coupling BFKL equation is equivalent to the usual DGLAP equation (with of course a suitable kernel). Hence at this order the existence of a BFKL-like equation is ensured by the existence of the DGLAP equation. One can show that the results of this section hold to any given order in the perturbative expansion [24]. But then this

implies that a BFKL-like equation for G holds at any given perturbative order, since we know that the DGLAP equation for G is an all order result. In other words, perturbative duality ensures that a BFKL-like equation for G holds also beyond LLx, even if our derivation of Eq. (1.109) was based on the k_T factorization (which is valid only at LLx). We stress that the BFKL equation holds for G: an explicit calculation shows that beyond NLLx it doesn't hold for the unintegrated gluon distribution.

The DLL approximation

In order to check Eq. (1.176) consider the DLL kernel, that is $\phi(M) = \frac{N_c}{\pi}\frac{1}{M}$. We know that in the DLL approximation the solution $G(N,t)$ is

$$G_{DLL}(N,t) \propto \exp\left[-\frac{N_c}{\beta_0 \pi N}\log\left(\alpha_s(t)/\alpha_s\right)\right] \tag{1.177}$$

In the DLL approximation the integrand of (1.176) is

$$f(N,M) \propto \exp\left[M\left(\frac{1}{\alpha_s(t)}\right) - \frac{N_c}{\pi\beta_0}\log M\right] = M^{-\frac{N_c}{\pi\beta_0 N}} e^{M\frac{1}{\alpha_s(t)}}, \tag{1.178}$$

that is we have to perform a Mellin inversion of M^{-k} with respect to the variable $z = 1/\alpha_s(t)$. The inversion can be done exactly with the result

$$f(N,t) \propto \left(\frac{1}{\alpha_s(t)}\right)^{\frac{N_c}{\pi\beta_0 N}}, \tag{1.179}$$

that is the correct (1.177) behaviour.

Quadratic kernel and asymptotic behaviour

Consider a generic kernel ϕ expanded around is minimum:

$$\phi(M) = c + \frac{k}{2}\left(M - M_{min}\right)^2 + \frac{h}{3!}\left(M - M_{min}\right)^3 + ... \tag{1.180}$$

It can be shown [18] that only the first two terms are relevant in order to derive the asymptotic small-x behaviour of G, the other terms lead to contributions that vanish in the $\xi \to \infty$ limit[6]. In this subsection then we will limit ourselves to quadratic kernels.

In this case the Mellin inversion (1.176) can be done exactly. If we set $M_{min} = 1/2$ (the minimum of χ_σ) and choose $M_0 = 1/2$ we get

$$G(N,t) = K(N) e^{1/(2\beta_0\alpha_s(t))} \mathrm{Ai}\left[z\left(\alpha_s(t), N\right)\right] \frac{I(N,t_0)}{N}, \tag{1.181}$$

[6]From here it is clear the importance of the symmetrizing procedure discussed in Sec. 1.4.3, since it ensures that order by order in the DL expansion the kernel χ has a minimum. Without symmetrizing this property is spoiled, see Fig. 1.10.

where K is a t-independent factor,

$$K(N) = e^{1/(2\beta_0\alpha_s)} \left(\frac{2\beta_0 N}{k}\right)^{\frac{1}{3}} \frac{1}{\pi}, \tag{1.182}$$

$$z(\alpha_s, N) = \left(\frac{2\beta_0 N}{k}\right)^{\frac{1}{3}} \frac{1}{\beta_0} \left[\frac{1}{\alpha_s} - \frac{c}{N}\right], \tag{1.183}$$

and $\mathrm{Ai}(z)$ is the Airy function, which satisfies

$$\mathrm{Ai}''(z) - zAi(z) = 0, \tag{1.184}$$

and that behaves asymptotically as

$$\mathrm{Ai}(z) = \frac{1}{2}\pi^{-1/2} z^{-1/4} \exp\left(-\frac{2}{3}z^{3/2}\right)\left(1 + O(z^{-3/2})\right). \tag{1.185}$$

In order to determine the large-ξ behaviour of $G(\xi, t)$ we must distinguish three cases, depending on the sign of c. Here we will discuss only the case $c > 0$, which is the one corresponding to the LO kernel χ_0. The interested reader can found an exhaustive treatment off all the possible cases in [18].
For large ξ, we may determine $G(\xi, t)$ by evaluating by saddle point the N-Mellin inversion integral of $G(N, t)$ (1.181). The saddle condition is dominated by the Airy function and has the form

$$\xi = \frac{d\mathrm{Ai}[z(\alpha_s, N)]/dN}{\mathrm{Ai}[z(\alpha_s, N)]}. \tag{1.186}$$

As ξ grows, the saddle is drawn towards the $N \to 0$; however for N small enough the derivative changes sign and the real saddle is lost. The saddle condition still has a pair of complex solutions, which can (for ξ large enough) be determined explicitly using the asymptotic expansion (1.185). We have $N\pm = e^{\pm i\pi/4}(a/\xi)^{1/2}$, with a a constant factor. The large ξ asymptotic behaviour is then dominated by the contribution from this pair of complex saddle point, which add to give cosine oscillations:

$$G(\xi, t) \sim \exp\left(\sqrt{2k\xi}\right) \cos\left(2k\xi\right). \tag{1.187}$$

As ξ becomes large, $G(\xi, t)$ becomes negative and starts to oscillate, so the solution looks unphysical. In order to solve this puzzling situation, consider the general solution of $G(N, t)$, Eq. (1.26), with boundary $G(N, t_0) = F_0(N)$:

$$G(N, t) = \Gamma(t, t_0, N) F_0(N), \tag{1.188}$$

with in this case

$$\Gamma(t, t_0, N) = \frac{G(N, t)}{G(N, t_0)} = e^{1/(2\beta_0)(1/\alpha_s(t) - 1/\alpha_s(t_0))} \frac{\mathrm{Ai}[z(\alpha_s(t), N)]}{\mathrm{Ai}[z(\alpha_s(t_0), N)]} \tag{1.189}$$

Since for large ξ the oscillations (1.187) are t-independent, they cancel in the ratio $G(N,t)/G(N,t_0)$, leaving Γ smooth and asymptotically monotonic in ξ as $\xi \to \infty$. The oscillations are then factored out in the initial condition.

From Γ we can extract the anomalous dimension

$$\gamma_A\left(\alpha_s(t), N\right) = \frac{d}{dt}\log G(N,t) = \frac{1}{2} + \left(\frac{2\beta_0 N}{k}\right)^{1/3} \frac{\mathrm{Ai}'[z(\alpha_s(t),N)]}{\mathrm{Ai}[z(\alpha_s(t),N)]}. \tag{1.190}$$

The large-N behaviour of γ_A is easily determined using the asymptotic expansion (1.185):

$$\gamma_A(\alpha_s, N) \sim \frac{1}{2} - \sqrt{\frac{2}{k}\left[\frac{N}{\alpha_s} - c\right]}, \tag{1.191}$$

which is the "naive" dual anomalous dimension, that is the anomalous dimension obtained by fixed-order duality with the replacement $\alpha_s \to \alpha_s(t)$.

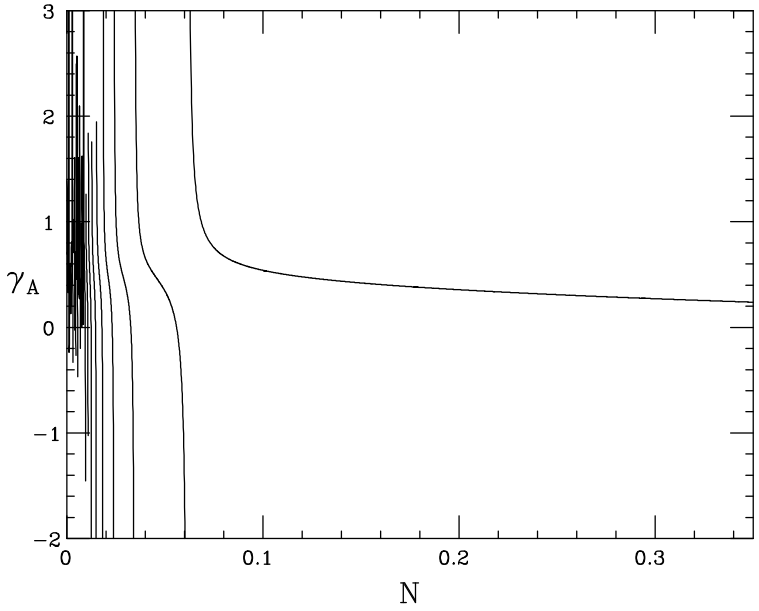

Figure 1.12: The Airy anomalous dimension γ_A for $c = 1$ and $\alpha_s = 0.2$

As N decreases γ_A increases indefinitely until it blows up for the value $N = N_0(t)$ corresponding to the first zero of the Airy function, $z_0 \approx -2.338$ (see Fig. 1.12). $\mathrm{Ai}'(z)$ is regular at $z = z_0$, so at $N = N_0$ the anomalous dimension has a simple pole.

From Eq. (1.189) it then follows directly the asymptotic behaviour of G: approximating the Airy function with its pole we get

$$G(\xi, t) \sim x^{-N_0(t_0)}. \tag{1.192}$$

Expanding the LO kernel χ_0 around its minimum we find $c \approx 2.65$, $k \approx 32$, which lead to $N_0 \approx 0.3$ for $Q_0^2 = 1$ GeV^2 and $N_0 \approx 0.25$ for $Q_0^2 = 10$ GeV^2. We see that the running coupling resummation softens the hard pomeron (1.123) prediction.

1.4.6 NL kernels with running coupling

If we want to evaluate the running-coupling kernels beyond LO accuracy, we must refine the approximations of the previous section. The asymptotic behaviour of γ is again determined by the quadratic approximation of χ near its minimum. Since the intercept and the curvature of χ_σ and χ_Σ are the same, we can expand χ_σ around the well-known minimum $M_{min} = 1/2$:

$$\chi_\sigma(\alpha_s, M) = c(\alpha_s) + \frac{1}{2}k(\alpha_s)\left(M - \frac{1}{2}\right)^2. \tag{1.193}$$

Beyond LO accuracy $c(\alpha_s) \to c(\hat{\alpha}_s)$,$k(\alpha_s) \to k(\hat{\alpha}_s)$. At NL accuracy it is sufficient to consider the linear term in the expansion of $c(\hat{\alpha}_s)$ and $k(\hat{\alpha}_s)$ in powers of $\hat{\alpha}_s - \alpha_s$ [4], that is

$$c(\hat{\alpha}_s) = c(\alpha_s) + (\hat{\alpha}_s - \alpha_s)c'(\alpha_s) + O\left[\left(\beta_0 \frac{d}{dM}\right)\right] \tag{1.194}$$

and similarly for k.

The solution of (1.176) can then be expressed in terms of the Bateman function. For a complete derivation we refer the interested reader to [4], here we will limit ourselves to cite the main results of the NL running coupling resummation. We saw that the small-x behaviour of G is determined by the leading singularity of the anomalous dimension. In Fig. 1.13 we report the dependence of this singularity on α_s for various anomalous dimensions.
Note that the general effect of resummation is to soften the small-x behaviour. The most accurate calculation (NLO Bateman) gives the softest behaviour prediction, say $G \approx x^{-0.2}$ for $\alpha_s \approx 0.2$.

For α_s large enough the NLO BFKL seems to produce a soft pomeron prediction. However, we can't trust this prediction because of the bad behaviour of the unresummed perturbative expansion of χ. Note instead that the resummed LO and NLO predictions are close to each other.

Consider now the full anomalous dimension and its associated splitting function, shown in Fig. 1.14. Note that the resummed NLO anomalous dimension follows closely the traditional one up to $N \sim 0.2$, then its rise grows faster because of the pole in the Bateman function. A careful analysis of these plots shows that up to very small x, say $x \sim 10^{-5}$, the difference between the full resummed splitting function and the DGLAP NL result is practically unnoticeable. Considerable differences start only from $x \sim 10^{-6}$. Hence, even if $\alpha_s \log 1/x \sim 1$ already for much larger values of x (say $x \sim 10^{-2}$ with $\alpha_s \sim 0.2$), their influence is negligible

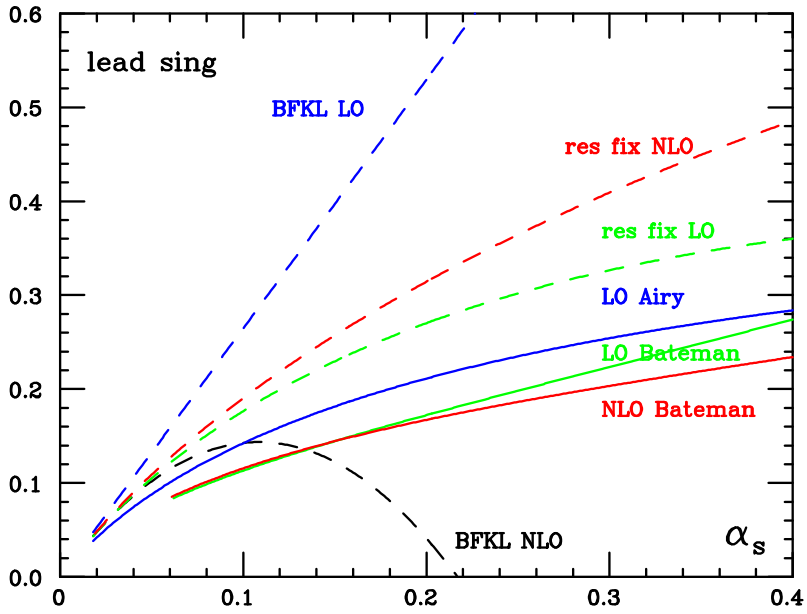

The rightmost singularity for various anomalous dimensions. BFKL LO, res fix LO and res fix NLO denote the location of the cut for respectively $\alpha_s\chi_0$, $\chi_{\sigma LO}$ and $\chi_{\sigma NLO}$ with $\beta_0 = 0$. LO Airy, LO Bateman and NLO Bateman denote the location of the pole for the running coupling resummation of the corresponding three curves. BFKL NLO denotes the location of the stationary point of the NLO kernel.

Figure 1.13: Leading singularity for various anomalous dimensions

in the perturbative HERA domain. This explain why standard phenomenological analysis of HERA data, which are based upon pure DGLAP evolution, are so successful even in the small-x region.

On the other hand, in the HERA domain these resummation effects cannot be responsible for "strange" phenomena, that is in this region saturation effects (if they are present) cannot be explained by perturbative resummations.

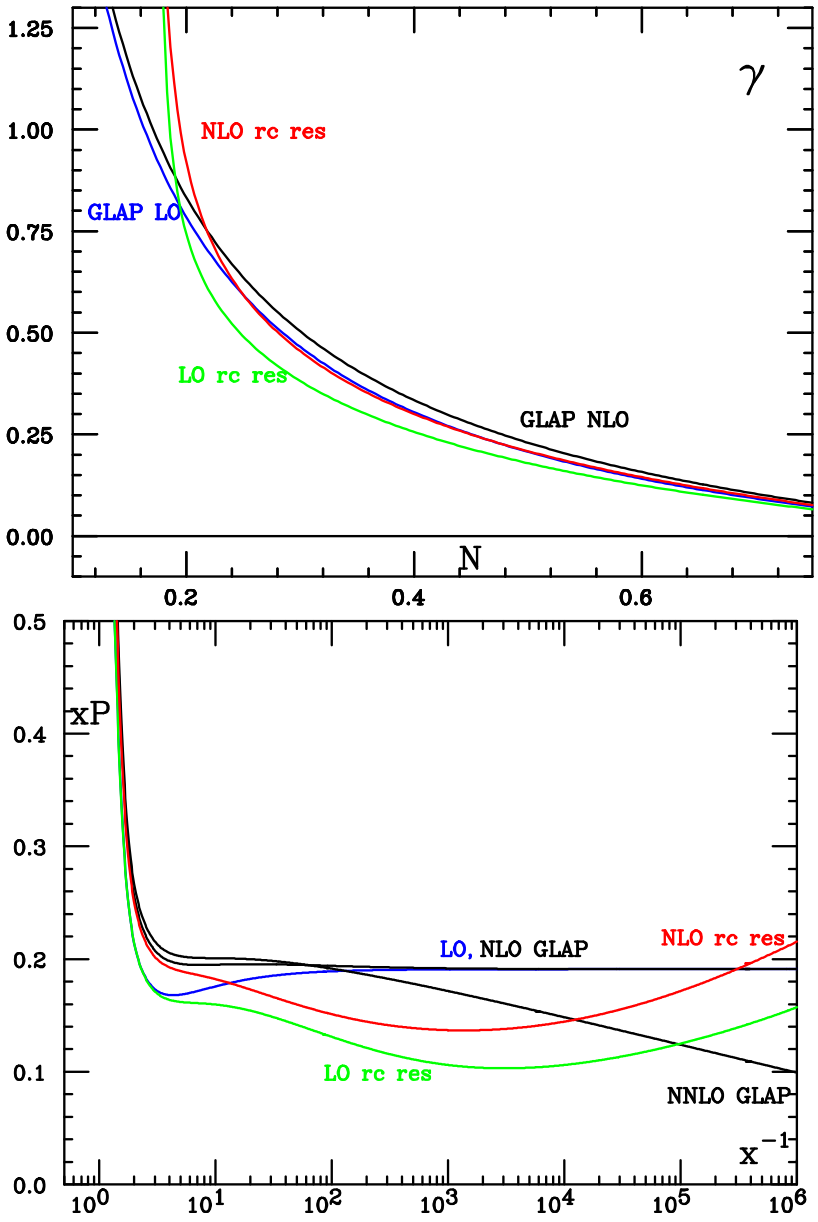

Comparison between resummed and traditional anomalous dimensions and splitting functions. GLAP LO and GLAP NLO are the traditional kernels, while LO rc res and NLO rc res are the running coupling resummed kernels.

Figure 1.14: Resummed evolution kernels

Chapter 2

High energy QCD

2.1 The idea of parton saturation

We saw that in the very high energy limit the traditional BFKL approach fails, since it violates the Froissart-Martin unitarity bound. In the early '80s Gribov, Levin and Ryskin [25] and somewhat later Mueller and Qiu [26] suggested that this breakdown could be due to saturation effects. In the high energy limit the gluon splitting leads to a very high gluon density, but this process cannot go on indefinitely: when the density inside the proton becomes too high gluons can no longer be treated as free. We must consider parton recombination, that is gluon fusion.

A schematic picture of this process is shown in Fig. 2.1, which depicts the x and Q^2 evolution of the parton distribution functions. Consider first the horizontal direction, i.e. DGLAP evolution. Using the uncertainty principle we can associate to each parton a typical size $r \sim 1/k_T$. The DGLAP kinematic regime of strong transverse ordering then implies that partons on the right are "smaller" than partons on the left. Now consider the vertical direction, i.e. BFKL evolution. We will show that in this case the ξ evolution is obtained through the emission of partons without ordering of transverse momenta, that is of partons with $k_{T_1} \simeq k_{T_2} \simeq ... \simeq k_{T_N} \simeq q^2$ (where k_{T_1} is the transverse momentum of the parent parton). Because of this kinematic constraint then the size of the upper partons is bounded to be of the same order as the original ones. Hence for a given Q^2 a point is reached where the finite size of the hadron will soon impose an upper bound to the number of partons that can be accommodated without overlapping. Conversely, for a given x there is a *saturation momentum* $Q_s(x)$ beyond which we cannot neglect parton recombination effects. Since we may expect that bigger partons reach a saturated regime sooner, the saturation scale $Q_s(x)$ should be an increasing function of x.

The first step towards a theory for the saturated regime was made by Balitsky [5] who constructed an infinite hierarchy of coupled equations for Wilson line operators in the small-x approximation. Indipendently Kovchegov derived in the *colour dipole* approach a non linear generalization of the BFKL equation, valid

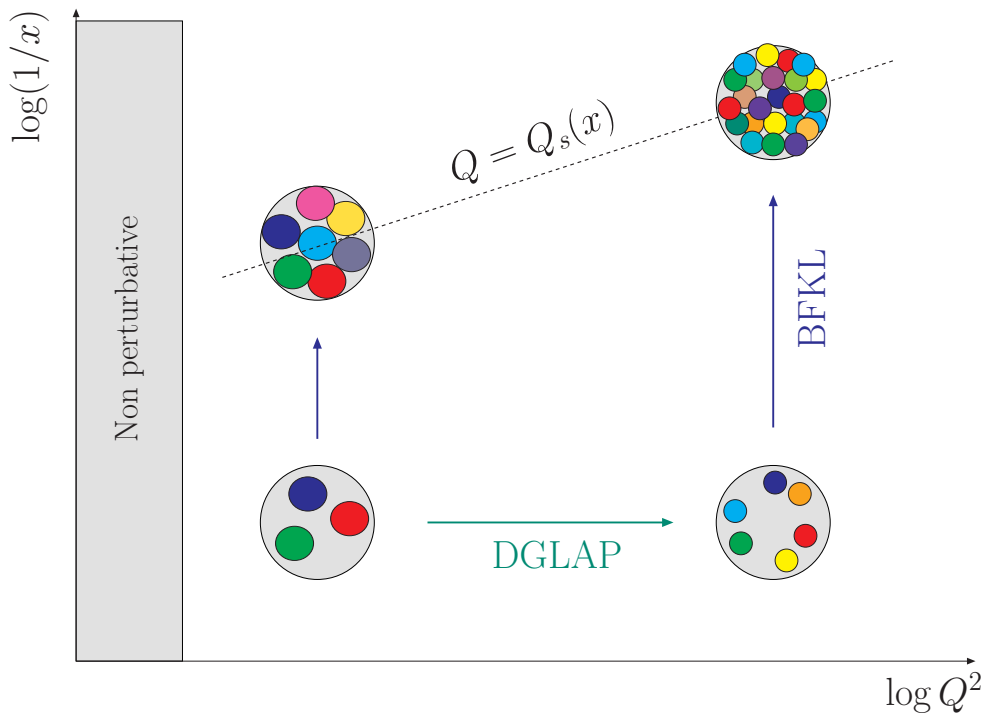

Figure 2.1: Schematic picture of parton saturation

in the large-N_c (see Appendix A) approximation and at leading $\log 1/x$ [7]. In the large-N_c limit the Balitsky hierarchy decouples and its first term reduces to the Kovchegov equation. Thus, this equation is usually referred as the Balitsy-Kovchegov (BK) equation. An alternative approach is the Jalilian-Marian-Iancu-McLerran-Weigert-Kovner-Leonidov (JIMWKL) hierarchy [6], that describes the change of the correlation functions of the colour charge density in the hadron wavefunction. This equation can be derived in the Color-Glass-Condensate (CGC) approach, an effective theory in which one consider the radiation of soft gluons in a strong background field. In the large N_c the JIMWKL hierarchy decouples and becomes equivalent to the BK equation.

An exhaustive presentation of all these derivation goes beyond the scope of this thesis. In the following we will limit ourselves to the Kovchegov theory, which is by far the simplest and it is model independent. Moreover, its link with the BFKL theory is transparent. To see this, we must derive the BFKL equation in the colour dipole formalism [21]. This chapter is hence organised as follows. In section 2.2 we introduce the colour dipole approach to DIS and within that context we give a precise definition of geometric scaling. Then in section 2.3 we use the dipole formalism to derive the BFKL equation and we evaluate the leading order kernel. This derivation is generalized in section 2.4 to multiple interactions, leading to the

BK equation. In section 2.5 we show how geometric scaling arises from the BK equation. Section 2.6 is devoted to the extended geometric scaling region, that is to geometric scaling above the saturation scale.

2.2 The colour dipole approach to DIS

The colour dipole is an alternative approach to DIS which at small x is very useful, since it shows that the $\gamma^* P$ interaction in this limit can be factorized in a $\gamma^* \to q\bar{q}$ part and in a $q\bar{q} - P$ interaction.

Consider indeed the structure of the interaction in the proton rest frame. In order to have non trivial QCD interactions the virtual photon must split in a $q\bar{q}$ pair, that is in a *colour dipole*. In addition, we will have in general several extra gluons. This situation is depicted in Fig. 2.2.

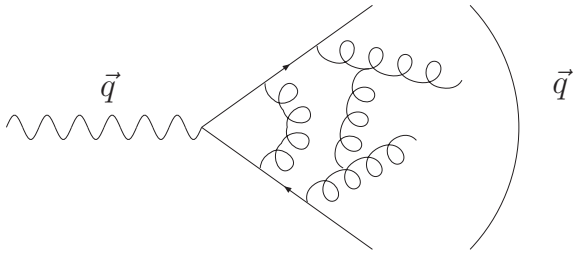

Figure 2.2: The virtual photon splitting

The effect of the extra gluons can be thought of as a binding energy. Hence we can write the energy difference between the $q\bar{q}$ state and the photon state as:

$$\Delta E = E_{pair} - E_{\gamma^*} = \sqrt{M_{pair}^2 + \vec{q}^2} - E_{\gamma^*} = \sqrt{M_{pair}^2 + Q^2 + E_{\gamma^*}^2} - E_{\gamma^*} =$$

$$= \frac{1}{2}\frac{M_{pair}^2 + Q^2}{E_{\gamma^*}} + O\left[\left(\frac{M_{pair}^2 + Q^2}{E_{\gamma^*}}\right)^2\right], \tag{2.1}$$

where M_{pair} is the invariant mass of the $q\bar{q}$ pair.
Remembering that in the proton rest frame $x = Q^2/(2m_P E_{\gamma^*})$, in the high virtuality limit $Q^2 \gg M_{pair}^2$ Eq. (2.1) reduces to

$$\Delta E = m_P\, x + O\left[(m_P\, x)^2\right]. \tag{2.2}$$

In the small-x limit we can then estimate the life time of the pair as $T_{pair} \sim \frac{1}{\Delta E_{pair}} \sim 1/(m_P\, x)$. On the other hand the typical interaction time is $T_{int} \sim R_p$, with R_p the proton radius. For small x then $T_{int} \ll T_{pair}$. This implies that in the high energy limit the $q\bar{q}$ pair is "frozen" during the interaction. Thus we can

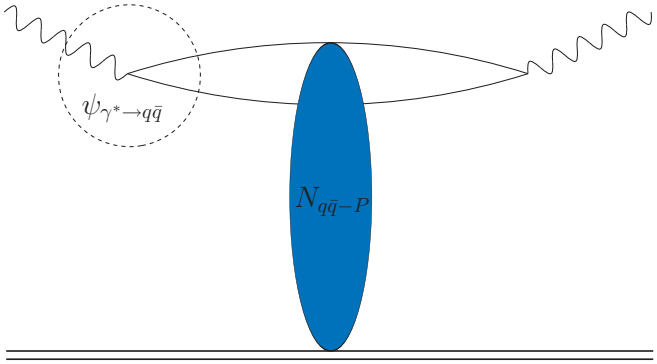

Figure 2.3: Colour dipole approach to DIS

factorize DIS in a $\gamma^* \to q\bar{q}$ splitting and in a fixed-size dipole scattering off a proton, as shown in Fig. (2.3).

All the above statement can formalised [27],[28]. The result is that it is possible to write the total cross section $\sigma_{tot}^{\gamma^* P}$ as

$$\sigma_{tot}^{\gamma^* P}(x, Q^2) = \sum_{i=T,L} \int d^2\mathbf{r} \int dz |\psi_i(r, z, Q^2)|^2 N(r, x), \tag{2.3}$$

where $\psi_{T,L}$ is the wave function for the splitting of a transverse (T) or longitudinal (L) polarized virtual photon into a $q\bar{q}$ pair and N is the total dipole cross section. In addition, $\mathbf{r}$ is the separation of the quarks in the $q\bar{q}$ pair and z is the light-cone momentum fraction of the photon carried by the quark (or antiquark).
The wave functions of the virtual photon can be calculated in perturbative QED. At the lowest order in α_{em} and neglecting quark masses they are given by [28]:

$$|\psi_T|^2 = \frac{3\alpha_{em}}{2\pi^2} \sum_f e_f^2 \left[\left(z^2 + (1-z)^2\right) z(1-z) Q^2 K_1^2 \left(\sqrt{z(1-z)} Qr\right) \right]$$

$$|\psi_L|^2 = \frac{2\alpha_{em}}{2\pi^2} \sum_f e_f^2 \left[4Q^2 z^2 (1-z)^2 K_0^2 \left(\sqrt{z(1-z)} Qr\right) \right], \tag{2.4}$$

where $K_{0,1}(x)$ are the Bessel-McDonanld functions.

The original geometric scaling observation [1] was made in terms of $\sigma_{tot}^{\gamma^* P}$, that is

$$\sigma_{tot}^{\gamma^* P}(x, Q^2) = \sigma_{tot}^{\gamma^* P}\left(Q^2/Q_s(x)^2\right). \tag{2.5}$$

Since F_2 is related to $\sigma_{tot}^{\gamma^* P}$ by

$$F_2(x, Q^2) = \frac{Q^2}{4\pi^2 \alpha_{em}} \sigma_{tot}^{\gamma^* P}. \tag{2.6}$$

we can express geometric scaling in terms of F_2:

$$\frac{F_2(x,Q^2)}{Q^2} = f\left(Q^2/Q_s(x)^2\right) \tag{2.7}$$

Using (2.4) it is straightforward to see that the geometric condition (2.5) is equivalent to

$$N(r,x) = N\left(rQ_s(x)\right), \tag{2.8}$$

thus in order to understand geometric scaling we can limit ourselves to the dipole cross section.

2.3 BFKL in the colour dipole approach

2.3.1 BFKL from Feynman graphs: general strategy

Before starting our derivation in the colour dipole approach, let us consider the connection between BFKL and Feynman graphs, as we did for DGLAP in Sec. 1.2.5. We have essentially two purposes: first to understand which diagrams are relevant in the BFKL theory and second to find out the correct kinematic regime. This section will be stopped half-way: the effective calculation of the BFKL kernel will be done in the next section, within the colour dipole formalism.

To obtain BFKL, we have to evaluate the kernel Γ shown in Fig. 1.6. We could use a technique similar to that used in Sec. 1.2.5: write down an evolution equation from a ladder graph. But how should this ladder be built? Since we are interested in small-x logarithms, which can arise by phase space integration in dx, we have to consider only terms which behave like $\sim 1/x$ near $x = 0$. Consider the basic "building blocks" of the DGLAP evolution, i.e. P_{ij}: only the gluon entries P_{gg} and P_{gq} have such a behaviour, hence only the $q \to gq$ and $g \to gg$ splitting are relevant in our ladder. Moreover, only the first "rung" of this ladder can be of quark type in a leading log approximation. Consider indeed Fig 2.4. The graph on the left has a quark rung in the middle of the ladder, associated to the subprocess $q \to gq$ (marked in green). Since P_{gq} is singular in $x = 0$, this emission will produce the desired term $\alpha_s \log 1/x$. But consider now the lower rung, marked in red in the figure. It must be associated to a $q \to q$ or to a $g \to q$ splitting. The corresponding splitting functions are regular in $x = 0$, hence this emission will lead to a factor α_s but unaccompanied by a $\log 1/x$ term. Thus this graph can be neglected in a leading log approximation. Consider now the ladder on the right. Since in this case the quark rung is the lowest one, there is only the $q \to g$ splitting. Hence this graph is leading order. Then in the leading log approximation only the first rung can be of quark type, i.e. quark emission cannot be iterated. Thus we may consider gluon-only ladders, the eventual first quark rung being only a trivial prefactor.

Until now we have considered only the DGLAP-relevant building blocks. In fact,

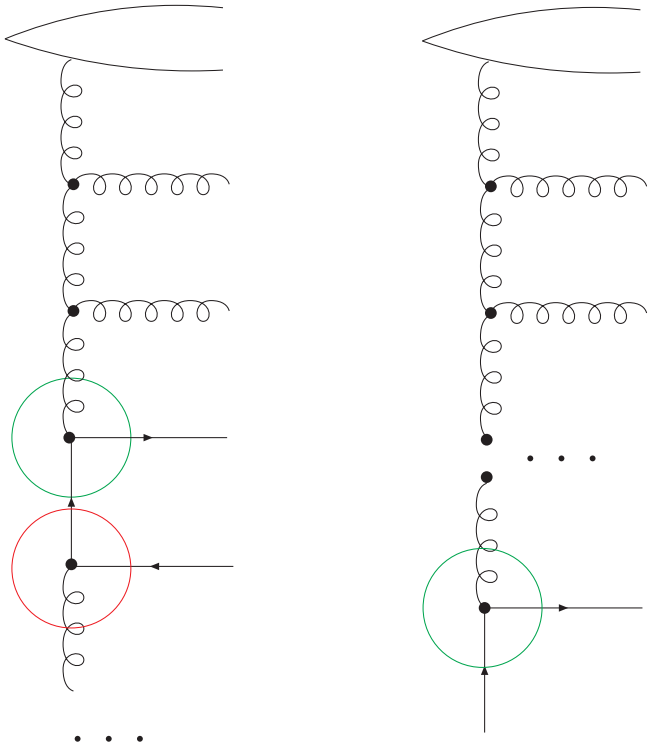

Figure 2.4: Quark and gluon ladder

there is another process which can produce large energy logarithms, namely a s-channel gluon emission. The two basic blocks of our ladder are then shown in Fig. 2.5.

Consider now the kinematics. In the $P\gamma^*$ center of mass frame we can write $p = (P, 0, 0, P)$, $q = \left(\sqrt{-Q^2 + P^2}, 0, 0, -P\right)$, hence $\sqrt{s} = E_P + E_{\gamma^*} = \sqrt{-Q^2 + P^2} + P$ and $P = \left(Q^2 + s\right) / \left(2\sqrt{s}\right)$. In the high energy limit $s \gg Q^2$ then we can write $p = \sqrt{s}/2(1, 0, 0, 1)$, $q = \sqrt{s}/2(1, 0, 0, -1)$. We can use these vectors as a basis for a Sudakov parametrization:

$$k_i = x_i p + y_i q + \mathbf{k}_i, \tag{2.9}$$

where $\mathbf{k}_i$ is the transverse momentum.
We want now to evaluate the phase space for the gluon ladder. For simplicity, we don't consider the dipole-proton interaction but a simpler process, namely a $q\bar{q}$ scattering with gluon emission. One can easily convince oneself that the results hold also in the $q\bar{q} - P$ case.

Consider then the $q\bar{q} \to q\bar{q} + g + g$ process shown in Fig 2.6, where the blob A represents one of the graphs in Fig. 2.5. In this case l_1 plays the role of p and l_2 of q, that is $k_i = x_i l_1 + y_i l_2 + \mathbf{k}_i$.

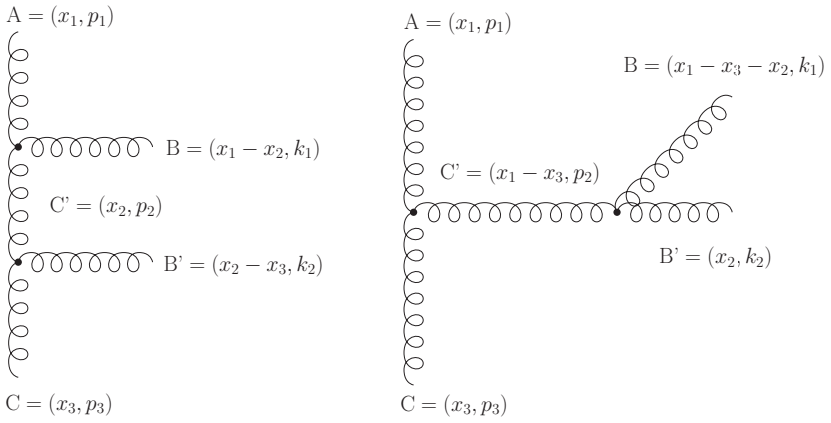

Diagrams for gluon emission contributing to the BFKL kernel χ_0. For each line the parton's energy (in units of p) and transverse momentum are indicated.

Figure 2.5: BFKL ladder building blocks

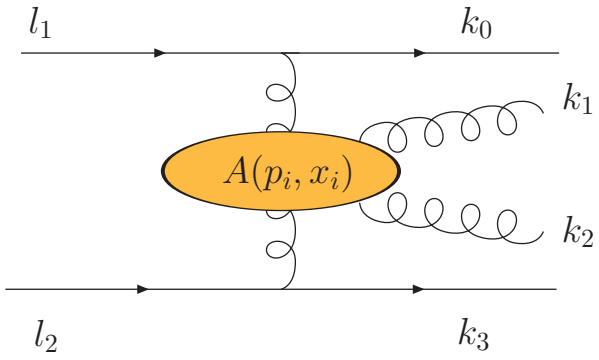

Figure 2.6: t-channel gluon emission

In the following we will assume that A stands for the t-channel gluon emission (Fig. 2.5 on the left). It can be shown with a similar procedure that the results are the same for the s-channel emission (Fig. 2.5 on the right).
Neglecting all the quark masses we can write the phase space for our process as

$$\int d\Phi_{2+2} = \int \frac{d^4k_0}{(2\pi)^3}\frac{d^4k_3}{(2\pi)^3}\frac{d^4k_1}{(2\pi)^3}\frac{d^4k_2}{(2\pi)^3}\delta\left(k_0^2\right)\delta\left(k_3^2\right)\delta\left(k_1^2\right)\delta\left(k_2^2\right)\cdot$$

$$\cdot(2\pi)^4\delta_4\left(l_1+l_2-k_0-k_3-k_1-k_2\right) = \frac{1}{(2\pi)^8}\int d^4p_1 d^4p_2 d^4p_3\cdot$$

$$\cdot\delta\left(\left[l_1-p_1\right]^2\right)\delta\left(\left[l_2+p_3\right]^2\right)\delta\left(\left[p_2-p_3\right]^2\right)\delta\left(\left[p_2-p_1\right]^2\right), \qquad (2.10)$$

where we have used in the first step the momentum-conservation δ_4 to eliminate the integration over k_2 and in the second step we have performed the change of variables $k_0 = l_1 - p_1$, $k_3 = l_2 + p_3$, $k_2 = p_2 - p_3$ and $k_1 = p_1 - p_2$. In the Sudakov parametrization Eq. (2.10) becomes

$$\int d\Phi^{2+2} = \left(\frac{s}{2}\right)^{1+2} \left(\frac{1}{2\pi}\right)^{(2+2)\cdot 3-4} \int \left(\prod_{i=1}^{2+1} dx_i dy_i d^2\mathbf{p}_i\right) \delta\left(-sy_1(1-x_1) - \mathbf{p}_1{}^2\right) \cdot$$

$$\cdot\delta\left(sx_3(x_3+y_3) - \mathbf{p}_3{}^2\right) \prod_{i=1}^{2} \delta\left(s(x_i - x_{i+1})(y_i - y_{i+1}) - (\mathbf{p}_i - \mathbf{p}_{i+1})^2\right), \qquad (2.11)$$

with the obvious n-gluon generalization

$$\int d\Phi^{2+n} = \left(\frac{s}{2}\right)^{1+n} \left(\frac{1}{2\pi}\right)^{3n+2} \int \left(\prod_{i=1}^{n+1} dx_i dy_i d^2\mathbf{p}_i\right) \delta\left(-sy_1(1-x_1) - \mathbf{p}_1{}^2\right) \cdot$$

$$\cdot\delta\left(sx_{n+1}(x_{n+1}+y_{n+1}) - \mathbf{p}_{n+1}^2\right) \prod_{i=1}^{n} \delta\left(s(x_i - x_{i+1})(y_i - y_{i+1}) - (\mathbf{p}_i - \mathbf{p}_{i+1})^2\right). \qquad (2.12)$$

The form (2.12) is totally generic, while we are interested in the leading log x (LLx) region. One can see that large x-logarithms arises by strong ordering of longitudinal momenta, that is $x_1 \gg x_2 \gg ... \gg x_{n+1}$, $|y_1| \ll ... \ll |y_{n+1}|$. Indeed it is easy to see that in this regime the phase space factor Eq. (2.12) simplifies to

$$\int d\Phi^{2+n} = \left(\prod_{i=1}^{n} \int_{x_{i+1}}^{1} \frac{dx_i}{x_i}\right) \prod_{i=1}^{n+1} d^2\mathbf{p}_i, \qquad (2.13)$$

with $|y_1| \approx \mathbf{p}_1{}^2/s$ and $x_{n+1} \approx \mathbf{p}_{n+1}^{\ 2}/s$. We recognize immediately the "logarithmic" term $\int_x^1 dx_1/x_1 \int_{x_1}^1 dx_2/x_2 ... \cdot \int_{x_{n-1}}^1 dx_n/x_n = 1/n! \log^n(1/x)$.
Consider now an evolution from x_0 to x, with both x_0 and x small, say $O(1/s)$ (and the same for y). Then from $s\, x_i y_{i+1} \approx (\mathbf{p}_i - \mathbf{p}_{i+1})^2$ we obtain $\mathbf{p}_i^2 \approx \mathbf{p}_k^2$. Hence the virtual gluons have transverse momenta of the same order. This implies that an emitted gluon has approximatively no transverse momentum. Then, since both x_i and y_i are small and $\mathbf{k}_i \approx 0$, the emitted gluons are soft, that is $k_i \ll l_1, l_2$. Let us summarize the main features of such an emission:

$$1 \ll x_1 \ll ... \ll x_{n+1} \approx \frac{\mathbf{k}^2}{s}, \quad 1 \ll |y_{n+1}| \ll ... \ll |y_n| \approx \frac{\mathbf{q}^2}{s},$$

$$\mathbf{p}_1^{\ 2} \approx \mathbf{p}_2^{\ 2} \approx ... \approx \mathbf{p}_{n+1}^2 \approx \mathbf{q}^2, \quad k_i \ \text{ soft}. \qquad (2.14)$$

Eq. 2.14 defines the *multi-Regge kinematics*. The BFKL theory holds exactly in this regime.

Now we have all the necessary tools to derive the BFKL equation: we can calculate the amplitudes for the graphs in Fig. 2.5 and write a x-evolution equation

exactly in the same way we did for DGLAP in Sec. 1.2.5. This is the fastest way to obtain BFKL, but it is not easily generalised for multiple scattering (i.e. for the non linear evolution). Moreover, the effective calculation is quite long and difficult, mainly because of the virtual corrections. We will adopt then a slightly different technique. BFKL can be viewed as an evolution equation for the probability that the gluon on the bottom of the ladder is generated by a parent gluon on the top through a x evolution. In the following we will derive a generating functional for this probability. Of course this is rather an awkward way to obtain BFKL, but with our generating functional we will be able to consider multiple scattering and hence to obtain in Sec. 2.4 the BK equation.

Our derivation of this generating functional will go through some steps. First we will calculate the probability P_n that our original $q\bar{q}$ dipole emits n gluons and express it through a generating functional. Then we will rewrite this generating functional in terms of creation/annihilation operators. This will enable us to evaluate the gluon ladder diagram and hence to obtain the BFKL equation. From the very beginning of our derivation we will work in the large-N_c limit (see Appendix A if you are not familiar with the large-N_c expansion). At the end we will show that for BFKL this is not an approximation, indeed all the leading log terms of BFKL are also leading N_c. Unfortunately this is not the case for the non linear generalizations.

2.3.2 The dipole branching generating functional

In order to obtain the probability for the n gluon emission, we first need the amplitude for the process $q\bar{q} \to q\bar{q} + ng$. We may write this amplitude as a wave function:

$$\psi^{(n)}_{\alpha\beta}(k_1, k_2, ..., k_n) = \langle \bar{q}_\beta(q - k_1 - k_2 - ... - k_n)\ q_\alpha(k_1)\ g(k_2)...g(k_n)|\psi\rangle\,, \quad (2.15)$$

where α and β are spinor indexes and $|\psi\rangle$ stands for our quark-antiquark pair (onium) of momentum q. Of course if $\alpha_s = 0$ we have $\left|\psi^{(0)}\right|^2 = 1$ and $\psi^{(n)} = 0$ for $n \neq 0$ (obviously as long as only QCD is involved).

We will work in the multi-Regge kinematic regime of strong longitudinal ordered ($(1-x_1), x_1 \gg x_2 \gg x_3...$) and soft ($k_i \ll k_1, k_0$) gluons. We will parametrize the emitted gluon four momenta and polarizations as

$$k_i = x_i p + y_i \eta + \mathbf{k}_i, \qquad \epsilon_i = \omega_i \eta + \epsilon_i, \quad (2.16)$$

with $p = (Q, 0, 0, Q)$ and $\eta = 1/(2Q)(1, 0, 0, -1)$. Note that x_i are defined as in the previous section (remembering the multi-Regge kinematics we have $x_i - x_{i+1} \approx x_i$), while y and ω are easily calculated respectively from the on-shell and transversality conditions:

$$y = \frac{\mathbf{k}^2}{x}, \qquad \omega = \frac{\mathbf{k}\cdot\epsilon}{x}. \quad (2.17)$$

In the multi-Regge regime we can use the *eikonal approximation*: we write the qqg vertex as $\bar{g}_s u(k_q + k_g)\gamma^\mu u(k_q) \approx g_s u(k_q)\gamma^\mu u(k_q) = 2g_s k_q^\mu$. This holds up to terms

which are suppressed by powers of x. Note that from this it follows that a quark propagates as a scalar particle. That is, when gluons are soft we can neglect the spin of the quarks.

We are ready now to calculate our wave function. We start with the simplest case, that is with $\psi^{(1)}$. The relation between this and the 0-gluon wave function is depicted in Fig. 2.7. Suppose we know $\psi^{(0)}$. Then we can evaluate $\psi^{(1)}$ by

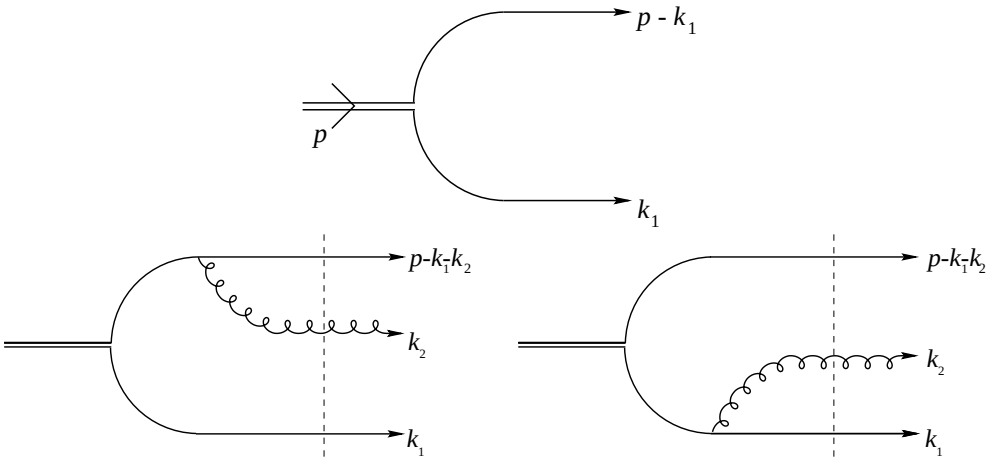

Figure 2.7: 0-gluon and 1-gluon onium wave functions

simply evaluating the Feynman graphs in Fig. 2.7. Up to an overall phase factor the result is:

$$\psi^{(1)}(k_1,k_2) = g_s t^A \left[\psi^{(0)}(k_1)\frac{k_0\cdot\epsilon_2}{k_0\cdot k_2} - \psi^{(0)}(k_1+k_2)\frac{k_1\cdot\epsilon_2}{k_1\cdot k_2}\right], \tag{2.18}$$

which in the multi-Regge limit simplifies to

$$\psi^{(1)}(\mathbf{k}_1,x_1,\mathbf{k}_2,x_2) \approx 2g_s t^A \left[\psi^{(0)}(\mathbf{k}_1,x_1) - \psi^{(0)}(\mathbf{k}_1+\mathbf{k}_2,x_1)\right]\frac{\mathbf{k}_2\cdot\epsilon_2}{\mathbf{k}_2^2}. \tag{2.19}$$

We see that the 1-gluon wave function is created from different configurations of the 0-gluon function. When we add more gluons, the number of possible configurations grows and the resulting function is very difficult to deal with. The situation is simplified if we Fourier-transform the transverse momenta:

$$\psi^{(n-1)}(\mathbf{b}_1,x_1,...,\mathbf{b}_n,x_n) = \int\prod_{i=1}^{n}\frac{d^2\mathbf{k}_i}{(2\pi)^2}e^{i\mathbf{k}_i\cdot\mathbf{b}_i}\psi^{(n-1)}(\mathbf{k}_1,x_1,...,\mathbf{k}_n,x_n). \tag{2.20}$$

Using the well-known result $\mathcal{F}\left[\mathbf{a}\cdot\mathbf{k}/\mathbf{k}^2\right] = i/(2\pi)\ \mathbf{a}\cdot\mathbf{b}/\mathbf{b}^2$ we obtain (once again neglecting an overall phase factor):

$$\psi^{(1)}(\mathbf{b}_1,x_1,\mathbf{b}_2,x_2) = \frac{g_s}{\pi}t^A\psi^{(0)}(\mathbf{b}_1,x_2)\left(\frac{\mathbf{b}_{02}}{b_{02}^2} - \frac{\mathbf{b}_{12}}{b_{12}^2}\right)\cdot\epsilon_2, \tag{2.21}$$

with $\mathbf{b}_{ij} \equiv \mathbf{b}_j - \mathbf{b}_i$, $\mathbf{b}_0 \equiv 0$.

What we are interested in is not the amplitude associated to the gluon emission, but its probability. We have then to evaluate the square of the wave function, summed over all colours and polarizations and integrated over the phase space, that is

$$\Phi^{(1)}(\mathbf{k}_1, x_1) = \sum_{col,\ hel} \int \frac{d^2\mathbf{k}_2}{2(2\pi)^3} \frac{dx_2}{x_2} \left| \psi^{(1)}(\mathbf{k}_1, x_1, \mathbf{k}_2, x_2) \right|^2 . \tag{2.22}$$

In terms of transverse coordinates we obtain

$$\Phi^{(1)}(\mathbf{b}_1, x_1) = \int_\rho d^2\mathbf{b}_2 \int_{x_0}^{x_1} \frac{dx_2}{x_2} \frac{\alpha_s C_F}{\pi^2} \frac{b_{01}^2}{b_{02}^2 b_{12}^2} \Phi^{(0)}(\mathbf{b}_1, x_1), \tag{2.23}$$

where ρ and x_0 are just cutoffs that will not appear in physical quantities. The integrand on the r.h.s. can be rewritten as

$$C_F \frac{b_{01}^2}{b_{02}^2 b_{12}^2} = C_F \left(\frac{1}{b_{02}^2} + \frac{1}{b_{12}^2} - \frac{2\mathbf{b}_{02} \cdot \mathbf{b}_{12}}{b_{02}^2 b_{12}^2} \right). \tag{2.24}$$

These terms are shown in Fig. 2.8 in the double-line representation. The first two terms correspond to the top two graphs, while the interaction term corresponds to the bottom ones.

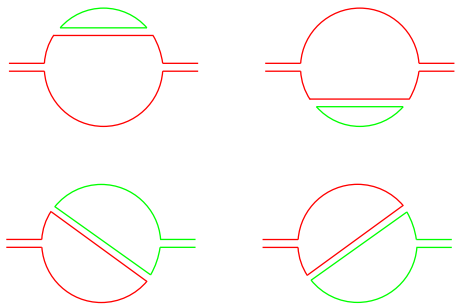

Figure 2.8: 1-gluon contributions to the onium squared wave function

All these contributions arise from planar graphs with one boundary quark loop. For large N_c we may then expect a behaviour like N_c. Indeed this is the case, since $C_F \to N_c/2$ in this limit.

Consider now the emission of an additional gluon. We have to evaluate two classes of diagrams, illustrated in Fig. 2.9. Graphs similar to A are planar, hence they have a colour factor $O(N_c)$, while graphs similar to B have only one colour loop and are associated with a colour factor $O(1/N_c)$. In the large-N_c approximation we retain only planar graphs. Consider the non-planar graph Fig. 2.9B. It corresponds to the interference between different dipoles. One can easily convince oneself that this is the case for all non-planar graphs. Our approximation hence corresponds to neglecting interference effects.

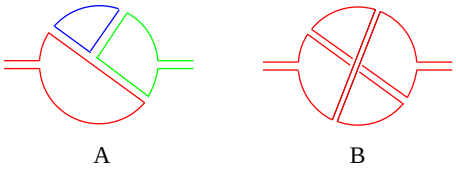

Figure 2.9: 2-gluon contributions to the onium squared wave function

Planar graphs can be thought of as composed by colour dipoles: the emission of the first gluon converts a single colour dipole into two colour dipoles. The "quark part" of the gluon line forms a colour dipole with the antiquark and conversely for the "antiquark part". From each new dipole a new gluon can be emitted. Obviously the emission of a quark part and of an actual quark would be in general different. But in the multi-Regge regime the only ggg relevant coupling for the emission of a soft gluon 3 from a gluon 2 is $2g_s k_2 \cdot \epsilon_3$, that is the emission of a dipole quark part is exactly the same as an emission of an actual quark (it can be easily shown that the quartic interaction is suppressed by factors of the form x_3/x_2).
Neglecting all the interferences, we obtain for the two-gluon emission the factorized form:

$$\Phi^{(2)}(\mathbf{b}_1, x_1) = \int d^2\mathbf{b}_2 d^2\mathbf{b}_3 \int_{x_0}^{x_1} \frac{dx_2}{x_2} \int_{x_2}^{x_1} \frac{dx_3}{x_3} I_{01\to 2} \left(I_{21\to 3} + I_{02\to 3}\right) \Phi^{(0)}, \quad (2.25)$$

where $I_{ij\to k}$ is the factor associated to the splitting of the dipole ij due to the emission of k:

$$I_{ij\to k} = \frac{\alpha_s C_F}{\pi^2} \frac{b_{ij}^2}{b_{ik}^2 b_{jk}^2} \to \frac{\alpha_s N_c}{2\pi^2} \frac{b_{ij}^2}{b_{ik}^2 b_{jk}^2}. \quad (2.26)$$

One can easily convince oneself that also the n-gluon term will be factorized in multiple splittings. This is the power of the large-N_c approximation: we can neglect interferences and then obtain the desired probability in a factorized form.

From this factorized form we could easily write down a BFKL equation for the unintegrated onium gluon distribution (see e.g. [2]). However we want a formulation that can be easily generalized to the case of multiple scattering, hence we must push the formalism a little further.
We can express the features of the dipole branching using a generating functional $Z(b_{01}, \xi_1, \xi, u)$. We define Z such that the probability of finding n dipoles of transverse size c with rapidity less than ξ generated from a parent of size b_{01} and rapidity ξ_1 is[1]

$$P_n(b_{01}, \xi_1, \xi, c) = \frac{1}{n!} \frac{\delta^n Z(b_{01}, \xi_1, \xi, u)}{\delta u(c)^n}\bigg|_{u=0}. \quad (2.27)$$

[1]Note that our definition of Z is slightly different from [21].

It is easy to obtain a perturbative equation for Z. In the trivial case $\alpha_s = 0$ we can have only the original dipole, that is $P_1(b_{01}, \xi_1, \xi, c) = \delta(b_{01} - c)$, (in the spirit of the multi-Regge kinematics we assume $\xi > \xi_1$), $P_n = 0$ for $n \neq 1$. Hence we can write $Z(b_{01}, \xi_1, \xi, u) = u(b_{01}) + O(\alpha_s)$. At the next order in α_s we may have one gluon emission, i.e. one dipole splitting. The probability for the splitting $b_{01}(\xi_1) \to b_{12} + b_{02}(\xi_2 < \xi)$ (that is for the emission of a gluon with transverse size b_2 and rapidity less than ξ) is

$$\tilde{P}(b_{01}, \xi_1, \xi, b_2) = \int_{\xi_1}^{\xi} d\xi_2 I_{01\to 2} \Phi^{(0)}(b_{01}, \xi_1) = \int_{\xi_1}^{\xi} d\xi_2 I_{01\to 2} + O(\alpha_s^2). \tag{2.28}$$

Then we have $P_2(b_{01}, \xi_1, \xi, b_2, b_3) = \tilde{P}(b_{01}, \xi_1, \xi, b_2)\delta(b_3 - b_{12})$+permutations, hence

$$Z(b_{01}, \xi_1, \xi, u) = u(b_{01}) + \int d^2\mathbf{b}_k \int_{\xi_1}^{\xi} dy I_{01\to k} u(b_k) u(b_{1k}) + O(\alpha_s^2). \tag{2.29}$$

By iterating this procedure it is easy to see that in the multi-Regge kinematics the full result is

$$Z(b_{01}, \xi_1, \xi, u) = u(b_{01}) + \int d^2\mathbf{b}_k \int_{\xi_1}^{\xi} dy I_{01\to k} Z(b_k, y, u) Z(b_{1k}, y, u). \tag{2.30}$$

This equation express nothing but the factorization of the probability, with the "branching ratio" given by $I_{ij\to k}$, as shown in Fig. 2.10.

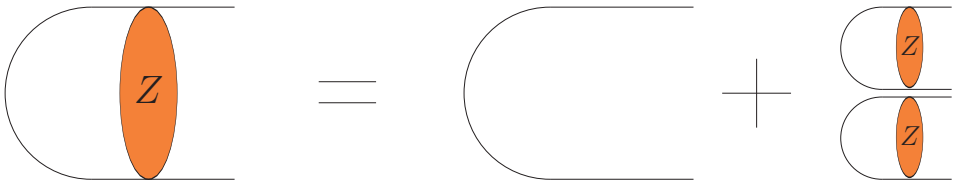

Figure 2.10: Graphical representation of Eq. (2.30)

However Eq. (2.30) can't be true. Consider indeed the normalization condition $\sum_n P_n = 1$. From Eq. (2.30) it follows $Z|_{u=0} = 0$, then we can write:

$$\sum_{n=1}^{\infty} P_n = \sum_{n=0}^{\infty} \left.\frac{\delta^n Z}{\delta u^n}\right|_{u=0} \cdot 1^n = Z|_{u=1}. \tag{2.31}$$

Now, it is easy to see from Eq. (2.30) that $Z|_{u=1} \neq 1$. This is because until now we have considered only real emissions, neglecting virtual corrections. The fastest way to encorporate these effects is to enforce the condition $Z = 1$ order by order in perturbation theory.
Start from $O(\alpha_s)$. From (2.30) we obtain

$$Z(b_{01}, \xi_1, \xi, 1) = 1 + \alpha_s \frac{C_F}{\pi^2}(\xi - \xi_1) \int_{\rho} \frac{d^2\mathbf{b}_k}{b_k^2 b_{1k}^2} b_{01}^2 + O(\alpha_s^2) =$$

$$= 1 + \alpha_s \frac{C_F}{\pi^2}(\xi - \xi_1) 4\pi \log\left(\frac{b_{01}}{\rho}\right) + O(\alpha_s^2). \tag{2.32}$$

In order to keep the correct normalization we must then shift the coefficient of the linear term in u from 1 to $1 - 4\alpha_s \frac{C_F}{\pi}(\xi - \xi_0)\log(b_{01}/\rho)$:

$$Z(b_{01}, \xi_1, \xi, u) = u(b_{01}) \left(1 - 4\alpha_s \frac{C_F}{\pi}(\xi - \xi_1)\log(b_{01}/\rho)\right) +$$

$$+ \int d^2\mathbf{b}_k \int_{\xi_1}^{\xi} dy I_{01\to k} Z(b_k, y, u) Z(b_{1k}, y, u) + O(\alpha_s^2) \tag{2.33}$$

Iterating this procedure we obtain for Z the correct result

$$Z(b_{01}, \xi_1, \xi, u) = u(b_{01}) \exp\left[-\frac{4\alpha_s C_F}{\pi} \log\left(\frac{b_{01}}{\rho}\right)(\xi - \xi_1)\right] +$$

$$\int d^2\mathbf{b}_k \int_{\xi_1}^{\xi} dy\; e^{-\frac{4\alpha_s C_F}{\pi}\log\left(\frac{b_{01}}{\rho}\right)(\xi - y)} I_{01\to k} Z(b_k, y, u) Z(b_{1k}, y, u). \tag{2.34}$$

2.3.3 The generating functional in operator language

In the previous section we have obtained a generating functional for the probability of the process $q\bar{q} \to q\bar{q} + ng$, with each gluon characterised by a transverse coordinate b_i (the Fourier transform of its transverse momentum) and having rapidity ξ_i less than a choosen value ξ. Moreover, in deriving Eq. (2.34) we have supposed $\xi_1 < \xi_2 < ... < \xi_n$, i.e. each splitting leads to an increase in rapidity. This is not yet what we need, that is an equation which describes the rapidity evolution of our original gluon ladder. In order to obtain such an equation we must rewrite our generating functional in terms of creation and annihilation operators. Within this approach indeed we will be able to link the gluon ladder with the generating functional. The evolution of the former will then follow immediately from the evolution of the latter. In this section therefore we will build up the operator formalism, while in the next one we will show the link between Z and the gluon ladder.

What we want to describe is the evolution in rapidity of an ensemble of dipoles. We will use an approach analogous to the classical perturbation theory in the interaction picture, with ξ playing the role of the time variable. We start by defining the states of our theory. To this purpose we define an operator $a^\dagger(\mathbf{b})$, which creates a dipole with transverse momentum $\mathbf{b}$, and an analogous annihilation operator $a(\mathbf{b})$, with fundamental commutator

$$\left[a(\mathbf{b}), a^\dagger(\mathbf{b}')\right] = \delta(\mathbf{b} - \mathbf{b}'). \tag{2.35}$$

The basic process of the theory is dipole branching, leading to a triple-dipole vertex carrying a factor $I_{ij\to k}$. We must consider the virtual correction too. From

(2.34) we obtain that the matrix element for the process $b_{01} \to b_{01}$ is not 1 but $1 - \int d^2\mathbf{b}_2 I_{01\to 2}$, thus in this case also we have a factor $I_{ij\to k}$. These interaction vertices are resumed in Fig. 2.11, where a double line stands for a dipole (note that this has nothing in common with the 't Hooft double line representation).

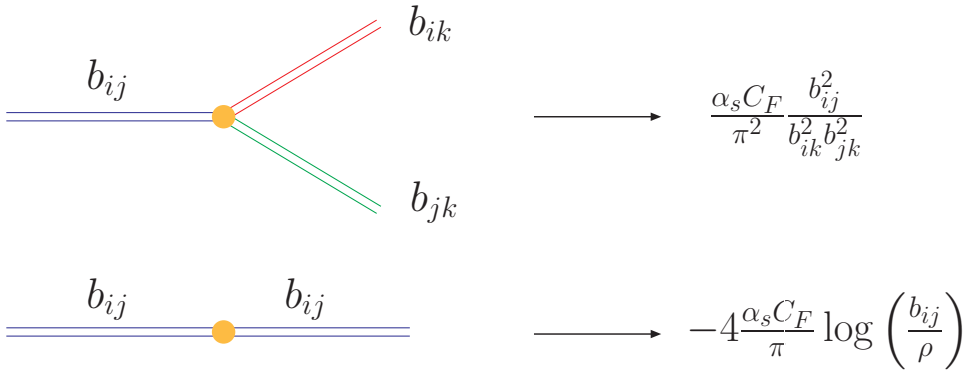

Figure 2.11: Feynman rules for the dipole picture

Our interaction Hamiltonian will be then $V = V_{real} + V_{virtual}$, with

$$V_{real} = \int d^2\mathbf{b}_{01} d^2\mathbf{b}_2 I_{01\to 2}\; a^\dagger(\mathbf{b}_2) a^\dagger(\mathbf{b}_{12}) a(\mathbf{b}_{01}) =$$

$$= \frac{\alpha_s C_F}{\pi^2} \int \frac{a^2}{b^2 c^2} \delta(\mathbf{a}+\mathbf{b}+\mathbf{c}) a^\dagger(\mathbf{b}) a^\dagger(\mathbf{c}) a(\mathbf{a})\; d^2\mathbf{a}\; d^2\mathbf{b}\; d^2\mathbf{c} \qquad \text{and}$$

$$V_{virtual} = -\int d^2\mathbf{b}_{01} d^2\mathbf{b}_2 I_{01\to 2}\; a^\dagger(\mathbf{b}_{01}) a(\mathbf{b}_{01}) =$$

$$= -\frac{4\alpha_s C_F}{\pi} \int d^2\mathbf{b} \log\left(\frac{\mathbf{b}}{\rho}\right) a^\dagger(\mathbf{b}) a(\mathbf{b}). \tag{2.36}$$

Consider now $P_k(\mathbf{b}_1, \xi_1, \xi, \mathbf{b}_2, ..., \mathbf{b}_k)$ in the operator approach. First of all we must create the dipole $\mathbf{b}_1$. Then we have to evolve in rapidity, considering all the possible branchings. Assume the rapidity is increased in $(\xi - \xi_1)/\delta\xi$ small steps. For each step the branchings are determined by the operator $1 + V\delta\xi$, hence we can write the rapidity-evolved state $|\mathbf{b}_1'\rangle$ as

$$|\mathbf{b}_1'\rangle = (1 + V\delta\xi)^{(\xi-\xi_1)\delta\xi} |\mathbf{b}_1\rangle . \tag{2.37}$$

In order to obtain P_k, all we have to do is to project $|\mathbf{b}_1'\rangle$ over the k-dipole state $\langle \mathbf{b}_2, ..., \mathbf{b}_k|$. In the limit $\delta\xi \to 0$ we obtain

$$P_k(\mathbf{b}_1, \xi_1, \xi, \mathbf{b}_2, ..., \mathbf{b}_k) = \left\langle 0 \left| a(\mathbf{b}_2)...a(\mathbf{b}_k) e^{V(\xi-\xi_1)} a^\dagger(\mathbf{b}_1) \right| 0 \right\rangle . \tag{2.38}$$

Note that because of our definition of V this is in fact a probability, and not an amplitude (and correspondingly a Feynman graph built up from Fig. 2.11 is in fact the square of a traditional Feynman graph, integrated over the phase space). From Eq. (2.38) it follows immediately an analogous expression for the generating functional Z:

$$Z(\mathbf{b}_1,\xi_1,\xi,u)=\left\langle 0\left|\exp\left(\int d^2\mathbf{c}\ u(\mathbf{c})a(\mathbf{c})\right)e^{V(\xi-\xi_1)}a^\dagger(\mathbf{b}_1)\right|0\right\rangle. \tag{2.39}$$

In order to verify that Eq. (2.39) is the correct form for Z, let us check the condition $Z|_{u=1}=1$. To simplify this calculation we must rewrite (2.39) in a slightly different way. We introduce the notation

$$a_u\equiv\int d^2\mathbf{b}a(\mathbf{b})u(\mathbf{b}),\qquad \left[a_u,a^\dagger(\mathbf{b})\right]=u(\mathbf{b}). \tag{2.40}$$

From this, using the Baker-Campbell-Hausdorff formula, it follows

$$\left[e^{a_u},a^\dagger(\mathbf{b})\right]=\left(\left[a_u,a^\dagger(\mathbf{b})\right]+\frac{1}{2}\left[a_u,\left[a_u,a^\dagger(\mathbf{b})\right]\right]+...\right)e^{a_u}=u(\mathbf{b})e^{a_u} \tag{2.41}$$

and hence

$$e^{a_u}f\left(a^\dagger(\mathbf{b})\right)=f\left(a^\dagger(\mathbf{b})+u(\mathbf{b})\right)e^{a_u}. \tag{2.42}$$

Since $e^{a_u}|\,0\rangle=|\,0\rangle$, we can then rewrite Eq. (2.39) as (dropping ξ_1):

$$Z(\mathbf{b}_1,\xi,u)=\left\langle 0\left|\exp\left((V(a,a^\dagger+u)\xi\right)\left(a^\dagger(\mathbf{b}_1)+u(\mathbf{b}_1)\right)\right|0\right\rangle, \tag{2.43}$$

with

$$V\left(a,a^\dagger+u\right)=\frac{\alpha_sC_F}{\pi^2}\int d^2\mathbf{a}\ d^2\mathbf{b}\ d^2\mathbf{c}\ \frac{a^2}{b^2c^2}\delta(\mathbf{a}+\mathbf{b}+\mathbf{c})\cdot$$
$$\cdot\left[\left(a^\dagger_{\mathbf{b}}a^\dagger_{\mathbf{c}}a_{\mathbf{a}}+u_{\mathbf{b}}a^\dagger_{\mathbf{c}}a_{\mathbf{a}}+a^\dagger_b u_{\mathbf{c}}a_{\mathbf{a}}+u_{\mathbf{b}}u_{\mathbf{c}}a_{\mathbf{a}}\right)-\left(a^\dagger_{\mathbf{a}}a_{\mathbf{a}}+u_{\mathbf{a}}a_{\mathbf{a}}\right)\right]. \tag{2.44}$$

If $u=1$ the linear term in a cancels, leaving only terms of the form $a^\dagger a$ or $a^\dagger a^\dagger a$. Then

$$\left\langle 0\left|e^{V(a,a^\dagger+1)}a^\dagger\right|0\right\rangle=0,\qquad \left\langle 0\left|e^{V(a,a^\dagger+1)}\cdot 1\right|0\right\rangle=1, \tag{2.45}$$

leading to the desired condition $Z|_{u=1}=1$.

2.3.4 The gluon ladder from the generating functional

Consider again Eq. (2.39), and expand the exponential e^{a_u}. Then Z becomes:

$$Z(\mathbf{b}_1,\xi,u)=P_{\mathbf{b}_1\to 0}+$$
$$+\int d^2\mathbf{b}_2u(\mathbf{b}_2)P_{\mathbf{b}_1\to b_2}+\frac{1}{2}\int d^2\mathbf{b}_2d^2b_3u(\mathbf{b}_2)u(\mathbf{b}_3)\left(P_{\mathbf{b}_1\to b_2b_3}+P_{b_1\to b_3b_2}\right)+... \tag{2.46}$$

Figure 2.12: Feynman rule for an external field u

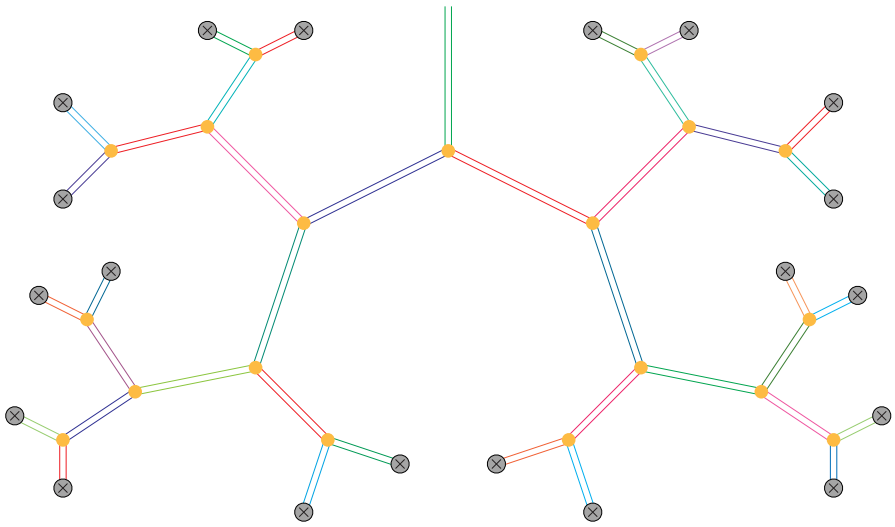

Figure 2.13: Graphical representation of a term contributing to Z

We can think of u as an external field coupled to our dipoles, with the associated Feynman rule shown in Fig. 2.12:
A typical contribution to the sum (2.46) is depicted in Fig. 2.13. By differentiating once w.r.t. u we select a dipole in the final state, thus differentiate w.r.t. u corresponds to cutting away a crossed external vertex and replacing it by an effective dipole. Consider now the external legs ending on a crossed vertex. Putting $u = 0$ or $u = 1$ corresponds respectively to destroying these legs or to summing over all the possible configurations (i.e. summing over all the possible dipole emissions), see Eq. (2.46).

Now we are ready to state the main result of the dipole approach to BFKL. Define

$$n_k\left(\mathbf{b}_0, \xi_0, \xi, b_1, b_2, ..., b_k\right) = \left.\frac{\delta^k Z(\mathbf{b}_0, \xi_0, \xi, u}{\delta u(\mathbf{b}_1)\delta u(\mathbf{b}_2)...\delta u(\mathbf{b}_k)}\right|_{u=1}, \tag{2.47}$$

then n_k represents the *inclusive* probability for the process $\mathbf{b}_0 \to b_1 + \mathbf{b}_2 + ... + \mathbf{b}_k$, obtained through an evolution in rapidity. Here inclusive means that we sum over all the possible dipole emissions.

Let us now go back to gluon-language. Then n_k gives the probability that a gluon $\mathbf{b}_0$ of rapidity ξ_0 evolves to a collection of k gluons with rapidities $\xi_0 < \xi_i \leq \xi$

through all the possible intermediate emissions of gluons. In particular, note that n_1 is nothing but our resummed gluon ladder! Moreover, this is exactly our ladder, hence in this case the large N_c limit is not an approximation.
In Fig. 2.14 we show some of the typical Feynman graphs resummed by n_k. These diagrams are usually referred as *fan graphs*.

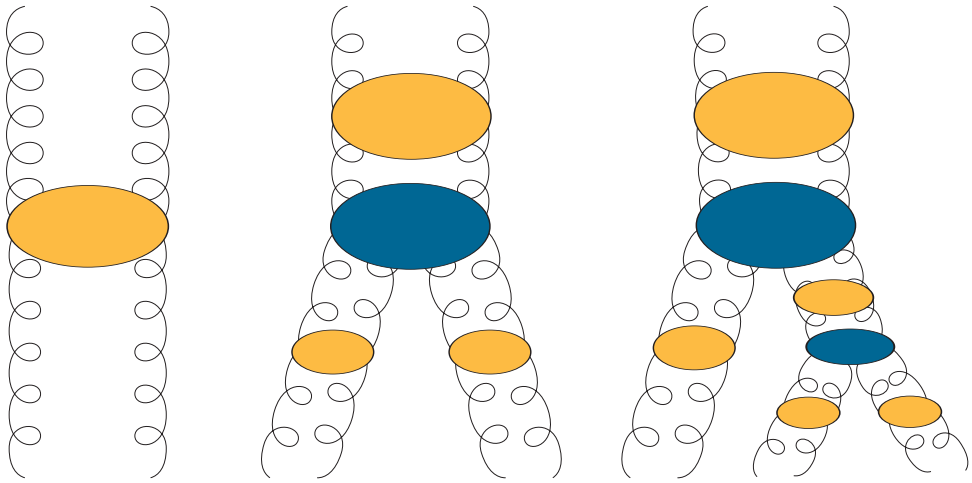

Representation of n_1, n_2, n_3. The yellow blob is the BFKL kernel Γ.

Figure 2.14: Ladder and fan graphs

2.3.5 The BFKL equation

Now we have all that we need to obtain the BFKL equation for the dipole cross section N.

We start by writing an evolution equation for n_1. From Eq. (2.34) it follows that

$$n_1(\mathbf{b}_{01},\xi,\mathbf{c}) = \delta(\mathbf{c}) \exp\left[-4\frac{\alpha_s C_F}{\pi}\log\left(\frac{b_{01}}{\rho}\right)\ \xi\right]\cdot$$
$$\cdot\frac{\alpha_s C_F}{\pi^2}\int_0^\xi dy e^{-4\frac{\alpha_s C_F}{\pi}\log\frac{b_{01}}{\rho}\ (\xi-y)}\int d^2\mathbf{b}_2\frac{b_{01}^2}{b_{12}^2 b_2^2}\left(n_1(\mathbf{b}_{02},\xi,\mathbf{c})+n_1(\mathbf{b}_{12},\xi,\mathbf{c})\right). \tag{2.48}$$

Differentiating w.r.t. ξ and recalling that in the large N_c limit $C_F = N_c/2$ we obtain the evolution equation:

$$\frac{d}{d\xi}n_1(\mathbf{b}_{01},\xi,\mathbf{c}) = \frac{\alpha_s N_c}{2\pi^2}\int d^2\mathbf{b}_2\frac{b_{01}^2}{b_{01}^2 b_2^2}\left(n(\mathbf{b}_2,\xi,\mathbf{c})+n(\mathbf{b}_{12},\xi,\mathbf{c})-n(\mathbf{b}_{01},\xi,\mathbf{c})\right), \tag{2.49}$$

which is the BFKL equation for the kernel n_1. Note that the dependence on the cutoff ρ has disappeared.

Consider now N. Using the k_T factorization we can write N as the convolution of the gluon ladder n_1 and a suitable proton (unintegrated) structure function $\phi_P(\mathbf{c})$:

$$N(\mathbf{b},\xi) = \int\frac{d^2\mathbf{c}}{c^2}\phi_P(\mathbf{c})n_1(\mathbf{b},\xi,\mathbf{c}). \tag{2.50}$$

Then N and n_1 obey the same evolution equation, that is

$$\frac{d}{d\xi}N(\mathbf{b}_1,\xi) = \frac{\alpha_s N_c}{2\pi^2}\int d^2\mathbf{b}_2\frac{b_1^2}{b_2^2 b_{12}^2}\left(N(\mathbf{b}_2,\xi)+N(\mathbf{b}_{12},\xi)-N(\mathbf{b}_1,\xi)\right). \tag{2.51}$$

To solve this it is convenient to consider the M-Mellin transform of N. Writing indeed $N(\mathbf{b},\xi)$ as

$$N(\mathbf{b},\xi) = \int_{c-i\infty}^{c+i\infty}\frac{dM}{2\pi i}\left(\frac{b^2}{c^2}\right)^M N(M,\xi) \tag{2.52}$$

and substituting (2.52) in Eq. (2.51) we obtain

$$\frac{d}{d\xi}N(M,\xi) = \alpha_s\chi_0(M)N(M,\xi), \tag{2.53}$$

with

$$\chi_0(M) = \frac{N_c}{2\pi^2}\int d^2\mathbf{b}^2\frac{b_1^2}{b_2^2 b_{12}^2}\left(\left(\frac{b_2^2}{b_1^2}\right)^M+\left(\frac{b_{12}^2}{b_1^2}\right)^M-1\right). \tag{2.54}$$

This is exactly the BFKL kernel Eq. (1.116).

2.4 Multiple scattering and the BK equation

In the previous section we have shown how the BFKL equation can be derived considering the scattering of a $q\bar{q}$ pair off a proton. In fact, we have considered only single dipole-parton interactions: writing N as the convolution $n_1 \otimes \phi_P$ we have implicitly assumed that the colour dipole "sees" only one parton, characterised by an unintegrated distribution ϕ_P. This approximation is acceptable if Q^2 is high and x is not too small, otherwise the partons within the proton overlap and the $q\bar{q}$ pair no longer sees a single parton. When x is very small then we have to consider interactions with an arbitrary number of partons. This situation is represented graphically in Fig. 2.15. On the left there is only one scattering, leading to the

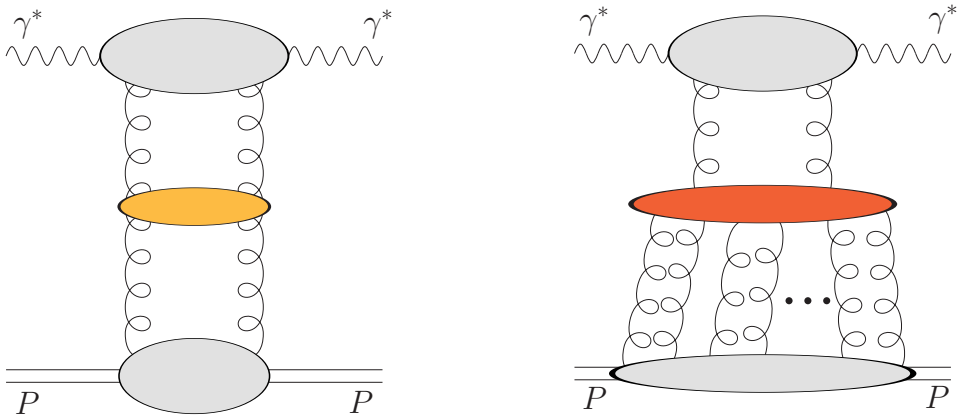

Figure 2.15: Multiple scattering

usual BFKL equation. On the right we have multiple scattering, neglected by the BFKL evolution.
In order to obtain a correct description of the small-x region we must consider all the possible scatterings. Here the power of our formalism becomes apparent: the resummed graphs for multiple scattering are nothing but fan graphs with 2,3,...,k,... endpoints, that is n_2, n_3,..., n_k... Thanks to the generating functional formalism we can take in account all these possible graphs.
The generalisation to multiple scattering is straightforward to obtain:

$$N = n_1 \otimes \phi \longrightarrow N = n_1 \otimes \phi + n_2 \otimes \phi \otimes \phi + ... + n_k \otimes \phi \otimes ... \otimes \phi + ...$$

There is only one subtlety we must be careful with: once convoluted, the gluons become identical particles. Hence we have to divide our probability n_k by $k!$ not to count k times the same configuration. Defining $\tilde{n}_k = n_k/k!$ and using Eq. (2.39) we obtain

$$\tilde{n}_2(\mathbf{b}_0, \xi, \mathbf{b}_1, b_2) = \frac{1}{2!} \left. \frac{\delta^2 Z(\mathbf{b}_0, \xi)}{\delta u(\mathbf{b}_1) \delta u(\mathbf{b}_2)} \right|_{u=1} = \frac{\alpha_s N_c}{2\pi^2} \int_0^\xi dy e^{-2\alpha_s \frac{N_c}{\pi} \log \frac{b_0}{\rho} (\xi - y)}.$$

$$\cdot \int d^2\mathbf{b}_k \frac{b_0^2}{b_k^2 b_{0k}^2} \left(\frac{1}{2!} \left(n^{(2)}_{k,1,2} + n^{(2)}_{0k,1,2} \right) + \frac{1}{2!} \left(n^{(1)}_{k,1} n^{(1)}_{0k,2} + \text{perm.} \right) \right), \tag{2.55}$$

where we set $n^{(k)}_{i,j,...,k+1} = n_k(\mathbf{b}_i, y, \mathbf{b}_j, ..., b_{k+1})$.
Consider the terms in the last line of Eq. (2.55): the $n_2/2!$ terms are nothing but our original $\tilde{n}_2$, while the terms in n_1 under convolution are all the same, giving a net contribution equal to $n_1(\mathbf{b}_k, y, \mathbf{b}_1) n_1(\mathbf{b}_{0k}, y, \mathbf{b}_2)$.
One can easily convince oneself that the solution for $\tilde{n}_i$ is the same as Eq. (2.55), but with the last line substituted by

$$\cdot \int d^2\mathbf{b}_k \frac{b_0^2}{b_k^2 b_{0k}^2} \left(\tilde{n}^{(i)}_{k,1,...,i} + \tilde{n}^{(i)}_{0k,1,...,i} + \sum_{l+m=i} n^{(l)}_{k,1,...,l} n^{(m)}_{0k,l+1,...,m} \right), \tag{2.56}$$

where we neglect the factorials and permutations in the spirit of the future convolution (i.e. Eq. (2.56) is wrong, but under convolution it is equivalent to the true solution).

From n_i we can immediately obtain the dipole cross section $\hat{N}$ (the reason for the hat will be clear in the following) by simply convoluting with ϕ_P and summing over i, with the result

$$\hat{N}(\mathbf{b}, \xi) = \phi_P(\mathbf{b}) e^{-2\alpha_s \frac{N_c}{\pi} \log \frac{b}{\rho} \xi} + \frac{\alpha_s N_c}{2\pi^2} \int_0^\xi dy e^{-2\alpha_s \frac{N_c}{\pi} \log \frac{b}{\rho} (\xi - y)} \cdot$$

$$\cdot \int d^2\mathbf{c} \frac{b^2}{c^2 (c-b)^2} \left(\hat{N}(\mathbf{c}, y) + \hat{N}(\mathbf{c} - \mathbf{b}, y) + \hat{N}(\mathbf{c}, y) \hat{N}(\mathbf{c} - \mathbf{b}, y) \right). \tag{2.57}$$

Assume that $\phi_P(\mathbf{b}) = \phi_P(b)$. Then $\hat{N}(\mathbf{b}, \xi) = \hat{N}(b, \xi)$, since the kernel of Eq. (2.57) depends only on b. This is a reasonable assumption: ϕ_P describes the propagation of a dipole in the proton, which we expect to be isotropic in the transverse plane. In the following we will make this assumption.
Differentiating Eq. (2.57) w.r.t. ξ we obtain the multiple-scattering generalization of the BFKL equation:

$$\frac{d}{d\xi} \hat{N}(b_{01}, \xi) = \frac{\alpha_s N_c}{2\pi^2} \int d^2\mathbf{b}_{02} \frac{b_{01}^2}{b_{02}^2 b_{12}^2} \cdot$$

$$\cdot \left(\hat{N}(b_{02}, \xi) + \hat{N}(b_{12}, \xi) - \hat{N}(b_{01}, \xi) + \hat{N}(b_{02}, \xi) \hat{N}(b_{12}, \xi) \right), \tag{2.58}$$

with initial condition $\hat{N}(\mathbf{b}, 0) = \phi_P(\mathbf{b})$.
However it is not difficult to see that the solution of Eq. (2.58) is always negative. It is convenient then to consider for our dipole forward amplitude not $\hat{N}$ but $N = -\hat{N}$. Then the dipole cross section obeys:

$$\frac{d}{d\xi} N(b_{01}, \xi) = \frac{\alpha_s N_c}{2\pi^2} \int d^2\mathbf{b}_{02} \frac{b_{01}^2}{b_{02}^2 b_{12}^2} \cdot$$

$$\cdot \left(N(b_{02}, \xi) + N(b_{12}, \xi) - N(b_{01}, \xi) - N(b_{02}, \xi) N(b_{12}, \xi) \right), \tag{2.59}$$

Eq. (2.59) is the celebrated Balitsky-Kovchegov (BK) equation. For $N \ll 1$, that is far from the unitarity bound, the BK equation reduces to the usual BFKL. For $N > 1$ its derivative w.r.t. ξ is negative, hence N decreases because of the N^2 term. We see that thanks to the non linear term the problems with unitarity vanish, even for very large ξ.

In order to show in the next section that Eq. (2.59) exhibits geometric scaling it is useful to return to the momentum space. It is also convenient to use a slightly different definition of Fourier transform:

$$N(k,\xi) \equiv \int \frac{d^2\mathbf{b}}{2\pi b^2} e^{-i\mathbf{k}\cdot\mathbf{b}} N(b,\xi), \qquad N(b,\xi) = b^2 \int \frac{d^2k}{2\pi} e^{i\mathbf{k}\cdot\mathbf{b}} N(k,\xi). \tag{2.60}$$

Exploiting the fact that $N(\mathbf{b},\xi) = N(b,\xi)$ Eq. (2.60) can be rewritten as

$$N(k,\xi) = \int_0^\infty \frac{db}{b} J_0(b\,k) N(b,\xi), \qquad N(b,\xi) = b^2 \int_0^\infty k dk J_0(b\,k) N(k,\xi). \tag{2.61}$$

With these definitions the geometric scaling condition now reads

$$N(k,\xi) = N\left(k/Q_s(\xi)\right). \tag{2.62}$$

In momentum space Eq. (2.59) can be written as

$$\frac{d}{d\xi} N(k,\xi) = \bar{\alpha}_s \chi_0(-\partial_L) N(k,\xi) - \bar{\alpha}_s N^2(k,\xi), \tag{2.63}$$

where $\bar{\alpha}_s = \alpha_s N_c/\pi$, χ_0 is the LO BFKL kernel Eq. (1.116) and $L = \log(k^2/k_0^2)$, with k_0 some fixed momentum scale. In the next section we will show that Eq. (2.63) admits scaling solutions.

2.5 Geometric scaling from the BK equation

Because of the non linear term Eq. (2.63) is quite difficult to study. However if we consider the case of a quadratic kernel the theory of non linear differential equations tells us that Eq. (2.63) asymptotically admits a scaling solution. It is interesting to note that this asymptotic behaviour is determinated only by the linear part of the equation, hence is quite general, since we have no doubt about the BFKL equation.
For a generic kernel we don't have similar results. However it is possible to show that in the saturated regime (i.e. where the non linearities become important) the solution exhibits again geometric scaling.

In the next section we will show how geometric scaling arises form the full BK equation but with a quadratic kernel. In Sec. 2.5.2 instead we will derive the geometric scaling using the full kernel but an approximate form of the BK equation.

2.5.1 The quadratic kernel and geometric scaling

Assume the full kernel χ_0 is replaced by its quadratic approximation near the minimum, as in Sec. 1.4.5:

$$\chi_0(-\partial_L) = c + \frac{d}{2}\left(\partial_L + \frac{1}{2}\right)^2 . \tag{2.64}$$

For the (fixed coupling) BFKL equation this should be a good approximation only if $L << \xi$. We may then assume that is the case also for the BK equation. In the quadratic approximation Eq. (2.63) reduces to a well-known differential equation, the Kolmogorov-Petrovsky-Piscounov (KPP) equation. To see how this happens, consider the change of variables:

$$t = \frac{\bar{\alpha}_s d}{2}(1-\bar{\gamma})^2\xi, \qquad x = (1-\bar{\gamma})\left(L + \frac{\bar{\alpha}_s d}{2}\,\xi\right),$$

$$u(t,x) = \frac{2}{d(1-\bar{\gamma})^2}\; N\left(\frac{2t}{\bar{\alpha}_s d(1-\gamma)^2}, \frac{x}{1-\bar{\gamma}} - \frac{t}{(1-\bar{\gamma})^2}\right), \tag{2.65}$$

with $\bar{\gamma} = 1 - \frac{1}{2}\sqrt{1+8c/d}$. Then Eq. (2.63) becomes

$$\partial_t u(t,x) = \partial_x^2 u(t,x) + u(t,x)\,(1-u(t,x))\,, \tag{2.66}$$

that is the KPP equation. It is known since a long time that for a certain class of initial conditions this equation admits a travelling wave solution, that is a solution which is function of $x - m(t)$ only. In terms of N this implies geometric scaling, as we shall now show.
First of all, let us be more specific about the initial conditions. It is known that if we choose an initial condition at time $t = t_0$ such that $u(t_0, x)$ decreases smoothly from 1 to 0 as x goes from $-\infty$ and $+\infty$ and has the asymptotic behaviour

$$u(t_0,x) \sim e^{-\beta x} \quad \text{for } x \to +\infty, \tag{2.67}$$

then the KPP equation admits travelling wave solutions at large times. This means that there exists a function w such that

$$u(x,t) \sim w\left(x - m_\beta(t)\right) \quad \text{for} \quad t \to \infty, \tag{2.68}$$

with

$$m_\beta(t) = \begin{cases} (1/\beta + \beta)t + O(1) & \text{for } \beta < 1 \\ 2t + \frac{1}{2}\log t + O(1) & \text{for } \beta = 1 \\ 2t - \frac{1}{2}\log t + O(1) & \text{for } \beta > 1. \end{cases} \tag{2.69}$$

Assume now to be in the supercritical case $\beta > 1$ (we will see in a while that this should be the case for QCD), then in terms of N Eq. (2.68) becomes

$$N(k,\xi) = N\left(k^2/Q_s^2(\xi)\right), \qquad \text{with } Q_s^2(\xi) = k_0^2 \xi^{-\frac{3}{2(1-\bar{\gamma})}} e^{\bar{\alpha}_s d\left(\frac{1}{2}-\bar{\gamma}\right)\xi}, \tag{2.70}$$

that is the travelling wave solution is nothing but a scaling solution.
Of course all this depends on the initial conditions. Munier and Peschansky (MP) suggested that the intial conditions for QCD could be in fact of the form of Eq.(2.67) [29]. Consider first the limit $x \to \infty$ at fixed $t = t_0$, that is the limit $L \to \infty$, ξ fixed. MP invoked colour transparency, leading to the asymptotic behaviour $N(k,\xi) \propto k^{-2}$. In terms of u this means $u(t_0, x) \sim e^{-\beta x}$, with $\beta = 1/(1-\bar{\gamma}) \approx 1.55$, hence the $x \to \infty$ limit has the correct form. Moreover, $\beta > 1$, then we are in the supercritical region. It has been shown [30] that in the supercritical regime logarithmic corrections to the initial condition (2.67) do not affect the asymptotic behaviour of the solution, that is we have geometric scaling even if $N(k,\xi) \propto k^{-2} \log^m k$. Consider now the limit $u(t_0, -\infty)$, that is $L \to -\infty$, ξ fixed. This is a non perturbative region, but MP suggested that N should have an upper bound because of strong absorption. In terms of u this leads to the desired condition $u(t_0, -\infty) < c$.
Then if these assumptions about the initial conditions are right, the BK equation provides a geometric scaling solution, with saturation scale given in Eq. (2.68). In terms of the Bjorken x the saturation scale reads $Q_s^2(x) = Q_0^2 x^{-\lambda} (\log(x))^{\eta} \approx Q_0^2 x^{-\lambda}$, with $\lambda = \bar{\alpha}_s d \left(\frac{1}{2} - \bar{\gamma}\right)$.

Of course this is an asymptotic results. Munier and Peschansky used a scaling ansatz to derive the principal subasymptotic correction, obtaining:

$$N(k/Q_s(\xi),\xi) = C\sqrt{\frac{2}{\bar{\alpha}_s \chi''(M_s)}} \log\left(\frac{k^2}{Q_s^2(\xi}\right)\left(\frac{k^2}{Q_s^2(\xi}\right)^{-\gamma_c} \cdot$$

$$\cdot \exp\left[-\frac{1}{2\bar{\alpha}_s \chi''(M_s)\xi} \log^2\left(\frac{k^2}{Q_s^2(\xi)}\right)\right], \tag{2.71}$$

with M_s being the solution of $M_s\chi'(M_s) = \chi(M_s)$.
They also tried to generalize these results to the case of running coupling. This is a very delicate point. First of all, we don't know if the BK equation holds also when the coupling runs. Furthermore, we don't know the argument of the running. Several possible arguments have been proposed for the non linear regime, but it still lacks a definitive result. Munier and Peschanski simply ignored these problems, assuming that BK equation still holds and that the coupling runs with the standard argument $\log k$. Note that with this choice $[\alpha_s(L), \chi(-\partial_L)] \neq 0$, hence there are ordering ambiguities. MP simply assumed that χ acts on N but not on the running coupling, that is they keep the coupling on the left of χ. If all these assumptions are correct, Munier and Peschanski get:

$$N(k/Q_s(\xi),\xi) = C\xi^{1/6}\left(\frac{k^2}{Q_s^2(\xi)}\right)^{-M_s} \cdot$$

$$\cdot \mathrm{Ai}\left[z_0 + \left(\frac{\sqrt{2bM_s\chi(M_s)}}{\chi''(M_s)}\right)^{1/3} \frac{\log\left(k^2/Q_s^2(\xi)\right)}{\xi^{1/6}}\right], \tag{2.72}$$

with the saturation scale given this time by

$$Q_s^2(\xi) = \Lambda_{QCD}^2 \exp\left[\sqrt{\frac{2\chi(M_s)}{bM_s}}\xi + \frac{3}{4}\left(\frac{\chi''(M_s)}{\sqrt{2bM_s\chi(M_s)}}\right)^{1/3} z_0\xi^{1/6}\right], \tag{2.73}$$

where $b = \frac{11N_c - 2n_f}{12N_c}$ and $z_0 = -2.338$ is the first zero of the Airy function.
All these results are valid only near the wavefront, that is only for $k \approx Q_s(\xi)$. Moreover, we stress once again that Eq. (2.71), (2.72) and (2.73) are not predictions of the BK theory, since they were obtained imposing a scaling ansatz. The only genuine prediction is that for a quadratic kernel with the coupling held fixed and a suitable boundary condition we may have an asymptotically scaling solution. However numerical studies [31], [32], [33] of the BK equation seem to suggest that the predictions Eq. (2.71), (2.72) and (2.73) are almost correct.

2.5.2 Geometric scaling in the saturated region

In the previous section we have seen that near the saturation momentum $Q_s(\xi)$ the solution of the BK equation with a quadratic kernel asymptotically displays geometric scaling. In this section we will investigate the saturated region, that is the region dominated by the non linear effects. We will follow explicitly the derivation given by Iancu and others [8].
In the saturated regime $N \approx 1$, hence we may write $N(b,\xi) = 1 - S(b,\xi)$. In terms of S the BK equation (2.59) becomes:

$$\frac{d}{d\xi}S(b_{01},\xi) = -\frac{\alpha_s N_c}{2\pi^2}\int d^2b_{02}\frac{b_{01}^2}{b_{02}^2 b_{12}^2}\left(S(b_{01},\xi) - S(b_{02},\xi)S(b_{12},\xi)\right). \tag{2.74}$$

If $S \approx 0$ we may neglect the quadratic term in (2.74). The resulting equation is ill-defined since it is ultraviolet divergent. But this is not a problem: we are in the saturated approximation, that is $q^2 \ll Q_s(\xi)^2$ or $b \gg 1/Q_s(\xi)$. Hence the saturation scale acts as a cutoff to our integral. The resulting equation is

$$\frac{d}{d\xi}S(b,\tau) = -\frac{\alpha_s N_c}{\pi}\log\left(b^2 Q_s(\xi)^2\right) S(b,\xi), \tag{2.75}$$

which shows that S is indeed a scaling solution. Note that we have cheated in this derivation: putting $Q_s(\xi)$ as a cutoff we have changed the ξ-dependence of S. However there are hints suggesting that at least to leading-log accuracy and for large b the result should be essentially correct [8].

Let us now determine an expression for the saturation scale. Following [8] we put in the BK equation a scaling solution and obtain then an expression for $Q_s(\xi)$. Note that once again we are using a scaling ansatz.
Before we start our calculation, note that for a scaling function $f(\zeta)$, with $\zeta = -\log\left(b^2 Q_s^2(\xi)\right)$ (we used this form for future convenience) we have

$$\frac{d}{d\xi}f(\zeta) = -\left(\frac{d}{d\xi}\log Q_s^2(\xi)\right) f'(\zeta) = b^2\frac{d}{db^2}f(\zeta)\left(\frac{d}{d\xi}\log Q_s^2(\xi)\right). \tag{2.76}$$

Hence assuming that S is a scaling solution we have

$$\int d^2b \frac{1}{b^2} \frac{d}{d\xi} S(b,\xi) = \pi \left(S(\infty,\tau) - S(0,\tau) \right) \frac{d}{d\xi} \log Q_s^2(\xi) = -\pi \frac{d}{d\xi} \log Q_s^2(\xi), \quad (2.77)$$

where we used the boundaries indicated in the previous section, that is $S(\infty,0) = 0$ and $S(0,\xi) = 1$. Therefore to obtain an equation for Q_s we have to divide by b^2 and integrate over d^2b the r.h.s. of Eq. (2.74):

$$\frac{d}{d\xi} \log Q_s^2(\xi) = \frac{\alpha_s N_c}{\pi} c, \qquad \text{with}$$

$$c = \int \frac{d^2b_{01} d^2b_{02}}{2\pi} \frac{1}{b_{12}^2 b_{02}^2} \left(S(b_{01},\xi) - S(b_{12},\xi) S(b_{02},\xi) \right). \quad (2.78)$$

It is easy to see that if S is a scaling solution then c is independent of ξ. Then the equation for Q_s becomes

$$\frac{d}{d\xi} \log Q_s^2(\xi) = \frac{\alpha_s N_c}{\pi} c, \quad \longrightarrow \quad Q_s^2(\xi) = Q_0^2 e^{\alpha_s N_c/\pi \; c\xi}, \quad (2.79)$$

in agreement with the result of the previous section.
The authors of [8] extended these results also to the case of running coupling. In this case they suggest that the typical scale of the problem is not Q^2 but the saturation scale Q_s^2 (for further discussion on this choice we refer the reader to the original paper). If this is the case the derivation of Q_s is exactly the same as in the fixed coupling case, but with the result

$$\frac{d}{d\xi} \log Q_s^2(\xi) = c \frac{N_c}{\pi} \alpha_s \left(Q_s^2(\xi) \right) \quad \longrightarrow \quad Q_s^2(\xi) = \Lambda_{QCD}^2 e^{\sqrt{2b_0 c(\xi+\xi_0)}}, \quad (2.80)$$

with $b_0 = \frac{12N_c}{11N_c - 2n_f}$ and ξ_0 an integration constant. Surprisingly enough, even in this case we obtain for Q_s a result in agreement with the one of the previous section. This situation is quite puzzling: we obtain the same result with two different arguments for the coupling! It is not yet clear why this happens. Incidentally, this is an indication that the running coupling version of the BK equation should be handled with care. In other words, a "true" running coupling BK equation is sorely needed. Some progress in this way have been made by Weigert, Kovchegov and others [34], [35], [36], but a final result is still missing.

2.6 The extended geometric scaling region

Until now we have considered only the region where the full BK equation differs from the original BFKL. Let us consider the low energy regime, where we can neglect all the non linear effects. Iancu and others have shown [8] that also in this regime there exists a region in which geometric scaling is approximatively valid. Such region is usually referred as the extended geometric scaling region.

The argument is very simple. Assume a function satisfies a saturation condition

$$f(\xi, Q^2)|_{Q^2=Q_s^2(\xi)} = 1, \tag{2.81}$$

then without loss of generality we can approximate this function near the saturation line as

$$f(\xi, Q^2) \approx \left(\frac{Q^2}{Q_s^2(\xi)}\right)^{\lambda(\xi)}, \tag{2.82}$$

with $\lambda(\xi) = \partial \log f / \partial \log Q^2|_{Q_s^2(\xi)}$. Assuming that this expansion can be extended up to values of Q^2 large enough that the non linear effects can be neglected, $\lambda(\xi)$ can be determined by solving the BFKL equation with the saturation boundary condition (2.81). Of course this doesn't imply that (2.82) is a scaling solution: this happens only if λ is independent of ξ. We shall see that this is the case with the BFKL evolution.

Consider indeed the solution to the (fixed coupling) BFKL equation:

$$N(b, \xi) = \int_{c-i\infty}^{c+i\infty} \frac{dM}{2\pi i} N(M, \xi_0) \exp Ml + \bar{\alpha}_s \chi_0(M)\xi, \tag{2.83}$$

with $l = \log(Q^2/\Lambda^2)$ $Q^2 \equiv 1/b^2$ and Λ is some fixed scale. We assume that ξ and l are large enough to evaluate the integral in the saddle point approximation. The saddle condition reads

$$\frac{d}{dM}\chi_0(M)|_{M_0} = -\frac{l}{\bar{\alpha}_s \xi} \equiv R. \tag{2.84}$$

This implies that $M_s(l, \xi) = M_0(R)$. Then defining $F(M, R) = -MR + \chi_0(M)$ and neglecting all the fluctuations around the saddle we can write the solution (2.83) as

$$N(b, \xi) \simeq e^{\bar{\alpha}_s \xi F(M_0(R), R)}. \tag{2.85}$$

Consider now the saturation criterion Eq. (2.81). In our case this criterion reads

$$N\left(b = 1/Q_s(\xi), \xi\right) = 1. \tag{2.86}$$

Strictly speaking, the r.h.s. of this equation is not exactly 1, since for $b \approx 1/Q_s$ we have seen that $S(b, \xi) \approx 0$ but it is not equal to 0. $N = 1$ is reached only asymptotically. However, replacing 1 by $k < 1$ would modify our following results by subleading terms of order $1/(\bar{\alpha}_s \xi) \cdot \log k$ (see [8]) which we may neglect to the accuracy of our calculation. In the following then we will suppose that Eq. (2.86) holds. This saturation criterion yields the following condition on F:

$$F\left(M_0(R_s), R_s\right) = 0 \quad \text{for} \quad R_s = \frac{1}{\bar{\alpha}_s \xi} \log \frac{Q_s^2(\xi)}{\Lambda^2}. \tag{2.87}$$

Note that R_s is a pure number and not a function of ξ. This implies

$$Q_s^2(\xi) = \Lambda^2 e^{R_s \bar{\alpha}_s \xi}, \tag{2.88}$$

in agreement with Eq. (2.79). Moreover, in this case the slope R_s can be easily computed. Indeed combining Eq. (2.84) and (2.86) and writing $M_0(R_s) = M_s$ we obtain

$$\chi_0(M_s) = M_s R_s = M_s \chi_0'(M_s). \tag{2.89}$$

Using for χ_0 its LO expression (1.116) we can solve this equation numerically, with the result

$$M_s = 0.6275..., \qquad R_s = 4.8833... \tag{2.90}$$

Assume now we want to evaluate N for R slightly above R_s, that is for values of b which, while still being much shorter than the saturation length $1/Q_s(b)$, are nevertheless close to it in logarithmic units. More precisely, we shall ask

$$0 < R - R_s \ll R_s, \quad \text{i.e.} \quad 1 < \log \frac{Q^2}{Q_s(\xi)^2} \ll \frac{Q_s^2(\xi)}{\Lambda^2}. \tag{2.91}$$

The condition $R > R_s$, that is $Q^2 \gg Q_s^2$, ensures that we are in the linear regime, while the condition $R - R_s \ll R_s$ allows us to write

$$F\left(M_0(R), R\right) = F\left(M_0(R_s), R_s\right)) + \frac{d}{dR} F\left(M_0(R), R\right)\Big|_{R=R_s} (R - R_s) + ... =$$
$$= -M_s(R - R_s) + ... \tag{2.92}$$

where we used both the saturation criterion $F(M_0(R_s), R_s) = 0$ and the fact that M_0 is a saddle point. This indeed implies:

$$\frac{d}{dR} F\left(M_0(R), R\right)\Big|_{R=R_s} = -M_0(R_s) + \frac{\partial F}{\partial M}\Big|_{M=M_0} \frac{\partial M_0}{\partial R}\Big|_{R=M_s} = -M_s. \tag{2.93}$$

Therefore above the saturation scale the dipole cross section N can be approximated as follows

$$N(b, \xi) \simeq e^{-\bar{\alpha}_s \xi M_s (R - R_s)} = \left(b^2 Q_s^2(\xi)\right)^{M_s}. \tag{2.94}$$

We see that neglecting the fluctuations around the saddle condition and keeping only the first non trivial term of the Taylor expansion (2.92) the solution of the BFKL equation exhibits geometric scaling. Let us relax these approximations. We don't consider corrections to the saddle point, since they are suppressed by $1/\bar{\alpha}_s \xi$. We consider instead the corrections coming from higher order terms in the expansion (2.92). These terms violate scaling. For instance, if we keep also the second order of the expansion, we obtain

$$N(b, \xi) \simeq \left(b^2 Q_s^2(\xi)\right)^{M_s} \exp\left[-\frac{M_s'}{2\bar{\alpha}_s \xi} \log^2 \frac{1}{b^2 Q_s^2(\xi)}\right], \tag{2.95}$$

with $M_s' = dM_0(R)/dR|_{R=R_s}$. The impact of higher order terms in the expansion (2.92) is controlled by the ratio $(R - R_s))/R_s$, hence the scaling behaviour holds in the window

$$1 < \log \frac{Q^2}{Q_s^2(\xi)} = \log \frac{Q^2}{\Lambda^2} - c\bar{\alpha}_s \xi \ll c\bar{\alpha}_s \xi. \tag{2.96}$$

Let us summarize the range of validity of our approximation. First, the saddle point approximation requires that both ξ and l are large. Second, we must have $Q^2 \gg Q_s^2$ in order to neglect the non linear effects. Third, $R - R_s \ll R_s$ in order to truncate the Taylor expansion (2.92) at the first non trivial term. These conditions define the extended geometric scaling region.

In summary, we have seen that geometric scaling persists also above the saturation scale in the kinematic window

$$1 \lesssim \log\left(\frac{Q^2}{Q_2^2}\right) \ll \log\left(\frac{Q_s^2}{\Lambda^2}\right). \tag{2.97}$$

Chapter 3

Geometric scaling: a systematic approach

3.1 The linear evolution: analytical results

3.1.1 Saddle point methods: general analysis

In the previous chapter we have seen that geometric scaling can be obtained also from the fixed coupling BFKL equation with a saturation boundary, but that derivation relied on two major approximations. First, we evaluated the inverse Mellin integral in a saddle point approximation. Second, we considered the saddle point only in the neighbourhood of the saturation line $t = \lambda\xi$, with λ constant. We may then ask where these approximations are reliable and if geometric scaling depends strongly on them. For example, if we consider also the third term in the Taylor expansion, does geometric scaling break down or does this only lead to a subasymptotic correction? Furthermore, it is important to understand whether the saturation ansatz is necessary to the scaling or not. Moreover, it is interesting to investigate if these results hold only for the BFKL kernel or if they are more general, i.e. if they are valid also for a DGLAP-like evolution. In this section we will answer these questions. In analogy with the analysis of the previous chapter, in a first step we will limit ourselves to the fixed coupling case. We will consider the running coupling case later.

We will start our analysis with the most delicate point, that is the Taylor expansion. In particular, what we wish to understand is the impact on geometric scaling of higher orders in the expansion. What we will do is to rewrite this Taylor expansion kernel in a way that makes evident if and where there is a scaling behaviour. We will write a (formal) all order expansion, from which it will follow that geometric scaling asymptotically holds for a very general class of evolution kernels, but also that far from the asymptotic region scaling violations may be very strong. We stress that what we are going to do is just a formal manipulation of the Taylor expansion: at the end we will come back to our starting point. This

may seem strange: usually we know a series expansion and we wish to resum it, here instead we do know the resummed result but we want a series expansion. One may ask why we aren't content with the traditional Taylor expansion. The answer is just that we don't want a generic series representation (remember that we have already the resummed form, a generic expansion will be totally useless), we want to find the very particular expansion which has a direct relation with the geometric scaling.

Let us define the terms of the question. First of all we have to write down an expression for the total $\gamma^* P$ cross section (which should scale) in terms of something that we can calculate, namely the parton distribution G:

$$\sigma_{tot}^{\gamma^* P} \propto \frac{F_2(\xi, t)}{Q^2} \approx A \frac{d}{d\xi} G(\xi, t) \Lambda_{QCD}^2 e^{-t}. \tag{3.1}$$

where A is just a numerical constant and the approximation is that we have neglected the term associated to the small eigenvector G^- of the splitting function matrix, which is asymptotically small at large ξ (see Sec. 1.2.6). We are interested in the asymptotic behaviour of the cross section, hence following what we have done in the previous chapter we consider only exponential terms, that is we write $G \approx e^{g(\xi,t)}$. From this definition it follows immediately that the condition for (asymptotic) geometric scaling is

$$g(\xi, t) - t = h(t - t_s(\xi)). \tag{3.2}$$

Hence as long as we are interested only in the asymptotic behaviour we can consider simply the function h.
For a BFKL evolution h has the form

$$h(\xi, t) = \chi(M)\xi + (M - 1)t, \tag{3.3}$$

with an associated saddle point condition

$$\left(\chi'(M)\xi + t\right)\big|_{M=M_s} = 0. \tag{3.4}$$

For a DGLAP evolution instead we have

$$h(\xi, t) = (\gamma - 1)t + N\xi, \qquad \left(\gamma'(N)t + \xi\right)\big|_{N=N_s} = 0. \tag{3.5}$$

Note that both the saddle conditions share an important property: they are not function of t and ξ separately but only of the ratio t/ξ. We will see that from this the scaling behaviour follows.

In order to stress that this is the only relevant property, we may generalize the situation by considering

$$h(x, t) = f\left(b\left(\frac{x}{y}\right)\right) y + b\left(\frac{x}{y}\right) x, \tag{3.6}$$

with the associated generalized saddle condition

$$f'\left(b\left(\frac{x}{y}\right)\right)+\frac{x}{y}=0. \tag{3.7}$$

Here f' means differentiation of f with respect to its argument. Of course with an appropriate choice of f and b Eq. (3.6) reduces to the usual expressions (3.3) and (3.5) for the BFKL and DGLAP evolutions.

Now that we have defined the terms of the question, we are ready to search for the expansion. Following the ideas of the previous chapter we expand around the saturation line $y=\lambda x$. Hence we may define a new variable $\tau=y-\lambda x$ and consider $h(x,y)\to h(\tau,x)$. Then we expand around $\tau=0$:

$$h(x,y)=\sum_{k=0}^{\infty}\frac{1}{k!}\,\frac{d^k}{\tau^k}h(x,y)\bigg|_{y=\lambda\xi}\tau^k. \tag{3.8}$$

For what concerns the geometric slope λ, we choose it such that $h(x,\lambda x)=0$. If this choice is possible we will show that geometric scaling asymptotically holds, without requiring any saturation criterion. From our definition of h (3.6) it follows that λ is defined implicitly by the equation

$$h(x,\lambda x)=f\left(b\left(\frac{1}{\lambda}\right)\right)\lambda x+b\left(\frac{1}{\lambda}\right)x=0\longrightarrow\lambda=-\frac{b(1/\lambda)}{f\left(b(1/\lambda)\right)}. \tag{3.9}$$

We can see immediately the purpose of this choice: with λ defined as in (3.9) the expansion start from $O(\tau)$. This ensures that for $\tau=0$ we doesn't have a residual x-dependence which can break scaling. With this choice then our expansion starts from the linear term. Since $d_\tau=d_t$, what we have to evaluate is the generic form of $d_t^k h(x,y)|_{y=\lambda x}$. A simple calculation shows that

$$d_y h(x,y)=f'b'\left(-\frac{x}{y^2}\right)y+b'\left(-\frac{x^2}{y^2}\right)+f=-\left(\frac{x}{y}\right)b'\left(f'+\frac{x}{y}\right)+f=f, \tag{3.10}$$

where in the last step we have used the saddle condition Eq. (3.7). For the next few terms we obtain

$$\begin{aligned}
d_y^2&=\frac{x^2}{y^3}b'\\
d_y^3&=-3\frac{x^2}{y^4}b'-\frac{x^3}{y^5}b''\\
d_y^4&=+12\frac{x^2}{y^5}+8\frac{x^3}{y^6}b''+\frac{x^4}{y^7}b'''
\end{aligned} \tag{3.11}$$

It is easy to generalize Eq. (3.11), with the result that for $k\geq 2$ the general term of this expansion has the form

$$d_y^k h(x,y)=(-)^k\left[a_1^{(k)}\frac{x^{1+1}}{y^{k+1}}b'+a_2^{(k)}\frac{x^{1+2}}{y^{k+2}}b''+...+\right.$$

$$+a_l^{(k)}\frac{x^{1+l}}{y^{k+l}}b^{(l)}+...+a_{k-1}^{(k)}\frac{x^k}{y^{2k-1}}b^{(k-1)}\Bigg], \tag{3.12}$$

with $l \leq k-1$. One obtains immediately that $\{a_1^{(k)}\} = \frac{1}{2}\{2!, 3!, ..., l!, ..., k!\}$, i.e. $a_1^k = k!/2$. For what concerns the others coefficients, some algebra shows that a recursion relation holds:

$$a_l^k = a_{l-1}^{k-1} + a_l^{k-1}(k-1+l). \tag{3.13}$$

We are now ready to regroup the expanded terms. The sum of terms proportional to b' is trivial:

$$b'\sum_{k=2}^{\infty}(-)^k\frac{x^2}{y^{k+1}}a_1^k\frac{\tau^k}{k!} = \frac{b'x^2}{2}\sum_{k=2}^{\infty}\left(\frac{-\tau}{y}\right)^k\frac{1}{y} = -\frac{b'}{2}\frac{x^2}{y}\frac{\tau}{y}\sum_{k=1}^{\infty}\left(\frac{-\tau}{y}\right)^k =$$

$$= \frac{b'}{2}\frac{x^2}{y^2}\frac{\tau^2}{\tau+y} \longrightarrow \frac{1}{2}\left.\frac{db}{dS}\right|_{S=1/\lambda}\frac{1}{\lambda^2}\frac{\tau^2}{\tau+\lambda x}. \tag{3.14}$$

For the other terms things are a little more complicated because of the $a_l^{(k)}$ coefficients, which cannot be written in terms of a generating function. However we are not directly interested in $a_l^{(k)}$ but rather in $a_l^{(k)}/k!$, which instead have a generating function representation. One indeed can easily prove by induction that

$$(-)^{k+l}\frac{a_l^{(k+l)}}{(k+l)!} = \frac{(-)^{l+1}}{(l+1)!}\frac{d^{k+1}}{dx^{k+1}}\frac{1}{(1+x)^l}. \tag{3.15}$$

Then for the l-term we have (up to an overall $(-)^{l+1}$ sign):

$$b^{(l)}x^{1+l}\sum_{k=l+1}^{\infty}\frac{a_l^{(k)}}{k!}\frac{\tau^k}{y^{l+k}} = b^{(l)}\frac{x^{1+l}}{y^l}\sum_{i=1}^{\infty}\frac{a_l^{k+l}}{(k+l)!}\frac{\tau^{k+l}}{y^{k+l}} =$$

$$= \frac{b^{(l)}}{(l+1)!}\frac{x^{1+l}}{y^l}\frac{1}{(1+\tau/y)^l}\left(\frac{\tau}{y}\right)^{l+1} \longrightarrow \frac{b^{(l)}}{(l+1)!}\frac{\tau^{l+1}}{\lambda^{2l+1}x^l}\frac{1}{(1+\tau/y)^l}. \tag{3.16}$$

Summing up all these contributions we obtain our final result

$$h(x,y) = f\tau + \tau\frac{1+z}{z}\sum_{k=2}^{\infty}\frac{(-)^k}{k!}\left(\frac{z}{\lambda(z+1)}\right)^k d_S^{k-1}b(S)|_{S=1/\lambda}, \tag{3.17}$$

with $z = \tau/\lambda x$.

We see that for a generic kernel only the first term $f\tau$ gives rise to geometric scaling, while all the others violate it. Whether or not the violations are strong, it depends on the form of the various kernel (and on the kinematic region). Note however that there are two regions in which geometric scaling holds for a very generic kernel. First, we may have $z \approx 0$. This correspond to $y \approx \lambda x$, x large. This is nothing but the extended scaling region of the previous chapter. In this region

geometric scaling holds up to subasymptotic contributes, hence the approximation of neglecting higher orders in the Taylor expansion is good. Unfortunately, since this behaviour is totally generic it tells us nothing about the underlying physics. In other words, the geometric scaling found in [8] has little to do either with a saturated or with an ordinary behaviour. However, this is something which is not generic and so that could gives us a hint about the evolution: the procedure explained above provides us a prediction for the saturation scale $\tau = 0$, that is it gives us a precise value for the constant λ. This value should be strongly kernel-dependent, hence a comparison with the phenomenology can give us an information about the kernel itself and hence about the evolution.

Apart from the extended geometric scaling region, there is another regime for which the scaling is asymptotically exact, and which definitely shows that the usual saturation-geometric scaling association must be handled with care. This is the region $z \gg 1$, that is $y \gg \lambda x$. For a DGLAP evolution this condition reads $t \gg \lambda\xi$. Now, all the saturation-based models say that in this limit geometric scaling should be broken[1]. Also in this case the effective parameters of the scaling are kernel-dependent. Furthermore, now apart from λ we have also a prediction for $b(1/\lambda)$, hence a comparison with the phenomenology in this region could give us more information about the evolution. One may object that this new geometric scaling region is in fact purely theoretical: we are working in a fixed coupling regime, while at large t the resummation of large logarithms and hence the introduction of the running coupling is necessary. We will deal carefully with the running coupling in the next section, for the moment we limit ourselves to one simple observation. As long as we consider a small t-evolution we can always work in a fixed coupling regime. Suppose indeed to work at a scale Q_0^2 large as we wish. Since physical quantities aren't affected by the definition of the renormalization scale, without loss of generality we can choose as renormalization scale just Q_0 . Thus the only logarithms that we can produce are of the form $\log\left(Q^2/Q_0^2\right)$. But then if the evolution is small, i.e. $Q^2 \sim Q_0^2$, we can't produce any large logarithm and hence we can work with fixed coupling (fixed of course at the renormalization scale Q_0).

Until now our arguments have been totally generic. Let us now study a specific case, that is a BFKL evolution with a quadratic kernel. Note that this is not a casual choice: this is the only one kernel for which we have a definitive analytic argument which states that the BK equation admits travelling waves, i.e. scaling solutions. The existence of travelling waves is often considered a claim of the deep connection between geometric scaling and saturation. But let us consider this case in a pure BFKL approach, without any scaling ansatz. In this case our kernel has the form

$$\chi(M) = \eta + \frac{\mu}{2}(M - M_0)^2, \tag{3.18}$$

[1]This is not completely correct. What really happens is that in this region all the arguments leading to the geometric scaling fail. Hence these models can't predict geometric scaling, but they also can't prove its breaking.

leading to the saddle condition

$$\chi'(M_s) + \frac{t}{\xi} = \mu(M - M_0) + \frac{t}{\xi} = 0 \longrightarrow M_s(S) = M_0 - S, \tag{3.19}$$

that is it gives a trivial condition for the saddle point as function of S. In other words, with a quadratic kernel the saddle point is not an approximation, it is the exact result. In this case all the further terms of the expansion die, we are left only with the scaling term and with the first violation, which behaves like $\sim 1/\xi$. From all of this it follows that we cannot see the scaling behaviour as a consequence of saturation. Of course, the range of validity of the quadratic approximation (and more in general of the saddle point approximation) and the parameters of the scaling (that is the exact value of λ) are not at all general, they depend on the kernel we are using. Hence if in a kinematic region the linear and non linear predictions are different, a careful analysis of the phenomenology can give us information about whether evolution is dominating. In the next sections we will perform such an analysis.

We may stress that geometric scaling arises trivially from a quadratic kernel only in the fixed coupling case: as we shall show with running coupling things change. In order to make a comparison with the BK case, we will work with a BFKL evolution. Note that because of duality this is totally generic: if geometric scaling holds for the BFKL solution, then it holds also for the DGLAP one, since duality states that these solutions are the same (with a suitable definition of the kernels). We consider then the running coupling solution to the BFKL equation, with the argument of the running coupling Q^2 as usual. We have shown in Sec. 1.4.5 that this solution can be written as

$$G(\xi, t) = \int_{c-i\infty}^{c+i\infty} \frac{dM}{2\pi i} \frac{dN}{2\pi i} G(M_0, N_0) \exp\left[Mt + N\xi - \frac{1}{\beta_0 N} \int \chi(M')dM'\right]. \tag{3.20}$$

In the previous chapter we evaluated the M-Mellin integral and we found an expression for the dual anomalous dimension. Now we perform first the N-Mellin inversion. Although it is possible to express exactly the result in terms of Bessel functions, in the spirit of this section we evaluate the integral in the saddle point approximation. This gives

$$G(\xi, t) \approx \int_{c-i\infty}^{c+i\infty} G(M_0, N_s) \frac{dM}{2\pi i} \exp\left[Mt + \sqrt{4A(M)/\beta_0}\sqrt{\xi}\right], \tag{3.21}$$

with $A(M) = \int \chi(M')dM'$. We see that we fall in the case previously discussed, provided that we expand in the new variable $\tau = t - \lambda\sqrt{\xi}$. This implies a change of our scaling law. In the next section we will consider more carefully the case of the quadratic kernel. For the moment we just note that, because of the square root and of the integral over χ, in the case of running coupling the relation between the quadratic kernel and the scaling behaviour is no longer a trivial condition and its reliability must be checked case by case.

Of course substituting an integral with its saddle point solution it is not in general a good approximation of reality, that is for large but finite t and ξ. Moreover, we know that with a running coupling quadratic evolution the saddle point is not reliable. Consider indeed the Airy anomalous dimension, which is an all-order resummation. It can be shown that this resummed anomalous dimension can be written as a saddle point term plus a (Borel) resummation of all the saddle corrections, that is we can write

$$\gamma_A(\alpha_s, N) = \gamma_s\left(\frac{\alpha_s}{N}\right) + \beta_0\alpha_s\Delta\gamma_{ss}\left(\frac{\alpha_s}{N}\right) + ..., \tag{3.22}$$

with

$$\gamma_s\left(\frac{\alpha_s}{N}\right) = \frac{1}{2} - \sqrt{\frac{2}{k}\left[\frac{N}{\alpha_s} - c\right]}, \quad \Delta\gamma_{ss}\left(\frac{\alpha_s}{N}\right) = -\beta_0\frac{\chi_0''(\gamma_s)\chi_0(\gamma_s)}{2\chi_0'^2(\gamma_s)}. \tag{3.23}$$

Note that if we limit ourselves to the saddle condition the leading singularity (that we know from the all order resummation being a simple pole) is a branch cut. Moreover, the term $\Delta\gamma_{ss}$ is singular near $M \sim 1/2$ because of the vanishing of the dominator. One can see by explicit calculations that also all the further terms of the expansion (3.23) behave badly near $M = 1/2$. We then see that at least in the case of quadratic running coupling BFKL evolution the saddle approximation is not a good one. But since we have said that asymptotically in ξ every kernel can by replaced by its quadratic approximation near the minimum, we see that this is the case of all BFKL evolutions when we let the coupling run. In the next section hence we will try to link geometric scaling to this all-order resummation, without relying on a saddle point approximation.

3.1.2 Asymptotic scaling with running coupling

In the previous section we have found that the saddle point derivation presented in [8] is not particularly appealing, since it is based on an approximation (the first term of a Taylor expansion) of an approximation (the saddle point). Moreover, being completely generic it doesn't tell us anything about the evolution. We have also shown that the saddle point is not a good approximation if the coupling runs. Now we want to see if geometric scaling is thus just an accident or if it is the sign of something more profound. Note that the former case looks unlikely: numerical simulations suggest that the scaling behaviour is a feature of both the full linear (BFKL) and non linear (BK) evolutions with the full kernel, where with full we mean that the evolution is (numerically) exact and it does not rely on a saddle approximation[2]. Indeed, in this section we will see that we are in the latter case: we will show that the all order running coupling resummation and geometric

[2]Typically here people invoke also phenomenology as a support of geometric scaling. However we will see that the effective phenomenological importance of this scaling law seems to be dubious, at least for HERA.

scaling are related, provided that we treat the factorization correctly. Let us see how all of this work.

It should now be clear that as long as we are interested only in the $\xi \to \infty$ asymptotics we can consider without loss of generality a quadratic BFKL kernel. We start hence by reviewing the main features of the Airy solution. In the next section we will show that this solution apart from a prefactor can be approximately written in terms of the difference $t - t_0$, where t_0 is the (fixed) factorization scale. Then in Sec. 3.1.2 we will show how to promote correctly $t_0 \to t_0(\xi)$. Finally we will obtain geometric scaling by simply identifying $t_0(\xi)$ with the saturation scale $t_s(\xi)$.

The Airy solution revisited

Consider the Airy solution in (N, t) space for the eigenfunction G, that is

$$G(N,t) = K(N) e^{M_0 t} \mathrm{Ai}\left[\left(\frac{2\beta_0 N}{k}\right)^{1/3} \frac{1}{\beta_0}\left(\frac{1}{\alpha_s(t)} - \frac{c}{N}\right)\right]. \tag{3.24}$$

In the previous chapter we have said that all its major problems (namely unphysical oscillations for large enough ξ) are in fact due to a wrong factorization: the oscillating terms are in fact factored out in the initial condition. In other words, what we are interested in it is not the solution Eq. (3.24) but rather the evolution factor:

$$\Gamma[N, t, t_0] = \frac{G(N,t)}{G(N,t_0)}. \tag{3.25}$$

Suppose now we want to Mellin transform Eq. (3.25). At ξ large enough the inversion integral will be dominated by the pole in $N = N_0 > 0$ of $G(N, t_0)$. Further singularities on the left of N_0 (as for example the boundary condition simple pole at $N = 0$) are suppressed in the high energy limit. It is straightforward to see that the position of this leading pole N_s is implicitly defined by

$$\frac{c}{N_s} = \frac{1}{\alpha_s(t_0)} - \beta_0 z_0 \left(\frac{k}{2\beta_0 N_s}\right)^{1/3}, \tag{3.26}$$

where $z_0 = -2.33811...$ is the first zero of the Airy function.

Then we can write the solution of (3.25) as

$$\Gamma[\xi, t, t_0] \propto e^{M_0(t-t_0)} \mathrm{Ai}\left[\left(\frac{2\beta_0 N_s}{k}\right)^{1/3} \frac{1}{\beta_0}\left(\frac{1}{\alpha_s(t)} - \frac{1}{\alpha_s(t_0)}\right) + z_0\right] e^{N_s \xi}, \tag{3.27}$$

where the last term $\exp(\xi N_s)$ is nothing but the exponential factor arising from the Mellin inverse transform. Apart from this term we note that the solution (3.27) has a remarkable property: it is function not of t and t_0 separately but only of

their difference $t - t_0$[3]. In other words, we can write $\Gamma(t, t_0)$ as

$$\Gamma(t, t_0) = f(t - t_0) \exp\left[N_s\left(t_0\right)\xi\right]. \tag{3.28}$$

But this has an immediate consequence in terms of geometric scaling. Remember indeed that the scaling law should hold not for G but for $G\exp(-t)$. Now, assume to choose the initial condition such that

$$t_0 = N_s\xi, \tag{3.29}$$

then we have geometric scaling in term of the variable $\tau = t - t_s$, with $t_s = N_s\xi$. In the next section we will show that in fact we cannot operate such a choice without harm, but for the moment we will neglect this problem and see where the naive scaling condition (3.29) leads us.

First of all we make some observations. We have derived geometric scaling only for the evolution factor. If the initial condition doesn't exhibit a scaling behaviour the total cross section won't scale either. However, numerical analysis of the BK and BFKL equations seems to suggest that for large enough rapidity the boundary condition are "washed out" by the evolution. If this behaviour is in fact true, then we recover geometric scaling, at least asymptotically.

Now we want to understand what our choice of the initial condition implies in terms of evolution. To this purpose consider the evolution of a point in the (t, ξ) plane. Geometric scaling says that considering the evolution of each point separately from all the others is in fact superfluous: points on the same $t - t_s(\xi) = \tau$ line indeed evolve at the same manner. In other words, geometric scaling implies that the evolution of a point automatically determines the evolution of the whole line where it lies, as shown in Fig. 3.1.

Assume indeed to consider two point on the same geometric line (in general this line could be a curve. In the picture we have assumed for simplicity a linear relation between t_s and ξ, but of course our argument holds for every curve), say A and B, and assume to evolve them. First we evolve A to A'. Consider now B. Since the evolution $B \to A$ doesn't affect the total cross section, the evolution operator $\mathcal{O}_{B\to A}$ is nothing but the identity operator (obviously we are thinking of such an operator acting on the cross section). Hence we may write

$$\mathcal{O}_{x\to x'}\ \sigma(B) = \mathcal{O}_{x\to x'}\mathcal{O}_{B\to A}\ \sigma(B) = \sigma(A'), \tag{3.30}$$

that is we have to know only the evolution of one point in order to know the evolution of the whole line[4] . It is clear then that in a geometric scaling context the natural boundary condition is not on a single point, but rather on a line.

[3]In fact this is not completely true, because of the t_0 dependence of N_s. We will see that in a particular situation this term can be factored out, just as we did for unphysical oscillations. However in general it gives rise to (subasymptotic) scaling violating terms.

[4]Note that this implies that geometric scaling cannot hold everywhere, it must have only a limited range of validity. Otherwise indeed we could know all the non perturbative information from the perturbative one. To see this, assume we want to determine the cross section in $Q_0 \sim \Lambda_{QCD}$. We may then walk up on the geometric line up to a perturbative scale $Q \gg \Lambda_{QCD}$, calculate the cross section and then walk back with our result to Q_0.

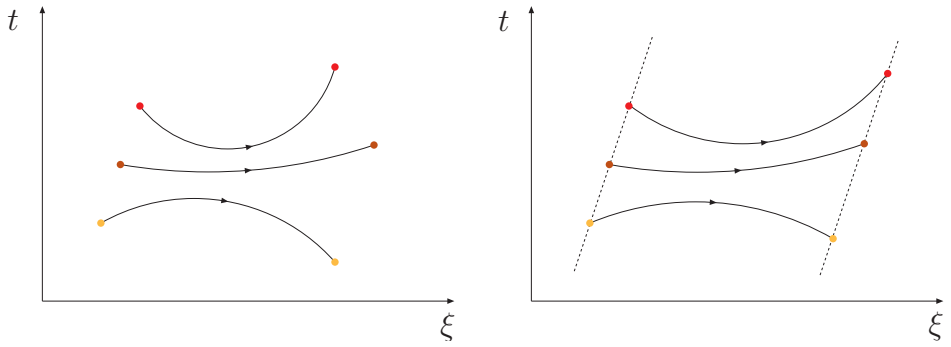

Evolution of the total cross section $\sigma_{tot}^{\gamma^* P}$ in a generic case (left) and in presence of geometric scaling (right). Points lying on the same geometric line leads to the same value for the total cross section

Figure 3.1: Evolution in presence of geometric scaling

Now that we have understood the meaning of our choice of the boundary, we may explore its consequences. Namely, we want to obtain a functional form for the saturation scale. From Eq. (3.27) and (3.29) it follows that the naive saturation scale t_0 is implicitly defined by

$$\frac{c\xi}{t_0} = \frac{c}{N_s} = \frac{1}{\alpha_s(t_0)} - \beta_0 z_0 \left(\frac{k}{2\beta_0 N_s}\right)^{1/3}. \tag{3.31}$$

Hence we must obtain an approximate form for $N_s(t_0)$. To his purpose, we may rewrite Eq. (3.27) as

$$\frac{c}{N_s} = \beta_0 t_0 - z_0 \beta_0 \left(\frac{k}{2\beta_0}\frac{1}{c}\left(t_0\beta_0 - z_0\beta_0\left(\frac{k}{2\beta_0}...\right)^{1/3}\right)\right)^{1/3}, \tag{3.32}$$

where we have put $1/\alpha_s(k) = \beta_0 k$. In the limit of large saturation scale t_0 we may express the solution of this equation as

$$\frac{c}{N_s} = \beta_0 t_0 + O\left(t_0^{1/3}\right). \tag{3.33}$$

Of course this is just a crude estimate. In general however the solution can be written as

$$\frac{c}{N_s} = a_0 t_0 + a_1 t_0^{1/3} + a_2 t_0^{1/9} + a_3 t_0^{1/27} + ... \tag{3.34}$$

In terms of the saturation scale this in turn implies

$$t_0 = N_s\xi \approx \frac{c\,\xi}{a_0 t_0 + a_1 t_0^{1/3}} \approx \frac{c\,\xi}{a_0 t_0}\left(1 - \frac{a_1}{a_0} t_0^{-2/3}\right), \tag{3.35}$$

where we have considered only the first two terms for simplicity. From this we obtain

$$t_0 = \sqrt{\frac{c\,\xi}{a_0}\left(1 - \frac{a_1}{a_0}t_0^{-2/3}\right)} = \sqrt{\frac{c\,\xi}{a_0}\left(1 - \frac{a_1}{a_0}t_0^{-2/3}\right)} =$$

$$= \sqrt{\frac{c\xi}{a_0}\left(1 - \frac{a_1}{a_0}\left[\frac{c\xi}{a_0}\right]^{-1/3}\right)} = \sqrt{\frac{c\xi}{a_0}} - \frac{1}{2}\frac{a_1}{a_0}\left(\frac{c}{a_0}\xi\right)^{1/6}, \tag{3.36}$$

where these manipulations are valid if we neglect all the terms $O\left(\xi^{1/9}\right)$. The generalization of Eq. (3.36) to higher order is trivial. Note that without any saturation or scaling ansatz we have recovered the same behaviour of the saturation scale of [37], that is

$$t_0(\xi) = A\sqrt{\xi} + B\xi^{1/6} + ... \tag{3.37}$$

Moreover, thanks to our all order resummation we are able to find the ξ dependence of the saturation scale up to any chosen accuracy, while in [37] the scaling ansatz provided only the first correction, that is the $\sim \xi^{1/6}$ term.
Let us now calculate the leading coefficients a_0 and a_1. From Eq. (3.32) and (3.34) it follows immediately

$$a_0 = \beta_0, \qquad a_1 = -z_0\beta_0\left(\frac{k}{2c}\right)^{1/3}, \tag{3.38}$$

from which

$$A = \sqrt{\frac{c\,\xi}{\beta_0}} = \sqrt{\frac{\chi(M_0)}{\beta_0}}\sqrt{\xi}. \tag{3.39}$$

All this seems very appealing, but there is a flaw in our argument: by assuming $t_0 = t_0(\xi)$ we have in fact changed the evolution equation. In the next section we will explain how this happens and we will show how to resume the correct evolution even with ξ-dependent boundaries.

ξ-dependence of the factorization scale

We have said that giving a ξ dependence to the initial scale t_0 we have modified the true evolution equation. At first sight this could seem strange: after all our starting result Eq. (3.24) was obtained in Mellin space, and the variable Mellin conjugate to M is t, not t_0. The initial scale enters in our equation only in a later stage of the calculation. Hence we may think that our choice of t_0 is totally legitimate. In fact this is not the case, as we shall now see.

From the definition of Γ Eq. (3.25) we see that t_0 is indeed the factorization scale. If this were not be so, we couldn't factor out the unphysical oscillations and hence we would get a totally absurd result. But if it is the factorization scale, it is

also the scale at which we define the starting condition for the running coupling. That is the definition Eq. (3.25) implies

$$\alpha_s(t) = \frac{1}{\beta_0 \log \frac{Q^2}{\Lambda^2_{QCD}}} = \frac{\alpha_s(t_0)}{1 + \beta_0 \alpha_s(t_0) \log \frac{Q^2}{Q_0^2}}. \tag{3.40}$$

Of course the two definitions are equivalent, hence even with our choice of t_0 the running still does not depend on ξ (which is obvious: the coupling, being an observable, cannot depend on the renormalization scale). However, only the second one is relevant when we calculate the Airy resummation, as one can see immediately by simply remembering what we have done in the Sec. (1.4.5). The variable t there defined is not the traditional $t_\Lambda = \log Q^2/\Lambda_Q CD^2$, but rather $t_{Q_0} = \log Q^2/Q_0^2$, with Q_0 being the factorization scale. Hence, if we want to give a ξ dependence to t_0 and we want that t_0 remains our factorization scale, we have to give a ξ dependence to t, where here with t we indicate not a precise scale but rather the Mellin conjugate to M. In order to keep track of t_0 in t, we can define a new variable for the Mellin conjugate to M, that is we may write $t = t_\Lambda - t_{0_\Lambda}$ and give a ξ dependence only to $t_{0\Lambda}$. From now on this new definition will be implicitly assumed, hence we can drop the Λ index in order to shorten the notation.

With this new definition it is easy to see how the evolution equation changes. Write indeed G in a Mellin representation:

$$G(\xi, t) = \int_{c-i\infty}^{c+i\infty} \frac{dM}{2\pi} e^{M(t-t_0(\xi))} G(M, t). \tag{3.41}$$

From this it follows immediately

$$\begin{aligned} \frac{d}{d\xi} G(\xi, t) &= \int_{c-i\infty}^{c+i\infty} \frac{dM}{2\pi} e^{M(t-t_0(\xi))} \left(-M \frac{dt_0}{d\xi} G(\xi, M) + \frac{dG(\xi, M)}{d\xi} \right) = \\ &= \int_{c-i\infty}^{c+i\infty} \frac{dM}{2\pi} e^{M(t-t_0(\xi))} \left(-M t_0' + \chi(\hat{\alpha}_s, M) \right) G(\xi, M), \end{aligned} \tag{3.42}$$

that is we do not have our starting BFKL equation any more.

However we can recast Eq. (3.42) in a traditional form by simply defining a new "geometric scaling" kernel, related to the traditional one by

$$\chi_{gs}(\hat{\alpha}_s, M) \equiv \chi(\hat{\alpha}_s, M) - M t_s', \tag{3.43}$$

where we have put $t_s = t_0$ since this will turn out to be the true geometric scale. As we shall now see, from a pure theoretical point of view the new term doesn't give any problem, since it is only a linear contribution. Assume indeed one considers a totally generic evolution kernel χ and one performs a Taylor expansion around $M = M_0$. Since the only interesting contribution for the asymptotic limit $\xi \to \infty$ comes from the quadratic part, we may separate it from the rest of the expansion,

i.e. we may write

$$\chi(M) = \sum_{i=0}^{\infty} \frac{d^k}{k! dM^k} \chi(M)\Big|_{M=M_0} (M - M_s)^k = c + \frac{k}{2} (M - M_0)^2 + \text{other terms}. \tag{3.44}$$

Now consider the the effect of a generic non quadratic term, say of the cubic $1/6\ \zeta(M - M_0)^2$ term for definiteness. In t space this contribution can be viewed as a differential operator acting on the solution without the cubic term. Suppose for simplicity that we have only the quadratic kernel plus a cubic correction. Then what we have said is that the full solution can be written as

$$G(N, t) = \exp\left(-\frac{1}{6}\zeta \frac{d^3}{dt^3}\right) G_2(N, t), \tag{3.45}$$

where G_2 is the solution with only the quadratic part. The generalization of Eq. (3.45) to other terms is obvious. Note that in general we can't deal easily with terms of the form (3.45), typically we can treat them only perturbatively. However for a linear terms things become trivial. Indeed the operator associated to such a term is nothing but

$$\mathcal{O}_1(\lambda) = \exp\left[-\lambda \frac{d}{dx}\right], \tag{3.46}$$

that is the generator of translations:

$$\mathcal{O}_1(\lambda) f(z) = f(z - \lambda). \tag{3.47}$$

Hence the effect of our linear term is nothing but a shifting of the argument of our solution. Furthermore, noting that

$$\frac{d}{dt} = \left(\frac{2\beta_0 N}{k}\right)^{1/3} \frac{d}{dz} \tag{3.48}$$

we can write the "geometric scaling" solution straightforwardly:

$$G_{gs}(N, t) = K(N) e^{M_0(t - t'_s)} \mathrm{Ai}\left[\left(\frac{2\beta_0 N}{k}\right)^{1/3} \frac{1}{\beta_0} \left(\frac{1}{\alpha_s(t)} - \frac{c}{N} - \beta_0 t'_s\right)\right]. \tag{3.49}$$

It is easy to see that this changes nothing in our previous argument, it simply changes the implicit definition of t_s:

$$\frac{\xi\ c}{t_s} = \left(\frac{c}{N_s}\right) \xi = \left(\frac{1}{\alpha_s(t_s)} + t'_s - \left(\frac{k}{2\beta_0 N_s(t_s)}\right)^{1/3} \beta_0 z_0\right) \xi. \tag{3.50}$$

Hence from a theoretical point of view we obtain the same results of the previous section. However Eq. (3.50) is very difficult to master, even if we limit ourselves to the first few terms of the expansion (3.34). Hence me may adopt a different strategy.

Assume indeed to perform a slightly different expansion of our original kernel, that is we expand it around a point near the minimum but which is not the minimum. For the moment we can choose this point as we like it, later we will see that the self consistency of our approach impose a unique choice. We can then write our original kernel as

$$\chi(\hat{\alpha}_s, M) = \hat{\alpha}_s \left(\chi(M_0) + \chi'(M_0)(M - M_0) + \frac{1}{2}\chi''(M - M_0)^2 \right) + ... \tag{3.51}$$

Then the geometric scaling kernel reads

$$\chi_{gs}\left(\hat{\alpha}_s, M\right) = \chi\left(\hat{\alpha}_s, M\right) - Mt'_s =$$

$$= \hat{\alpha}_s \left(\chi(M_0) + \chi'(M_0)(M - M_0) + \frac{1}{2}\chi''(M - M_0)^2 \right) - Mt'_s. \tag{3.52}$$

Our strategy will be the following: we search a value M_0 such that the term $-Mt'_s$ cancels exactly the linear term of our geometric scaling term. Acting this way we obtain a new kernel which is quadratic, to which we can apply all the formalism derived in the previous section. Of course the new kernel will be in general different from the starting one, hence we will obtain different parameters for the saturation scale.

We can treat the running coupling perturbatively. It can be shown [18] that expanding the Airy solution we find exactly the same terms obtained by the perturbative expansion of the running coupling, this ensure that our procedure will lead to the correct result. The advantage of this perturbative approach is that the expansion is finite, since our kernel is a polynomial of degree two. Namely, one found that the geometric scaling kernel can be written as

$$\chi_{gs}(\alpha_s, M) = \left[\alpha_s\left(\chi - \chi' M_0\right) + \alpha_s^2\beta_0\chi' - \alpha_s^2\beta_0\chi'' M_0 - \alpha_s^3\beta_0^2\chi''\right] +$$

$$+ \left[\alpha_s\chi' + \alpha_s^2\beta_0\chi'' - t'_s\right] M + \left[\alpha_s\frac{1}{2}\chi''(M - M_0)^2\right], \tag{3.53}$$

where $\alpha_s = \alpha_s(t_s)$. Assume now that we want to consider the leading behaviour of the saturation scale. Accordingly this reduces to

$$\chi_{gs}(\alpha_s, M) = \alpha_s\left(\chi - \chi' M_0\right) + \left(\alpha_s\chi' - t'_s\right) M + \alpha_s\frac{1}{2}\chi''(M - M_0)^2. \tag{3.54}$$

Following our program then we have to solve

$$t'_s = \alpha_s\chi' = \frac{1}{\beta_0 t_s}\chi', \tag{3.55}$$

leading to the following definition for the saturation scale:

$$t_s = \sqrt{\frac{2\chi'}{\beta_0}\xi} \tag{3.56}$$

in analogy with [37]. But remember that the procedure of the previous sections leads to the prediction

$$t_s = \sqrt{\frac{c}{\beta_0}\xi}. \tag{3.57}$$

Hence, our approach is self consistent only if $c_{gs} = 2\chi'$. But $c_{gs} = \chi(M) - \chi' M_0$, hence we must have $\chi'(2 + M) = \chi$. This fix uniquely M_0 at a value slightly different from the one argued in [37].

At last, we can say that the total cross section has indeed a scaling behaviour, that is

$$\sigma_{tot}^{\gamma^* P} \propto e^{-(t-t_s)(1-M_0)} \mathrm{Ai}\left[\left(\frac{2\beta_0 N_s}{k}\right)^{1/3}(t - t_s) + z_0\right]. \tag{3.58}$$

The scaling law is broken by the residual ξ dependence of N_s. However assume that we are very close to the saturation scale, that is that we have $t \approx t_s$. Then we may expand the Airy function and factor out N_s in the boundary condition, just as we have done with the oscillating behaviour. In this case we obtain

$$\sigma_{tot}^{\gamma^* P} \approx \left(\frac{Q_s^2(x)}{Q^2}\right)^{1-M_0} \log \frac{Q^2}{Q_s^2(x)}, \tag{3.59}$$

in agreement with [37].

In this section we have clarified that geometric scaling cannot be claimed as a prerogative of the BK equation. However, note that all our predictions share a common property: they blow up when $\xi \to \infty$. In the case of running coupling this bad high energy behaviour is reduced w.r.t. the fixed coupling case, however from a theoretical point of view this is not a good situation. We have shown that geometric scaling is neither a proof nor a hint for the existence of a non linear regime, but such regime (or something very similar) must exist in order to ensure unitarity. Hence the true "original" prediction of the non linear equation is not geometric scaling but the saturation of the cross section for small x. As far as we know all the solutions of the linear equations blow up at very high energy. With the naive kernel χ_0 this growth is very rapid and leads to unitarity violations even for not so small x. However with the resummed kernels of Sec. 1.4 this rise is softened, hence the problems with unitarity arise only at very high energies. So, it is not yet clear where the non-linear effects become relevant. However there must come a point for which non linearities are relevant, hence requiring the full BK equation. For what concerns the BK prediction, there is a point that we must clarify. Because of the non linear damping term we have seen that Eq. (2.59) gives rise to saturation, and this is totally general. However, it is not clear how this saturation is reached and if the travelling wave solution (i.e. geometric scaling) is universal or not. We have said that geometric scaling arises only for a particular class of the boundary conditions, and also the behaviour of the cross section at high energy may depend strongly on them. Hence, even if the BK equation is a perturbative result, its predictions could be dominated by the non perturbative

input. Of course one should say that this is the case of all QCD phenomena, but this is not completely true. For example, the DGLAP prediction for F_2 is universal for sufficiently large t, that is the contribution of the boundary is subasymptotic with respect to the contribution of the perturbative evolution: the non perturbative information enters only as a trivial overall constant. We don't know if this is the case of BK equation. However, it seems that in the region interesting for the actual DIS phenomenology the solution may be boundary-condition dependent.

3.2 Geometric scaling at HERA

Until now we have worked on a totally theoretical plan, but all our theories must be tested with the existing experimental results. In this thesis we will focus on HERA data on deep inelastic scattering. Applications to other processes, namely experiments with heavy ions, may be found in [38] and references therein.

As we have mentioned in the introduction, a correct understanding of the true nature of the evolution in the HERA kinematic window is fundamental. Throughout all this thesis we have shown that from a theoretical point of view knowing the correct evolution in a given kinematic range is very useful, since it can give information about possible saturation effects. But also from a phenomenological point of view the knowledge of the real evolution at HERA is of the highest importance: all the parton distribution functions extracted from HERA data are evolved according to a DGLAP theory. If this turn out to be wrong, all our PDF are distorted and hence they introduce systematic errors when we use them as input for the calculation of others processes. Note that this is not a minor problem: just to make an example, the Higgs production via gluon fusion at LHC is strongly dependent on the small-x PDFs.

Hence a careful analysis of the HERA phenomenology is needed. This section is devoted to such analysis. In fact, in order to perform a more flexible analysis we won't work directly with HERA data, but we rather use an interpolation based on a neural network parametrization. Thus, before starting our true analysis we will give in Sec. 3.2.1 a short introduction of the neural network approach to deep inelastic structure functions fitting and we will specify parameters of the net that we have used.

In order to test our theories, the first task we will accomplish is to understand what is the exact kinematic window for the geometric scaling at HERA. In Sec. 3.2.2 then we will test the scaling behaviour in different kinematic ranges. Once stated where the geometric scaling holds, we will extract from the available data the parameters of the scaling law, namely the geometric slope λ. We will do such an analysis in Sec. 3.2.3, both with fixed and running coupling. Finally, in Sec. 3.2.5 we will compare the traditional predictions based on the DGLAP evolution with the ones based on the BFKL/BK theories.

3.2.1 The neural network parametrization of DIS data

As we have mentioned in the introduction of this section, in our analysis we won't to use directly the experimental data, but rather a suitable interpolation F_{exp}. This allows us to perform a much more flexible analysis. But of course in order to obtain reliable results F_{exp} must contain all the available information about the data. From a theoretical point of view one can obtain F_{exp} quite easily: one has only to choose a basis in an appropriate function space and to expand F_{exp} on this basis. Note the result of this expansion is totally independent of the chosen basis. Then all one has to do is to obtain the appropriate coefficients of this expansion from experimental data. But of course a non trivial function space has infinite dimension, hence we would have to determine an infinite number of coefficients. In other words, we would need an infinite number of experiments. In fact what one does is to truncate the infinite expansion and to fit the finite number of coefficients with all the existing data. However in this case the result is dependent on the chosen basis. The determination of the basis hence leads to a systematic error which is very difficult to deal with.

In our case we will use a different interpolation system, neural networks. The main advantage of this approach is that we don't have to say anything about the functional form of our F_{exp}. The strategy of the neural network parametrization we will use is the following (see Ref. [39]): first with Monte Carlo methods one generates a probability measure in the function space such that it gives a faithful representation of F_{exp} evaluated in the known experimental points, then one feeds the neural network with this measure. The result is an interpolation extended to the whole (x, Q^2) plane. Of course we can trust this interpolation only in a region where we have experimental data.

The neural network we will use was trained with all the existing experimental DIS data (in reality some very old and inaccurate data were removed), that is with the result of 13 charged lepton-proton scattering experiments. The kinematic coverage of these experiments in shown in Fig. 3.2. The characteristic triangular form can be easily understood if one takes in account the relations between x, Q^2 and the centre of mass energy $\sqrt{s}$:

$$y_{min} s < \frac{Q^2}{x} < s, \tag{3.60}$$

where y_{min} depends on the experiment. At HERA $\sqrt{s} \approx 314$ GeV and $y_{min} \approx 0.04$. The interested reader can found a more detailed description of these experiments in [39] and references therein. With respect to what we have said in the previous sections, we must specify that at sufficiently high virtualities DIS can be mediated not only by a virtual photon but also by a Z. However our net was built in order to handle both this cases.

The output of the net is the structure function F_2 with the relative error and correlations. This output not only agrees with the experimental results with which the net had been trained, but it has also passed various reliability test. Hence we

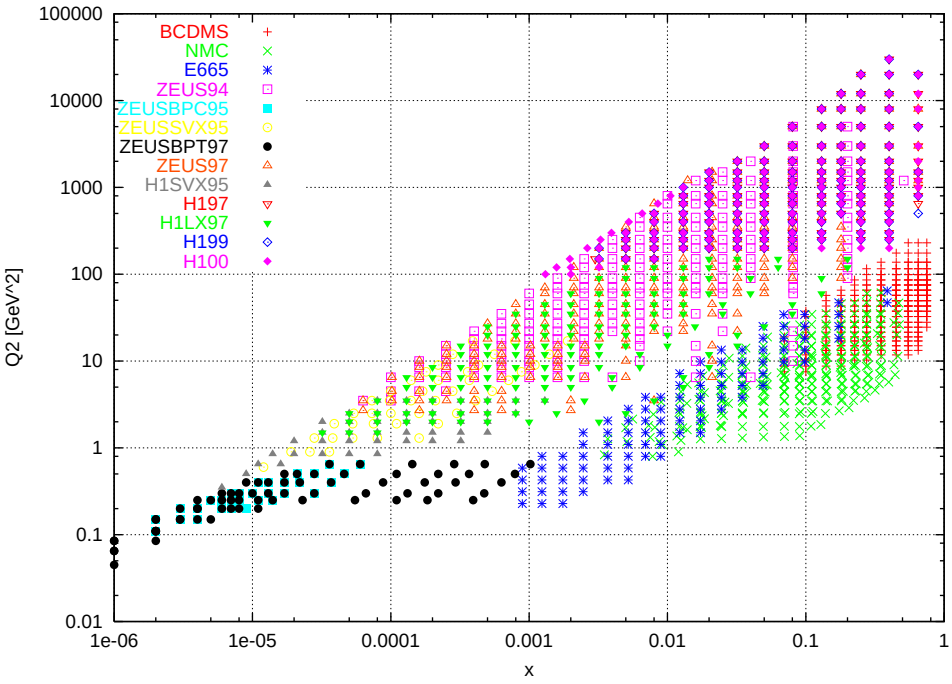

Figure 3.2: HERA kinematic range

can safely trust it, provided that we stay in the kinematic region shown in Fig. 3.2.

3.2.2 The geometric scaling window

In order to study the geometric scaling at HERA, first of all we have to know the kinematic region where the scaling behaviour holds. The goal of this section is just the determination of this kinematic range.
As a warm-up, we want to reproduce the original geometric scaling observation [1]. To this purpose, we have generated a grid of 1685 points in the $\left(x, Q^2\right)$ plane, with the condition $x < 0.01$. At HERA this bound implies $x \in \left[1.14 \cdot 10^{-6}, 0.01\right]$ and $Q^2 \in \left[0.05\ \text{GeV}^2, 450\ \text{GeV}^2\right]$. Since the natural variables in our theories are not x and Q^2 but rather ξ and t, we have chosen our points equally spaced in logarithmic units. Our sample is shown in Fig. 3.3, where we have also depicted two (fixed coupling) geometric lines, $Q^2 \cdot x^\lambda = 10$ and $Q^2 \cdot x^\lambda = 0.01$. Note that we have followed carefully the contours of the HERA triangle, in order to be absolutely sure about the output of the net.

As a starting point for our analysis we use the fixed coupling form for the saturation line. For λ we use the same value of [1], that is $\lambda = 0.29$. We hence plot

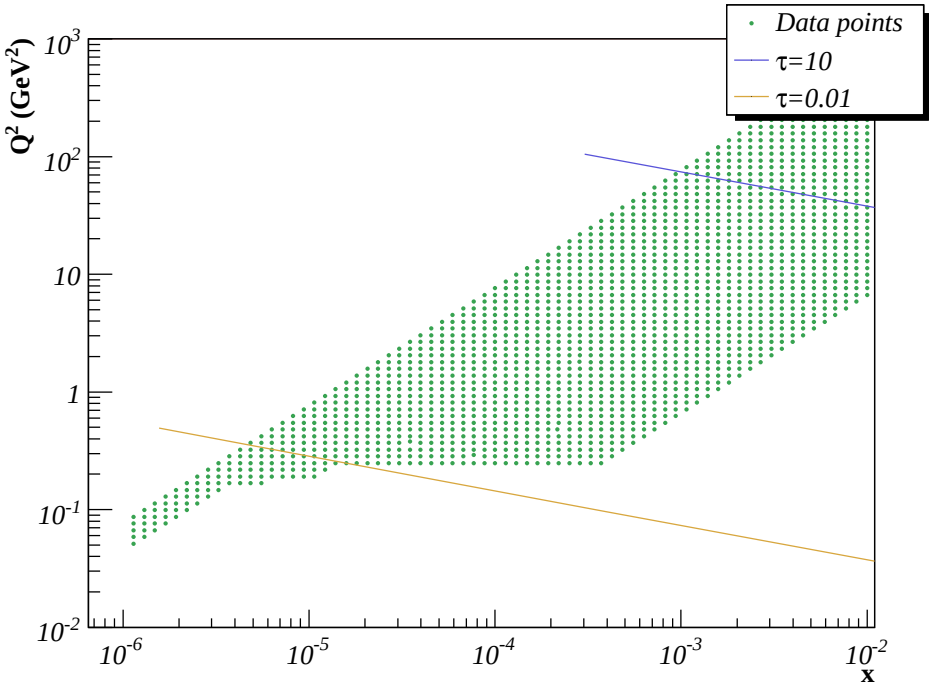

Figure 3.3: Data sample

the output of the net in function of the fixed coupling scaling variable[5] $\tau = Q^2 \cdot x^\lambda$. The resulting plot is shown in Fig. 3.4. At first sight geometric scaling seems to hold almost exactly. However note that the plot is in logarithmic units: the Q^2 range is so wide that the error bars aren't even visible. Hence this plot should be interpreted with care. Furthermore, dimensional analysis tells us that for large τ, and hence for large Q^2, the cross section should drop as $1/Q^2$ up to logarithmic corrections. Hence in Fig. 3.4 what we are seeing, at least for large τ, could be only this trivial asymptotic behaviour, which masks all the other interesting subasymptotic contributions.
In order to quantify what we have just said, we can consider

$$F(x) = \sigma_{tot}^{\gamma^* P}\left(x, Q^2 = \tau/x^\lambda\right), \tag{3.61}$$

that is the total cross section in function of x at fixed τ. If geometric scaling holds, then $F(x)$ is a constant. In Fig. 3.5 we plot F for different values of τ. Note that the scaling behaviour approximatively holds, but these plots clarifies that the geometric scaling description of HERA data is not as good as one can

[5]Note that in this section we use a different definition for τ: here $\tau = Q^2/Q_s(x)^2$, while in the previous section we have defined $\tau = t - t_s(\xi)$.

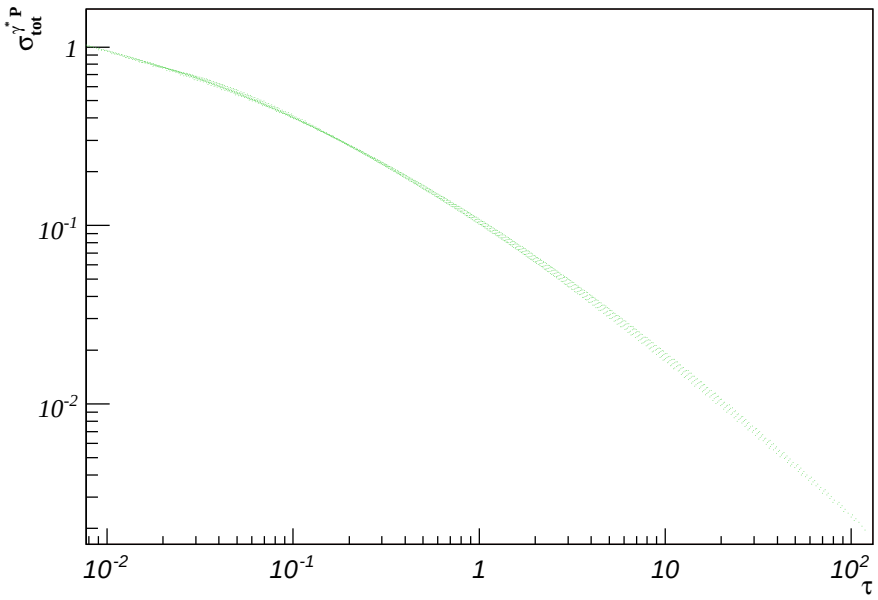

Figure 3.4: Geometric scaling in the original kinematic window

naively think from Fig. 3.4. In particular, we will see in Sec. 3.2.5 that the double scaling prediction (i.e. the pure DGLAP prediction) is a better description of HERA data (of course only in the kinematic range where the DGLAP theory can be applied).
Note that for small or large τ we have only few points (one can understand this immediately by inspecting Fig. 3.2), for very small τ we may have just one point for each different value of τ. But then in this region Fig. 3.4 doesn't tell us nothing about the scaling behaviour.

In order to understand if what we are seeing is in fact the geometric scaling predicted in the previous sections, we can adopt the following strategy. Our scaling law should hold for BFKL/BK-like evolutions, hence it should be relevant only at large ξ. Moreover, all our analytical analysis have shown that the scaling behaviour should be exact only in the asymptotic limit $\xi \to \infty$. Hence if we enlarge the kinematic window in order to consider also points with smaller rapidities, i.e. with $x > 0.01$, we may expect that the scaling behaviour disappears or at least that we can see some violations. But this is not the case of HERA data, as shown in Fig. 3.6: geometric scaling holds up to large values of x, say $x \sim 0.1$. This may be a first hint that in fact the scaling behaviour of the cross section is not directly related with the BFKL/BK geometric scaling prediction, at least for large τ (that is for large Q^2 and x).

Note however that the true non linear prediction, that is saturation, seems to

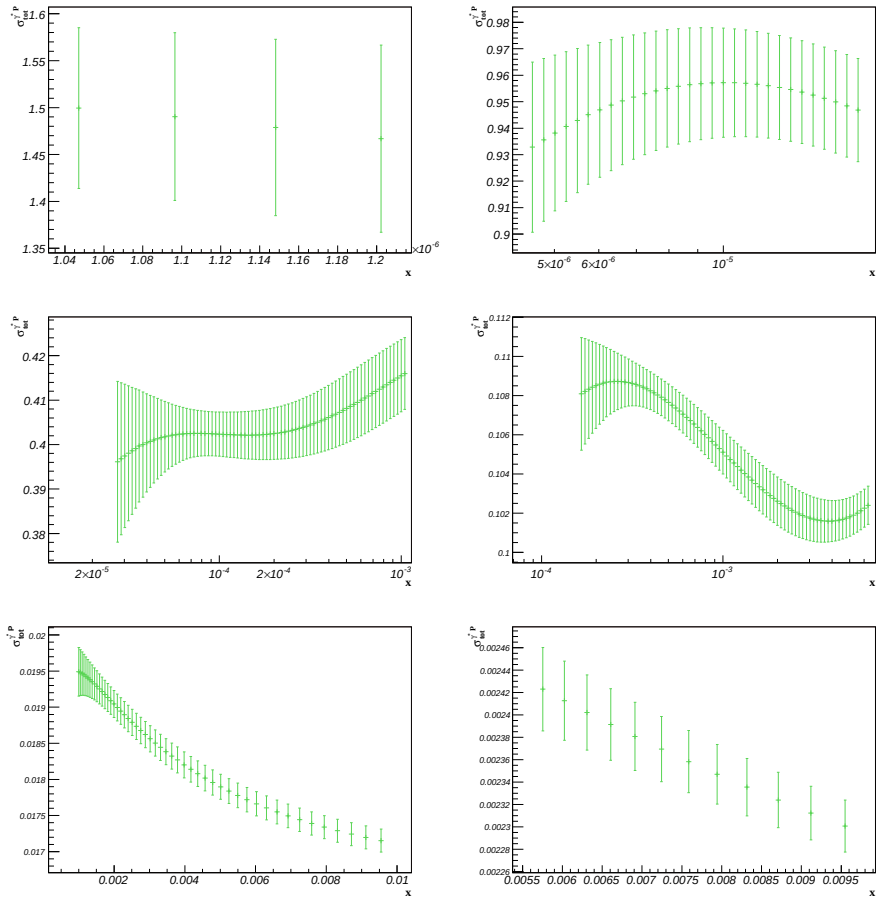

Plots of $F(x)$ for different values of τ. From left to right and from top to bottom: $\tau = 0.001,\ 0.01,\ 0.1,\ 1,\ 10,\ 100$.

Figure 3.5: Total cross section at fixed τ

be visible in the region on the extreme left of the plot. This is of course a region of very large rapidities, hence our theories should apply, but unfortunately it is also a region of low virtualities, hence perturbation theory is not reliable: we even reach values such that $Q^2 < \Lambda^2_{QCD}$, that is we go through the Landau pole of QCD. There are arguments showing that one could use perturbation theory even in this regime, but no one seems to us totally plausible.

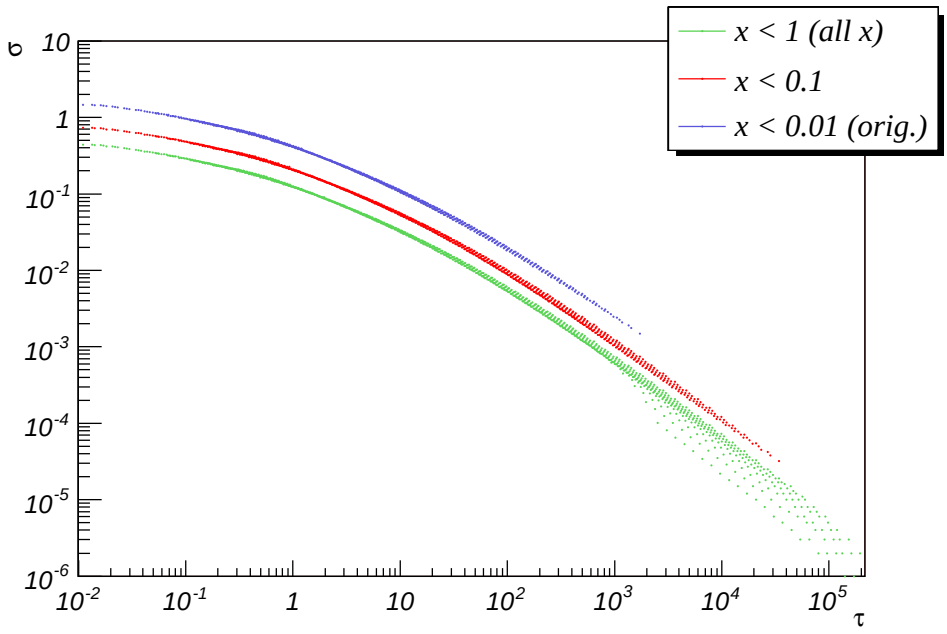

Figure 3.6: Geometric scaling in different kinematic windows

3.2.3 The geometric slope

In order to understand whether the observed scaling behaviour is geometric scaling or not, we may extract from the experimental data the saturation slope λ and compare it with our theoretical predictions. However this is not a trivial task: we do not have a well-defined function to fit. All our analytical predictions indeed hold only in the asymptotical regime $\xi \to \infty$, while at HERA the largest value of ξ is 13. Furthermore, data with large rapidities have also small virtualities, hence our leading order predictions aren't reliable. Hence our asymptotic expressions are inappropriate at HERA. Thus in order to extract a phenomenological value of λ we won't fit an analytical expression but we rather follow the approach proposed in [40]. Our strategy will be the following. We will associate to each possible value of λ a quality factor which express the goodness of the scaling behaviour. Then we will perform a scan in λ and choose as λ_{exp} the one with the highest quality factor.

Our expression for the quality factor is

$$Q(\lambda) = \left[\sum_i \frac{(y_{i+1} - y_i)^2}{(x_{i+1} - x_i)^2 + \epsilon^2} \right]^{-1}, \tag{3.62}$$

where x and y are rescaled τ and $\sigma_{tot}^{\gamma^* P}$, such that $0 < x_i, y_i < 1$, while ϵ is just a small number. It is easy to see that Eq. (3.62) accomplishes its task. Consider

indeed two successive points x_i, x_{i+1}. If we have the scaling behaviour, that is if it exists a function $\sigma(x_i)$ such that $y_i = \sigma(x_i)$, we may expect that the images through σ of x_i and x_{i+1}, that is y_i and y_{i+1}, should be very close. Otherwise, we expect that y_i is not related to y_{i+1}. We then see that Eq. (3.62) is a good definition for a quality factor. The role of ϵ is very simple: it prevents the sum to blow up if we have two points with the same x.

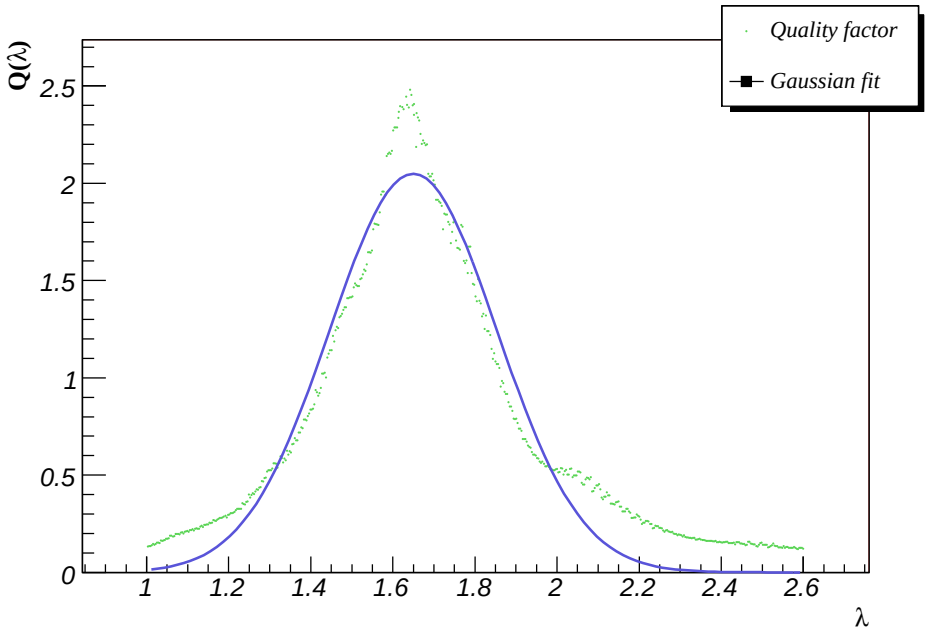

Figure 3.7: Quality factor in the running coupling case

We have used the quality factor Eq. (3.62) to extract λ_{exp} both for fixed and for running coupling geometric scaling, that is with geometric lines defined by $t - \lambda_{fix}\xi$ and by $t - \lambda_{run}\sqrt{\xi}$. In Fig. 3.7 a typical quality factor plot is shown. In order to extract a value from such a plot, we perform a gaussian fit (also shown in Fig. 3.7). Our best fit results are $\lambda_{fix} = 0.28 \pm 0.04$, $\lambda_{run} = 1.62 \pm 0.17$, in agreement with the results found in [40].

We can now replot our cross section using these new best fit parameters. In the case of fixed coupling the shape is almost identical to the one shown in Fig. 3.4, hence we do not report the plot. Consider instead the running coupling version of geometric scaling. In this case too the scaling behaviour seems very good, as shown in Fig. 3.8. But in this case too the same argument of the previous section applies. In particular if we plot the cross section at fixed τ in function of x we obtain a behaviour analogous to that depicted in Fig. 3.5.

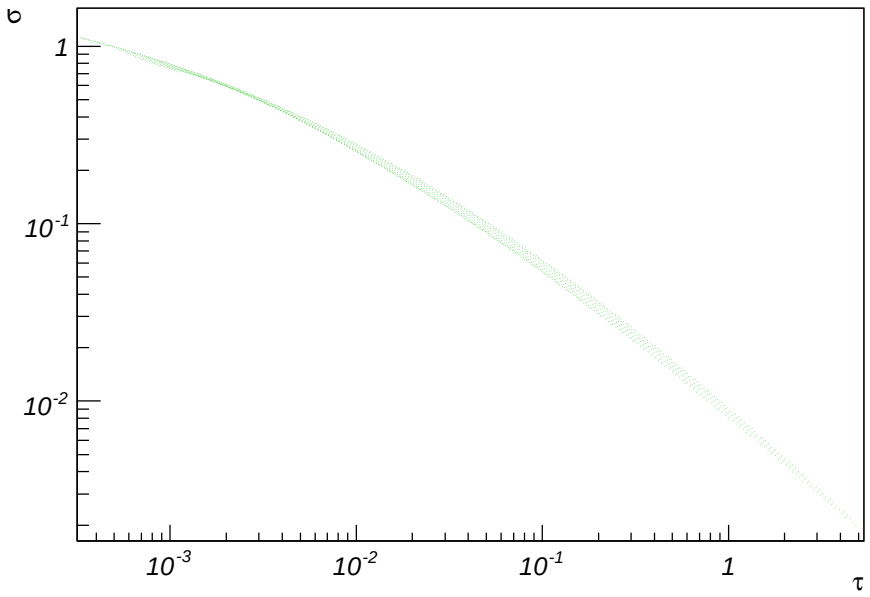

Figure 3.8: Running coupling geometric scaling

3.2.4 Comparison with the theoretical predictions

In the previous sections we have seen that geometric scaling holds in a very wide kinematic regime, both in the case of running and fixed coupling. But this seems at least strange: for Q^2 very large and for a large kinematic window we could expect a failure of a fixed coupling theory. Note that here we have huge Q^2: with the bound $x < 0.1$ at HERA we can have Q^2 up to 9000 GeV^2. Hence we cannot trust seriously a theory which neglects systematically all the large logarithms of Q^2.

In fact, we have not yet said that the scaling behaviour of HERA data and the geometric scaling predicted in the previous chapter are the same. In order to make a comparison, we will quote the main results that we have obtained in the previous chapter and in the first sections of this chapter. Let us start with the fixed coupling case. With the BK evolution in the quadratic approximation the geometric slope is obtained as the speed of the travelling wave solution, that is

$$\lambda_{BK,\ fix} = \bar{\alpha}_s \chi''\left(\frac{11}{2}\right)\left(\frac{1}{2} - 1 + \frac{1}{2}\sqrt{1 + 8\frac{\chi(1/2)}{\chi''(1/2)}}\right) \approx 4.6287\bar{\alpha}_s. \tag{3.63}$$

With the saddle point approximation of the BFKL equation instead one obtains

$$\lambda_{BFKL,\ fix} = \bar{\alpha}_s \chi'(M_s), \qquad \chi(M_s) = M_s \chi'(M_s), \tag{3.64}$$

leading to the prediction $\lambda \approx 4.8833\bar{\alpha}_s$. Note that the two predictions are comparable, but both fail completely do describe the data for realistic values of α_s. These predictions lead to a phenomenologically acceptable λ value only for $\alpha_s \approx 0.06$, while in the small-x region of HERA we can typically set $\alpha_s \approx 0.2$. We could have expected this failure: in such a wide kinematic range we cannot neglect running coupling effects. Let us then consider the running coupling version of geometric scaling. In [37] using a scaling ansatz the authors obtained

$$\lambda_{ansatz,\ run} = \sqrt{\frac{2\chi'(M_0)}{\beta_0}}, \qquad \chi(M_0) = \chi'(M_0)M_0, \tag{3.65}$$

leading to the prediction $\lambda \approx 3.75$. In the first section of this Chapter instead we obtained from the Airy anomalous dimension

$$\lambda_{Airy,\ run} = \sqrt{\frac{2\chi'(M_0)}{\beta_0}}, \qquad \chi(M_0) = \chi'(M_0)(2 + M_0), \tag{3.66}$$

leading to the prediction $\lambda \approx 1.78139$. We see that in this case too the theoretical and phenomenological values disagree. Note however that our prediction is closer to the phenomenological value. Moreover, in this case too we could have expected a failure of the Airy prediction: we have seen in the previous Chapter that the Airy approximation is not so good, in order to obtain a correct description of the phenomenology one should consider the Bateman anomalous dimension. We obtain a value which is not so bad because we are considering only the leading asymptotic behaviour of the Airy anomalous dimension, which is not so different from the Bateman one.

In order to have a representation of the errors of our theoretical estimates, in Fig. 3.9 we plot the cross section in function of τ_{teor}. The theoretical fixed coupling predictions are not universal, they depend on the value of the coupling. For the plot in Fig. 3.9 we have chosen the typical value $\alpha_s = 0.2$. There are some interesting observation about Fig. 3.9. We will left for later the more obvious, i.e. that the Airy prediction is very good. Consider the two plot on the top of the figure, that is the fixed coupling and the scaling ansatz running coupling solution. We note that the running coupling prediction is better than the other. This is nothing but a further signal saying that in this kinematic window we can't neglect large Q^2 logarithms (and hence DGLAP evolution). We note also that in the limit of small τ, i.e. of small t and large ξ, the theoretical predictions seem to capture the main features of the evolution. This is of course plausible: in this region the $\log Q^2$ terms are not so large, hence we may neglect them. Towards the saturation region all the theoretical predictions seems to furnish a correct representation of the data. However in this region we don't have experimental information enough for a definitive affirmation: as we have said, in this region the points are just a few (see Fig. 3.5), so it is not so strange that they lie on the same line. However this seems not to be just an accident, as we can see in Fig. 3.10. Unfortunately, as

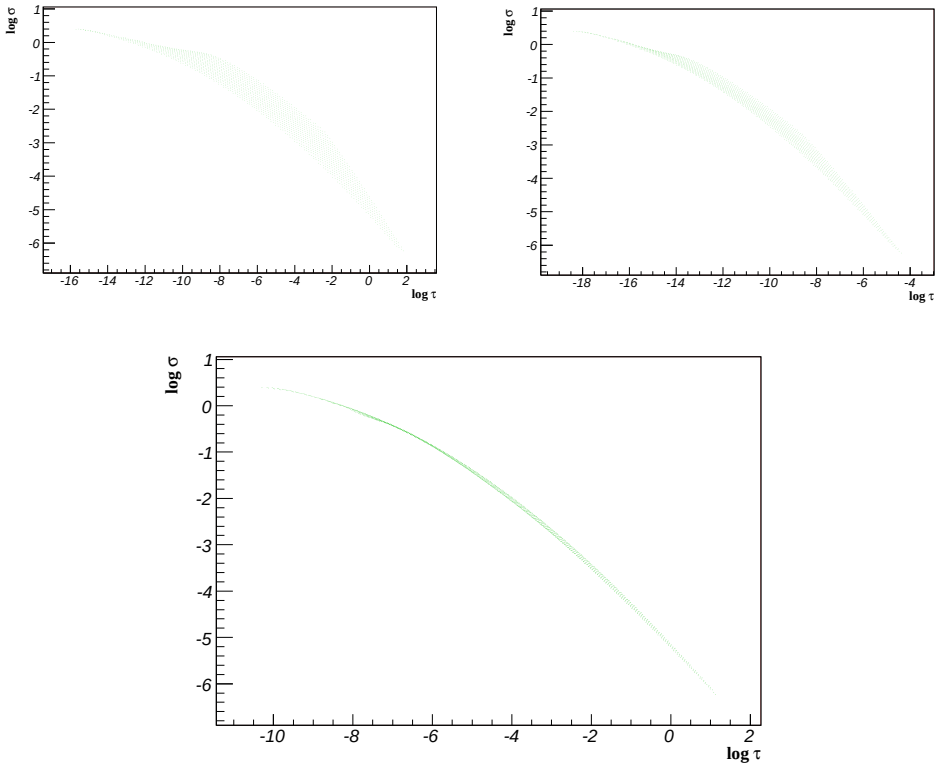

From left to right,top to bottom: the fixed coupling prediction $\lambda_{fix} \approx 0.93$, the scaling ansatz prediction $\lambda_{run} \approx 3.75$ and the Airy prediction $\lambda_{run} \approx 1.78$.

Figure 3.9: Geometric scaling with theoretical slopes.

we have said this region corresponds to very small momenta, hence it is dubious if we can apply standard perturbative theory, even if we are at large rapidities. We may say hence that at small τ we have a hint that our theories are correct, but we have no definitive argument.

Let now consider in detail the case of the Airy scaling. From Fig. 3.9 it seems that the Airy theory can explain all the HERA kinematic window. This should be strange, since from other analysis it emerges that the Airy anomalous dimension is not a good approximation of the true evolution [4]. However, we have never said that the Airy scaling is the correct description of HERA data, we just have shown that its prediction for the geometric slope is quite accurate. This of course is a necessary condition for a correct description of the data, but it is not sufficient. We have fitted the experimental points with a function of the form of the Airy prediction, that is

$$\sigma_{tot}^{\gamma^* P} = A \left(\frac{1}{\tau}\right)^{1-M_0} \log \frac{\tau}{B}. \tag{3.67}$$

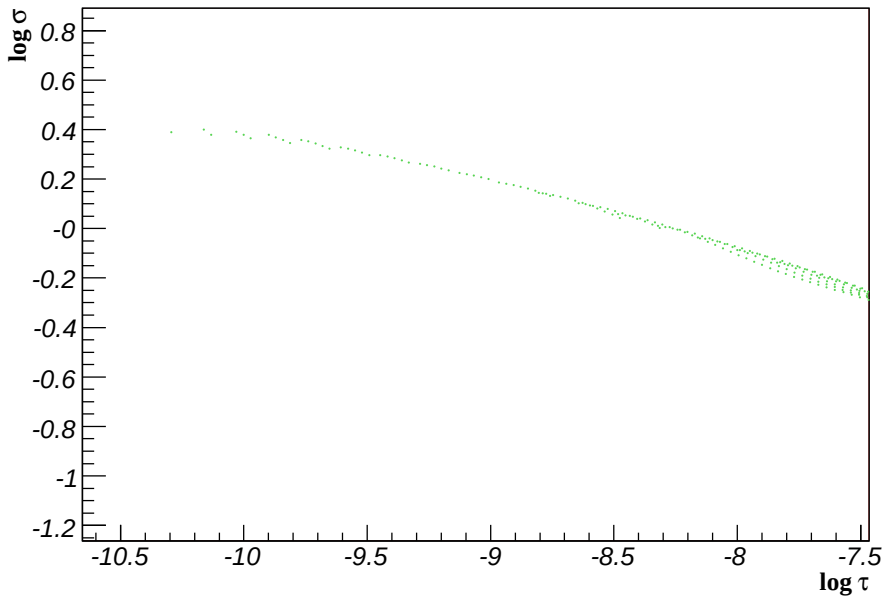

Figure 3.10: Enlargement of the small τ region.

In Fig. 3.11 we plot our result. Note that there is an agreement with the data only for small x. Note that with our theory we can't predict the actual values of A and B. From Fig. 3.11 it would seem that the small τ region of HERA data can be explained in terms of perturbative resummation only, that is there is no strong evidence of saturation effects. However, this region is highly non perturbative, hence it is dubious whether our analysis applies or not.

Note that the most of HERA data can't be described in term of the Airy scaling, hence our theories seems to fail for not so small τ. This is because until now we have neglected the real relevant evolution, that is the DGLAP evolution. In the next section we will see that the DGLAP solution explains perfectly the data in the whole kinematic window where it can be applied (that is at sufficiently large Q^2).

3.2.5 DGLAP evolution

One may legitimately wonder what is the role of DGLAP evolution in the HERA kinematic range. In this section we will show that for $Q^2 > 10$ GeV^2 the DGLAP solution reproduces all the available data with great accuracy. At first sight this may seem strange, since we can't find an analytic scaling prediction. However the DGLAP solution scales almost perfectly, as we show in Fig. 3.12. This behaviour is easily understood. Consider indeed the two pair of conjugate variables $\tau_\pm = t \pm \lambda\xi$.

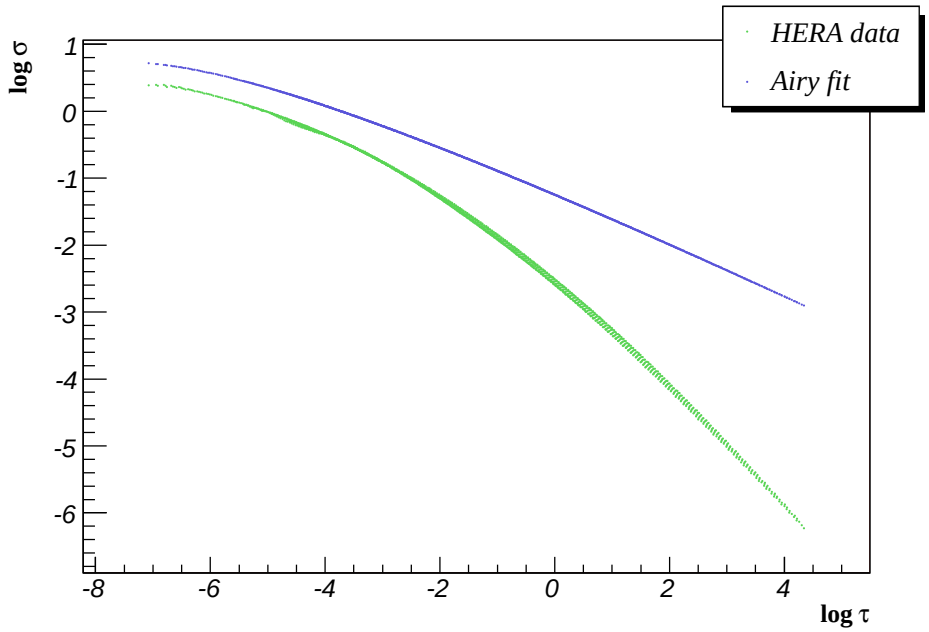

Figure 3.11: Airy fit

If for a value of λ the derivative of σ_{teor} with respect to τ_+ is small, then we have the scaling behaviour. Now, this is exactly the case of our experimental value $\lambda_{exp} = 0.28$. The same argument applies also to the case of running coupling scaling.

Hence the original geometric scaling observation in most of the kinematic window is nothing but a simple approximation to the DGLAP evolution. Note that this explains why the scaling behaviour persists also for not so small values of x.

Moreover, in this kinematic window we can consider an approximate solution to the DGLAP evolution, that is the double scaling prediction. In order to see that in this kinematic window the double scaling solution is in fact the correct description of the phenomenology, we plot the experimental results rescaled with the full asymptotics and subasymptotics double scaling predictions. In other words, consider the double scaling prediction for F_2:

$$F_2(t,\xi) = \mathcal{N}\frac{\gamma}{\sqrt{\sigma}\rho}\exp\left(2\gamma\sigma - \delta_+\frac{\rho}{\sigma}\right), \tag{3.68}$$

with σ, ρ, γ and δ_+ defined as in Sec. 1.2.6. Eq. (3.68) hence implies that the rescaled function

$$\sqrt{\gamma\sigma}\frac{\rho}{\gamma}e^{\delta_+(\sigma/\rho)-2\gamma\sigma}F_2 \tag{3.69}$$

should in fact be a constant. In Fig. 3.13 and 3.14 we plot this function of ρ and σ, for values of Q^2 smaller than 25 GeV^2, this way we do not have to consider

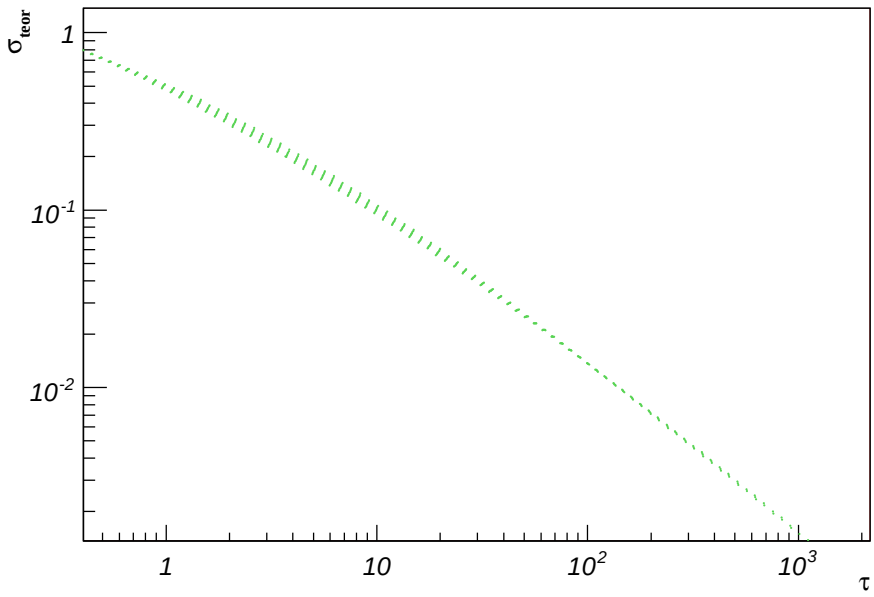

Figure 3.12: The theoretical DGLAP cross section for $Q^2 > 10$ GeV^2

bottom quark contribution and hence we can always put $n_f = 4$. Note that in this case the agreement with the expected prediction is better than in Fig. 3.5. In other words, as long as $Q^2 > 10$ GeV^2 the true small x evolution is just a pure DGLAP evolution.

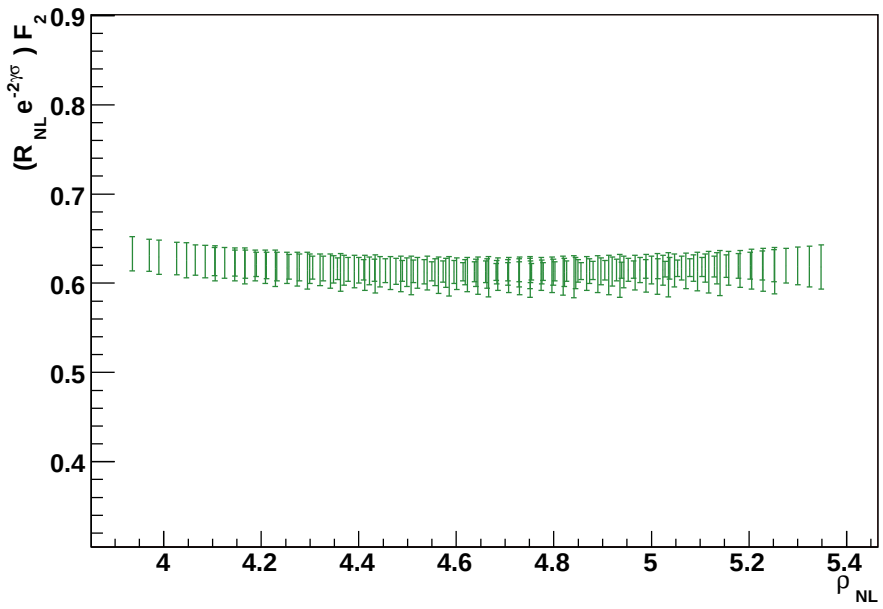

Figure 3.13: Double scaling in the variable ρ

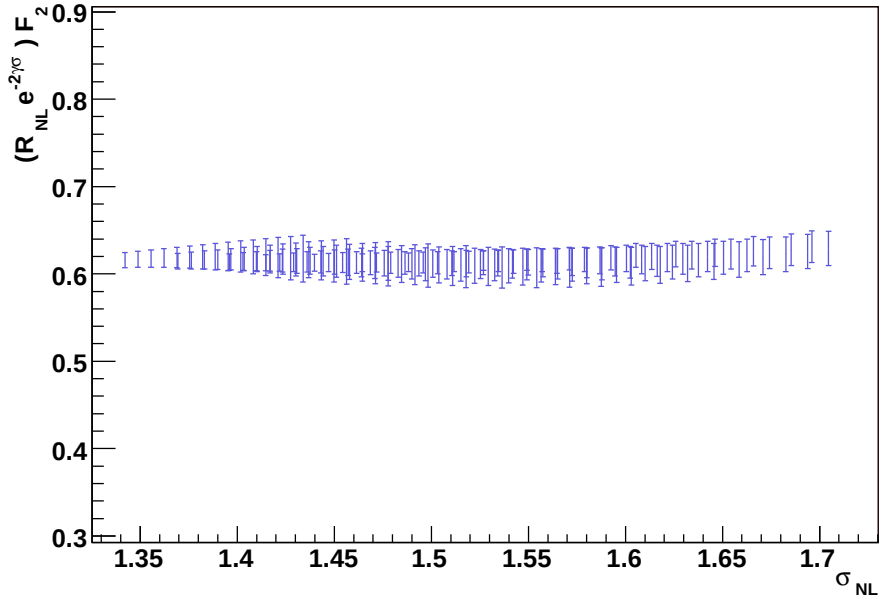

Figure 3.14: Double scaling in the variable σ

Summary and future work

In this thesis we studied perturbative QCD in the small-x limit. In particular we have tried to understand the phenomenon of geometric scaling observed at HERA. In the first chapter we have introduced the traditional evolution equations of perturbative QCD, namely the DGLAP and the BFKL equations. We have shown their utility and their limits. Then we have shown how one can improve these equations. First we have considered perturbative resummations, which enable us to deal with two large scales. Second, we have unitarized the BFKL equation by considering a generalization to multiple scattering of the standard BFKL theory. This has led us to the non linear BK equation. Finally we have shown how geometric scaling arises from the non linear evolution. The last chapter was devoted to an intensive study of geometric scaling. First we performed an analytical study of the linear equations and we showed that also in the linear regime we can have asymptotic geometric scaling. This implies that geometric scaling is not directly related to saturation. However, the saturation and the linear predictions for the parameters of the scaling behaviour (that is for the geometric slope λ) are different, hence a careful analysis of the phenomenology can give us an information about the true evolution. Hence in the last section of the thesis we have tested our theories with data. We focused on the deep inelastic scattering data, which are traditionally considered one of the most striking proofs of geometric scaling. In fact, we have shown that the geometric scaling observed at HERA has little to do with non linear effects (i.e. with saturation): it is nothing but a "masked" manifestation of the traditional double scaling behaviour of the structure function F_2. However, in the region of very large rapidities data may be compatible with a BK evolution. Unfortunately in this region we have very few data points, hence our affirmations can't be definitive. Moreover, this is a region characterised by small values of Q^2, hence all the perturbative approach is dubious.

We conclude this thesis by realizing that there is still a lot of work to do in order to achieve a deep understanding of the small x and large Q^2 region. First of all, a true running coupling version of the BK equation is sorely needed. Moreover, it is interesting to see the effects of non linearities on perturbative resummations. Furthermore, one may investigate the impact of next to leading order terms in the framework of the BK theory. Once a next to leading theory is available, one could perform a NL HERA data analysis, in order to check the accuracy of our LO results.

Of course the phenomenological implications of high energy QCD aren't limited to deep inelastic scattering. Other interesting applications include heavy ions physics and also astrophysics. The theory can be fruitfully applied also to hadron-hadron scattering. Hence we expect that the future LHC results will lead to a deep insight of the small-x perturbative QCD.

Appendix A: The large N_C QCD expansion

In this Appendix we will sketch the main features of the large-N_c QCD expansion. We will limit ourselves to derive the result that we use in the text. For a complete exposition we refer to the existing literature, for example to [41] and references therein.

The main idea of the large N_c limit, first introduced by 't Hooft [20], is to consider the limit $N_c \to \infty$ with $\alpha_s N_c$ held fixed. The small parameter of the theory is then $1/N_c$. In QCD $N_c = 3$, so one may think that this is a bad approximation. To see that this is not a valid objection, consider QED: $e^2/4\pi = 1/137 \to e = 0.3$. Thus we can hope that the large N_c limit can give some interesting results.

Consider the general Lagrangian of a $SU(N)$ theory, written in the form

$$\mathcal{L} = \frac{N}{g^2}\left[\bar{\psi}_a\left(i\partial_\mu + A^a_{\mu b}\right)\gamma^\mu\psi^b - m\bar{\psi}_a\psi^a - \frac{1}{4}F^a_{\mu\nu b}F^{\mu\nu b}_a\right]. \tag{A.1}$$

Than the propagators of our theory are

$$\left\langle\psi^a(x)\bar{\psi}_b(y)\right\rangle = \frac{1}{N}\delta^a_b S(x-y) \tag{A.2}$$

$$\left\langle A^a_{\mu b}(x)A^c_{\nu d}(y)\right\rangle = \frac{1}{N}\left(\delta^a_d\delta^c_b - \frac{1}{N}\delta^a_b\delta^c_d\right)D_{\mu\nu}(x-y) \tag{A.3}$$

if S and $D_{\mu\nu}$ are the propagators of respectively a single Dirac and gauge field. Since we are interested in the large N limit, we can drop the term proportional to $1/N^2$ in the gluon propagator. This way we can easily follow indices along a line in a Feynman graph: along a quark line the index doesn't change, while along a gluon line the pair at the beginning is the same as the pair at the end.

We can use this observation to derive an alternative way of drawing Feynman graphs, the 't Hooft double-line representation. We simply draw one line for each index rather than one line for each virtual particle. Hence quark lines will be represented by a single line, while gluon lines by a double line. The standard Feynman rules in the double-line representation are shown in Fig. A.1. The correspondence between traditional and double-line graphs is not one to one: to

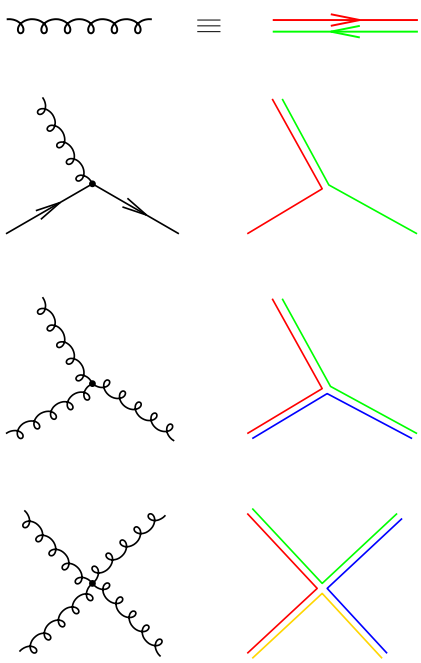

Figure A.1: Double-line representation of Feynman rules

one traditional graphs can correspond several double-line graphs, each for every possible different way of assigning index. The power of $1/N$ carried by a graph is very difficult to calculate for a traditional graph, while it becomes trivial for a double-line graph.

Consider first a vacuum-to-vacuum graph, that is a graph in which every line must close to make an index loop. We can think of every loop as the perimeter of a polygon. We can assign an orientation to each polygon by the direction of the arrows around its perimeter and the right hand rule. Now, if two adjacent edges (of two different polygons) lie on the same double line (i.e. on the same gluon propagator), we "glue" them together. This way we have constructed an oriented surface. The power of N associated to this surface is easily calculated. Each face is a loop integral, thus it carries a N factor from the sum over all the possible values of the index. Every vertex is a Feynman vertex, thus it carries a N factor (see (A.1)). Every edge is a quark or gluon propagator, so it carries a factor $1/N$ (be careful not do double count the glued edges). Thus the graph is proportional to

$$N^{F+V-E} \equiv N^{\chi}, \tag{A.4}$$

where χ is the *Euler characteristic* of the surface.

Every oriented surface is topologically equivalent to the sphere S^2 with some numbers of holes and some number of handle. If H is the number of handles and

B the number of holes, it can be shown that the Euler characteristic is

$$\chi = 2 - 2H - B. \tag{A.5}$$

Thus the leading vacuum-to-vacuum diagrams are proportional to N^2 and are those topologically equivalent to a sphere. Consider first a diagram with only gluons. The simplest one is the gluon loop, Fig. A.2: the two faces (oppositely oriented) with glued perimeters can be assembled to form the sphere S^2. As can be

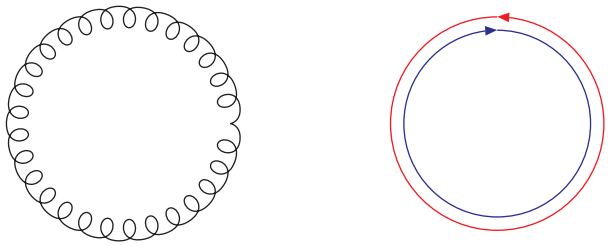

Figure A.2: Gluon loop

easily seen this is the case of all planar graphs made up only of gluons. Conversely, remove a generic face from a spherical surface with no holes and no handles. The result will be a spherical surface with one hole, that is a surface topologically equivalent to a plane, that is a planar graph. Thus we obtained that the leading large N_c graphs are *planar graphs made up only of gluons*. Since they have no holes and no handles, they behave like N^2.

Consider now a quark loop. Since it is a single (unpaired) line, it corresponds to a hole. The leading quark graphs then have one hole and no handles. As we noted before, a spherical surface with one hole is equivalent to a plane. Thus the leading graphs are planar graphs. The only difference with the previous situation is that now the outer boundary of the resultant planar graph is the quark loop. Thus when quarks are involved the leading graphs are *planar graphs with only one quark loop forming the boundary of the graph*. Since these graphs have one hole, they behave like N.

These analysis can be easily generalized to graphs with external lines. Note that we obtained these results using the equivalence (A.4), valid only if in the Lagrangian (A.1) the prefactor is N_c/g^2. In other words, the "correct" large N_c expansion is with $\alpha_s N_c$ held fixed. If we for example hold $\alpha_s N_c^2$ fixed, no interesting result can be found.

In Fig. A.3 several graphs relevant for the dipole picture are reported. Even though they are not vacuum-to-vacuum graphs, our previous analysis is unaltered. Consider indeed the graph (a). Its vacuum-to-vacuum equivalent should be a closed quark loop, that is a $O(N)$ graph. Here we don't have loops, but we have N possible different quark-antiquark pairs, so this graph too behaves like N. This argument can be easily generalized to all onium-to-onium graphs. Using our results we then expect that in the large N_c limit only (a), (b) and (c) are relevant, since

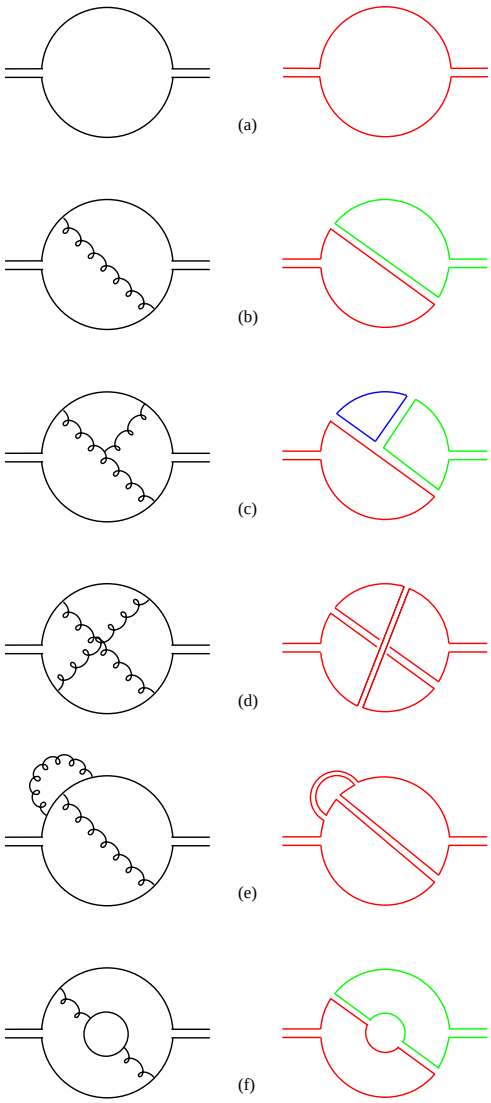

Figure A.3: Double-line onium graphs

they are planar graphs with the quark loop on the boundary. Let us check out if this is the case. First consider (a). We have N different quark-antiquark pairs, so this graph is $O(N)$ as expected. In (b) we have two faces, three edges and two vertices, so this too behaves like N. In (c) we have three faces, six edges and four vertices, hence $\chi = 1$. (d) is not a planar graph. It has one hole and one handle, so we expect it being proportional to N^{-1}. In fact it has only one loop index, four vertices and six propagators, that is it is $O(N^{-1})$. (e) is planar, but the boundary is not the quark loop. Hence it has one hole and one handle, so it is $O(N^{-1})$. Indeed it has one colour loop, four vertices and six propagators. (f) should be

suppressed: having two holes it should be $O(1)$. That is the case: we have two colour loops, four vertices and six propagators. But in QCD there are more than one flavour, so this graph is enhanced by a power of n_f. This is a delicate point in the large-N expansion. However, for our purposes we can simply neglect this complication and act as if there were only one flavour.

Bibliography

[1] A. M. Stasto, K. J. Golec-Biernat and J. Kwiecinski, Phys. Rev. Lett. **86** (2001) 596 [arXiv:hep-ph/0007192].

[2] R. K. Ellis, W. J. Stirling and B. R. Webber, *QCD and Collider Physics*. Cambridge Univ. Press, 1996.

[3] L.N. Lipatov, Sov. J. Nucl. Phys. **23** (1976) 338; E.A. Kuraev, L.N. Lipatov and V.S. Fadin, Zh. Eksp. Teor. Fiz **72**, 3 (1977) (Sov. Phys. JETP **45** (1977) 199); Ya.Ya. Balitsky and L.N. Lipatov, Sov. J. Nucl. Phys. **28** (1978) 822.

[4] G. Altarelli, R. D. Ball and S. Forte, Nucl. Phys. B **742** (2006) 1 [arXiv:hep-ph/0512237].

[5] I. I. Balitsky, Nucl. Phys. **B463**, 99 (1996) [arXiv:hep-ph/9509348];

[6] J. Jalilian-Marian, A. Kovner, A. Leonidov and H. Weigert, Nucl. Phys. B **504** (1997) 415 [arXiv:hep-ph/9701284]; E. Iancu, A. Leonidov and L. D. McLerran, Nucl. Phys. A **692** (2001) 583 [arXiv:hep-ph/0011241]; H. Weigert, Nucl. Phys. A **703** (2002) 823 [arXiv:hep-ph/0004044].

[7] Y. V. Kovchegov, Phys. Rev. **D60**, 034008 (1999) [arXiv:hep-ph/9901281]; Y. V. Kovchegov, Phys. Rev. **D61**, 074018 (2000), [arXiv:hep-ph/9905214].

[8] E. Iancu, K. Itakura and L. McLerran, Nucl. Phys. A **708** (2002) 327 [arXiv:hep-ph/0203137].

[9] S. Catani, M. Ciafaloni and F. Hautmann, Phys. Lett. B **307** (1993) 147; S. Catani and F. Hautmann, Phys. Lett. B **315** (1993) 157; S. Catani and F. Hautmann, Nucl. Phys. B **427** (1994) 475 [arXiv:hep-ph/9405388].

[10] R. K. Ellis, H. Georgi, M. Machacek, H. D. Politzer and G. G. Ross, Phys. Lett. B **78** (1978) 281; R. K. Ellis, H. Georgi, M. Machacek, H. D. Politzer and G. G. Ross, Nucl. Phys. B **152** (1979) 285.

[11] S. Weinberg, Phys. Rev. 118 (1960) 838: in: *The Quantum Theory of fields*. Cambridge Univ. Press, 1996.

[12] V. Del Duca, arXiv:hep-ph/9503226.

[13] S. Marzani, R. D. Ball, P. Falgari and S. Forte, arXiv:0708.3994 [hep-ph].

[14] T. Jaroszewicz, Phys. Lett. B **116** (1982) 291.

[15] R. D. Ball and S. Forte, Phys. Lett. B **405**, 317 (1997) [arXiv:hep-ph/9703417].

[16] V. S. Fadin and L. N. Lipatov, Phys. Lett. B **429**, 127 (1998) [arXiv:hep-ph/9802290].

[17] L. N. Lipatov, Sov. Phys. JETP **63** (1986) 904 [Zh. Eksp. Teor. Fiz. **90** (1986) 1536].

[18] G. Altarelli, R. D. Ball and S. Forte, Nucl. Phys. B **621** (2002) 359 [arXiv:hep-ph/0109178].

[19] M. E. Peskin and D. V. Schroeder, *An Introduction To Quantum Field Theory.* Addison-Wesley, 1995

[20] G. 't Hooft, Nucl. Phys. B **72** (1974) 461.

[21] A. H. Mueller, Nucl. Phys. B **415** (1994) 373.

[22] G. Altarelli, R. D. Ball and S. Forte, Nucl. Phys. B **599** (2001) 383 [arXiv:hep-ph/0011270].

[23] T. Jaroszewicz, Phys. Lett. B **116** (1982) 291; S. Catani, F. Fiorani, G. Marchesini, Phys. Lett. B **336** (1990) 18; S. Catani et al., Nucl. Phys. B **361** (1991) 645.

[24] R. D. Ball and S. Forte, Nucl. Phys. B **742** (2006) 158 [arXiv:hep-ph/0601049].

[25] L. V. Gribov, E. M. Levin and M. G. Ryskin, Nucl. Phys. B **188** (1981) 555; Phys. Rep. **100**(1983).

[26] A. H. Mueller and J. w. Qiu, Nucl. Phys. B **268** (1986) 427.

[27] J. D. Bjorken, J. B. Kogut and D. E. Soper, Phys. Rev. D **3** (1971) 1382.

[28] N. N. Nikolaev and B. G. Zakharov, Z. Phys. C **49** (1991) 607; Z. Phys. C **53** (1992) 331; Z. Phys. C **64** (1994) 651; JETP 78 (1994) 598.

[29] S. Munier and R. Peschanski, Phys. Rev. Lett. **91** (2003) 232001 [arXiv:hep-ph/0309177].

[30] M. Bramson, Memoirs of the American Mathematical Society 285 (1983).

[31] M. Braun, Eur. Phys. J. C **16**, 337 (2000) [arXiv:hep-ph/0001268].

[32] E. Levin and K. Tuchin, Nucl. Phys. B **573**, 833 (2000) [arXiv:hep-ph/9908317]; Nucl. Phys. A **691**, 779 (2001) [arXiv:hep-ph/0012167]; N. Armesto and M. A. Braun, Eur. Phys. J. C **20**, 517 (2001) [arXiv:hep-ph/0104038]; M. Lublinsky, Eur. Phys. J. C **21**, 513 (2001) [arXiv:hep-ph/0106112]; K. Golec-Biernat, L. Motyka and A. M. Stasto, Phys. Rev. D **65**, 074037 (2002) [arXiv:hep-ph/0110325].

[33] J. L. Albacete, N. Armesto, A. Kovner, C. A. Salgado and U. A. Wiedemann, arXiv:hep-ph/0307179.

[34] E. Gardi, J. Kuokkanen, K. Rummukainen and H. Weigert, Nucl. Phys. A **784** (2007) 282 [arXiv:hep-ph/0609087].

[35] Y. V. Kovchegov and H. Weigert, Nucl. Phys. A **784** (2007) 188 [arXiv:hep-ph/0609090].

[36] Y. V. Kovchegov and H. Weigert, Nucl. Phys. A **789** (2007) 260 [arXiv:hep-ph/0612071].

[37] S. Munier and R. Peschanski, Phys. Rev. D **69** (2004) 034008 [arXiv:hep-ph/0310357].

[38] D. d'Enterria, arXiv:0706.4182 [hep-ex].

[39] L. Del Debbio, S. Forte, J. I. Latorre, A. Piccione and J. Rojo [NNPDF Collaboration], JHEP **0503** (2005) 080 [arXiv:hep-ph/0501067].

[40] F. Gelis, R. Peschanski, G. Soyez and L. Schoeffel, Phys. Lett. B **647** (2007) 376 [arXiv:hep-ph/0610435].

[41] S. Coleman, *Aspects of Symmetry*. Cambridge Univ. Press, 1988.

Ringraziamenti

Vorrei innanzitutto ringraziare il Professor S. Forte, per il suo sostegno e la sua disponibilità davvero eccezionali.
Voglio anche ringraziare i miei amici Giovanni per le lunghe discussioni fatte e Salvatore per aver risolto praticamente ogni mio problema con LaTeX. Un grazie va poi ai miei genitori, che mi hanno sopportato in questi mesi di frenetico lavoro e a mia sorella, che praticamente ha vissuto gli ultimi sei mesi da figlia unica. Allo stesso modo devo ringraziare tutti i miei amici, che mi hanno sempre supportato nonostante io li abbia parecchio trascurati in questi ultimi tempi.

Da ultimo, vorrei ringraziare Arthur Rubinstein, Glenn Gould, Sviatoslav Richter e Johann Sebastian Bach per non avermi mai lasciato solo durante la lunga stesura di questo testo.